NASA Tech Briefs

National Aeronautics and
Space Administration

March 1988
Volume 12 Number 3

**1482°C—
Too Hot
To Handle?
Nope—see
page 12.**

In space: looking back to look forward.

What can the nature and origin of the universe tell us about the future of Earth? To help answer that question, we make craft and instruments for traveling billions of miles in space and seeing as far as 15 billion years back in time. Martin Marietta was the integrator and builder of two Viking landers, which sent back remarkable photos of the surface of Mars, examined soil samples, and studied Martian weather and seismic activity. For the Voyagers we provided instrumentation that reported on electromagnetic activity near Jupiter and Saturn—Voyager 2 went on to Uranus, some 2 billion miles from Earth. That was nine years after launch; next destination, Neptune, in 1989. These are but a few results of Martin Marietta's ability to create survivable, mystery-solving craft and their instruments—from concept through mission completion.

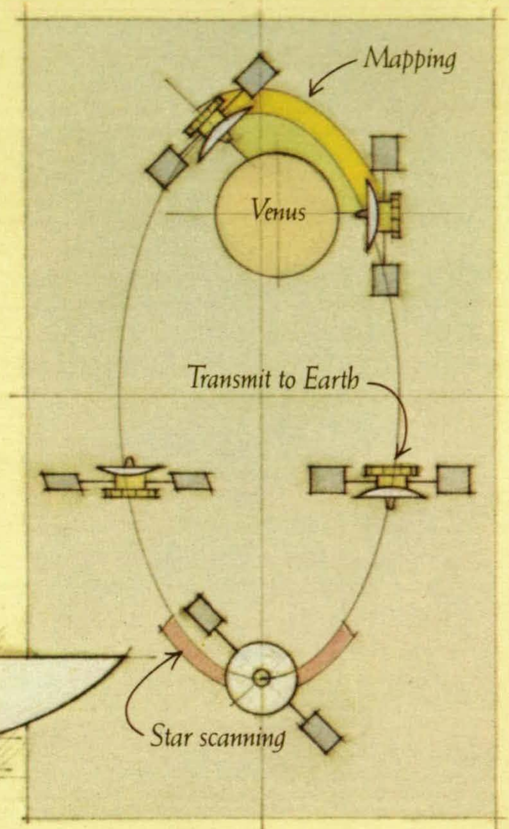

Orbit and orientation

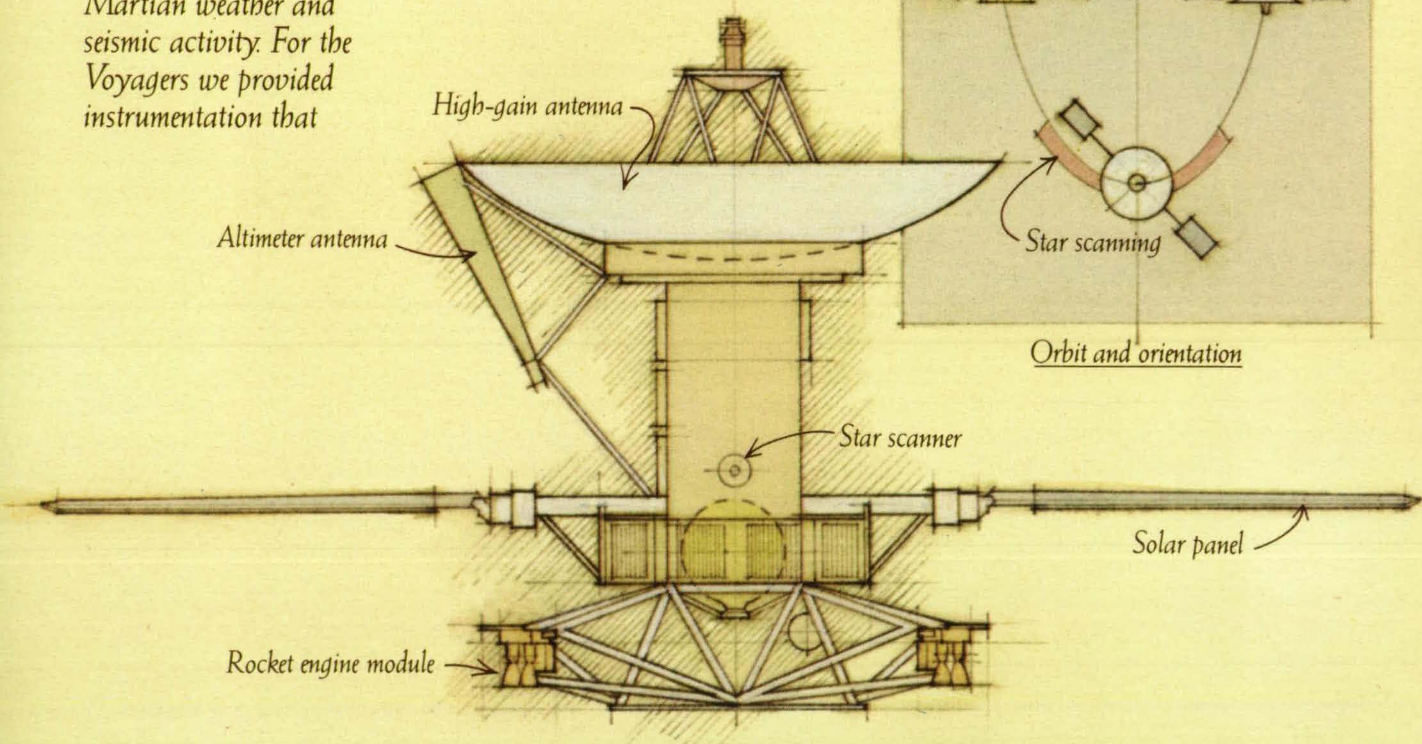

Magellan Spacecraft

Mission: map Venus.

From orbit, Magellan's radar will penetrate the planet's thick, gaseous cloud cover and send back photo-like images of nearly 90% of its surface. Our role: design, integrate, build and test the craft.

The earlier you "think cost-efficient you

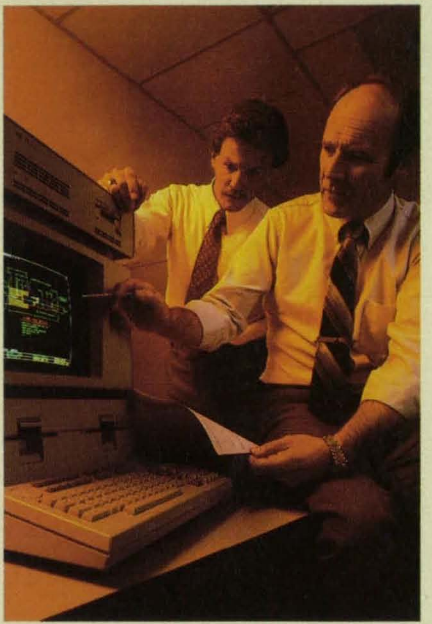

Du Pont CAD/CAM facilities assist in the development of VESPEL parts.

Du Pont resources help every step of the way

VESPEL polyimide parts from Du Pont give you something you just don't get anywhere else—assistance and accountability from resins straight through to finished parts.

From years of experience, our sales engineers can show you how ultra-performance VESPEL parts can simplify entire assemblies. How they let you combine several parts into one. Eliminate lubrication systems. Cut machining costs. Minimize downstream maintenance costs and warranty claims.

In short, we show how it pays to "think VESPEL" from the start—instead of using materials that can't perform as well or last as long, and could be the cause of costly failures.

Quality control so good, some customers let us do all the inspecting

Our custom molding techniques insure consistency—part-to-part and order-to-order. And we follow through with Statistical Process Control—a quality procedure so rigorous, many of our customers forego their own inspections.

So when you get VESPEL parts from Du Pont, you can be sure they have the quality you want. Otherwise, we wouldn't let them out of the house.

VESPEL parts give you the best of plastics, metals and ceramics

VESPEL polyimide parts are in a class by themselves—for resilience and compressive strength, for dimensional stability, for resistance to wear and friction.

They retain their properties at temperatures from cryogenic to 500°F, with excursions to 900°F. They can take PVs up to 1 million psi-fpm lubricated. And an unmatched 300,000 psi-fpm without lubrication.

VESPEL parts can carry loads at temperatures that turn ordinary plastics into puddles. Their compliant surface seals tighter than machined metal-to-metal seals. And like ceramics, they offer insulating properties and excellent wear resistance at temperatures where lubricants cannot function.

Computer video scanning insures dimensional accuracy of VESPEL parts.

Vespel,®" the more total design can be.

A guide to resin selection for VESPEL parts

Resin	Description	Characteristics
SP-1	Unfilled base resin	Provides maximum physical strength, elongation and toughness, and best electrical and thermal insulation.
SP-21	15%, by weight, graphite filler.	Graphite added to provide low wear and friction for bearings, thrust washers, and dynamic seals.
SP-22	40%, by weight, graphite filler.	Same as SP-21 for wear and friction plus improved dimensional stability. It has the lowest coefficient of thermal expansion.
SP-211	15%, by weight, graphite and 10%, by weight, Teflon® fluorocarbon resin fillers.	Has lowest coefficient of friction over wide range of operating conditions. Also, has lowest wear rate up to 300°F.
SP-3	15%, by weight, molybdenum disulfide.	MoS_2 added to provide lubrication for seals and bearings in vacuum or dry environments.

A VESPEL sampler: from auto check valves to aircraft bushings

VESPEL parts earned their wings the hard way, replacing bronze bushings inside jet engines at 650°F. Today, they're outperforming metals and other materials in hundreds of applications. Just a small handful are shown and listed below.

- Spline couplings
- Electrical coil bobbins
- Thrust washers
- Standard balls for check valves
- Glide blocks
- Flanged bushings
- Split bushings
- Insulating bushings
- Rubbing blocks
- Insulators
- Brake shoes

"Think VESPEL" on your next design

When your product calls for performance *and* economy, do the smart thing—come to Du Pont for VESPEL parts, and all the help that comes with them. Just call 800-527-2601, or complete the coupon below.

DU PONT

REG. U.S. PAT. & TM OFF

Du Pont Company • VESPEL, Room X50272-DN • Wilmington, DE 19898

Please send free literature on VESPEL parts.

Name__________ Title__________

Company__________

Address__________

City__________ State__________ Zip__________

Phone__________ Industry/Application__________

Circle Reader Action No. 582

NASA Tech Briefs
National Aeronautics and Space Administration

MARCH 1988
Volume 12 Number 3

ABP BPA

SPECIAL FEATURES

TECHNICAL SECTION

Results from flight tests of the X-29A airplane (above) at the NASA Western Aeronautical Test Range in California are transmitted via satellite to the Grumman Aerospace Corp. in New York, allowing Grumman's research team to participate in tests as they occur. See page 26.

DEPARTMENTS

This issue's technical section features new research in the field of fiber optics. See pages 20, 58, and 70. *(Photo courtesy Corning Glass Works, Corning, NY)*

ON THE COVER: This fused quartz coil helps heat a thermal analysis system recently introduced by Texas-based Ruska Instrument Corporation. The system's heating chambers are insulated with thermal tiles originally developed for NASA's Space Shuttle. The tiles provide protection at up to 1482°C. For more on this Mission Accomplished story, turn to page 12. *(Photo courtesy NASA)*

NASA Tech Briefs, ISSN 0145-319X, USPS 750-070, copyright © 1988 in U.S., is published monthly except July/August and November/December (10x per year) by Associated Business Publications Co., Ltd. 41 E. 42nd St., New York, NY 10017-5391. The copyrighted information does not include the individual Tech Briefs which are supplied by NASA. Editorial, sales, production and circulation offices at 41 E. 42nd Street, New York, NY 10017-5391. Subscriptions for non-qualified subscribers in the U.S., Panama Canal Zone, and Puerto Rico, $75.00 for 1 year; $125.00 for 2 years; $200 for 3 years. Single copies $15.00. Remit by check, draft, postal or express orders. Other remittances at sender's risk. Address all communications for subscriptions or circulation to NASA Tech Briefs, 41 E. 42nd Street, New York, NY 10017-5391. Second-class postage paid at New York, NY and additional mailing offices.

POSTMASTER: please send address changes to NASA Tech Briefs, 41 E. 42nd Street, Suite 921, New York, NY 10017-5391.

Project #8: Building a two-channel fiber optics communications link.

Learn, Apply, Advance Fiber Optics

Start with the basics, or explore today's most advanced applications with Newport's new Fiber Optic Projects Kit for teachers, students and engineers.

Newport's **Projects in Fiber Optics** was developed by professional éducators and researchers to help you acquire state-of-the-art skills and hands-on experience.

Ten applications-oriented projects will lead you from optical fiber fundamentals and on to explore advanced applications, such as interferometric sensors and data communication.

The projects can be ordered individually or in sets, making **Projects in Fiber Optics** ideal both as an elective course for students and as an efficient independent study program for engineers.

Each Kit Includes...

- **A complete set of research-quality equipment:** Light sources, fibers, detectors, optics and optomechanical components.
- **Informative Applications Handbook:** Clear, complete, illustrated step-by-step lab guide including theory and references.

By project completion, you will be able to use the same equipment with other compatible Newport components to explore new areas of interest. What better way to start a fiber optics lab?

Call our technical staff for more information and send for your free copy of Newport's new 400 page catalog of other fiber optics equipment and electro-optics components.

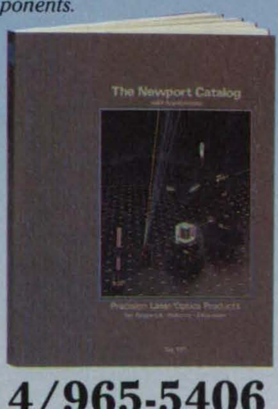

714/965-5406

18235 Mt. Baldy Circle
Fountain Valley, CA 92708
IN EUROPE; Newport GmbH: 06151-26116
IN UK; Newport Ltd: 05827-69995

Circle Reader Action No. 540

Newport Corporation

NASA Tech Briefs

National Aeronautics and Space Administration

NASA Tech Briefs:

Published by .... Associated Business Publications
Editor-in-Chief/Publisher .... Bill Schnirring
Associate Publisher .... Frank Nothaft
Associate Publisher .... Robin J. DuCharme
Managing Editor .... R. J. Laer
Associate Editor .... Joseph T. Pramberger
Technical Advisor .... Dr. Robert E. Waterman
Production Manager .... Rita Nothaft
Traffic Manager .... James E. Cobb
Circulation Director .... Anita Weissman
Controller .... Neil B. Rose
Awards Manager .... Evelyn Mars
Reader Service Manager .... Arlene Berrios

Technical Staff:

Briefs prepared for National Aeronautics and Space Administration by **Logical Technical Services Corp.**, NY, NY

Technical/Managing Editor .... Ted Selinsky
Art Director .... Ernest Gillespie
Administrator .... Elizabeth Texeira
Chief Copy Editor .... Lorne Bullen
Staff Editors .... Dr. James Boyd, Dr. Larry Grunberger, Jordan Randjelovich, George Watson, Oden Browne, Joseph Renzler, Dr. Theron Cole, Jr.
Graphics .... Luis Martinez, Vernald Gillman, Charles Sammartano
Editorial & Production .... Bill Little, Frank Ponce, Ivonne Valdes, Paul Marcus

ABP BPA

NASA:

NASA Tech Briefs are provided by the National Aeronautics and Space Administration, Technology Utilization Division, Washington, DC:

Administrator .... Dr. James C. Fletcher
Assistant Administrator for Commercial Programs .... James T. Rose
Deputy Assistant Administrator (Programs) .... Henry J. Clarks
Deputy Director TU Division (Publications Manager) .... Leonard A. Ault
Manager, Technology Utilization Office, NASA Scientific and Technology Information Facility .... Walter M. Heiland

Associated Business Publications
41 East 42nd Street, Suite 921, New York, NY 10017-5391
(212) 490-3999 FAX (212) 986-7864

President .... Bill Schnirring
Executive Vice President .... Frank Nothaft
Vice President Marketing .... Mark J. Seltman

Advertising:
New York Office: (212) 490-3999

Sales Manager .... Robin DuCharme
Account Executive (Mid-Atlantic) .... Dick Soule
Account Executive (Midwest) .... Michelle Larsen
Marketing Research Manager .... Leo D. Kluger
Advertising Coordination Manager .... Erving Dockery, Jr.
Account Executives (Eastern MA, NH, ME, RI) .... Lee Arpin at (617) 899-5613; Bill Doucette at (617) 278-7792
Account Executive (Western MA, CT, VT) .... George Watts at (413) 596-4747
Account Executives (No. Calif., UT) .... for Area Code 415—Janice Richey King and for Area Code 408—Richard Cassidy at (415) 656-3613
Account Executives (So. Calif., AZ, NV, NM) .... for Area Codes 818/213/805—Thomas Stillman or Dana Gindoff and for Area Codes 619/714—Leslie Alley at (213) 541-4699

NTBM-Research Center

Project Director .... Mark J. Seltman
Account Supervisor .... Lourdes Del Valle

NASA has submitted to Congress an $11.48 billion budget request for Fiscal 1989, a $2.46 billion increase over 1987. The proposed budget includes $967 million for the full-scale development of Space Station, $100 million for the new Pathfinder program designed to develop technology for future manned lunar and Mars missions, and $88 million for development of an advanced Space Shuttle solid rocket motor, which would increase Shuttle payload by 15,000 pounds. According to NASA Administrator Dr. James C. Fletcher, the increased budget is a vital step in carrying out President Reagan's new national space policy, announced February 11, which sets NASA on a course toward development of a manned lunar base and extensive solar system exploration.

NASA will receive real-time remote sensing data from Japan's Earth Resources Satellite (ERS-1) under terms of an agreement recently signed by NASA Administrator Dr. James C. Fletcher and Hiroyuki Osawa, President of the National Space Development Agency of Japan (NASDA). Data from the ERS-1 synthetic aperature radar and optical sensor will be transmitted to a ground station at the University of Alaska, Fairbanks. The ERS-1 is scheduled to be launched by NASDA in early 1992.

Andrew J. Stofan, Associate Administrator for Space Station, will retire from NASA on April 1. Stofan, 53, said he has met the objectives he set when appointed to the Space Station management position in June, 1986. "We have the management team in place, the development and support contractors are on board, the international negotiations are in their final stages, and the President has submitted a one billion dollar budget for the next fiscal year," stated Stofan. "The program is on track now and it's an appropriate time to retire from government."

Canada is the first international partner to reach agreement on its participation in Space Station. Negotiators from NASA and the Canadian government agreed on a memorandum calling for Canada to provide a robot arm for use in assembly and maintenance of the station. In exchange, Canada will participate in management of Space Station, and Canadian researchers will have access to the facility's full capabilities. The next step is formal approval of the agreement by the two governments. NASA is also negotiating with Japan and the European Space Agency.

NASA will sponsor feasibility studies on launching unmanned scientific spacecraft to better understand black holes, quasars, nucleosynthesis solar particles, and unexplored layers of the Earth's atmosphere. Costing between $100,000 and $400,000 each, the four studies are part of the Explorer Concept Program, designed to develop intermediate-size space experiments.

"Space Challenge '88," the Fourth National Space Symposium sponsored by the United States Space Foundation, will be held April 12-15 in Colorado Springs, CO. Scheduled speakers include NASA Administrator Dr. James C. Fletcher, Dr. James Abrahamson, Director of the Strategic Defense Initiative Organization, and Dr. David Webb, a member of the National Commission on Space.

CONTRACT AWARDS

Calspan Corp., Buffalo, N.Y.: $52,622,508—for operation, maintainance, and engineering support of aerodynamic test calibration and support services at Ames Research Center;

Wyle Laboratories, Scientific Services and Systems Group, Hampton,VA: $45,365,000—from Langley Research Center for instrument support services;

McDonnell Douglas Corp., Houston, TX: $18,743,808—for applications and analysis support at Johnson Space Flight Center;

Ford Aerospace, Houston, TX: $11,755,921—from Johnson Space Flight Center for advanced digital avionics system support for Space Shuttle training aircraft.

Mission Accomplished

A NASA Spinoff Cools The Fire

Fresh from a 1316°C oven, the glowing cube provides the only illumination in this photo.

Glowing white-hot, a ceramic cube is extracted from a 1316 degree Centigrade oven. Seconds later, an engineer grasps the cube in his bare hand—without injury. Amazingly, the cube's surface has already cooled to room temperature. This demonstration by a Lockheed Missiles and Space Company engineer illustrates the lightning speed with which heat is dissipated by a silica fiber material developed by Lockheed for NASA's Space Shuttle thermal protection system. Combining the low thermal conductivity of fiber board with the compressive strength of insulating fire brick, the silica material can withstand temperatures exceeding 1482°C.

The silica insulation evolved from years of research aimed at finding a reusable form of spacecraft heat shield. Before the Space Shuttle, protection from the searing heat of reentry was provided by ablative shields that burned away as the spacecraft plunged earthward. But the Shuttle required insulation that would repeatedly handle the 1260°C reentry heat without shrinking or melting. The answer: the silica fiber "thermal tile" (later modified to include alumina fiber and boron nitride powder for greater thermal strength) which could be cut into some 34,000 shapes and fitted to the Orbiter's underside. By dissipating over 90 percent of the Shuttle's surface heat, the tiles ensure that the temperature of the craft's aluminum frame never exceeds 177°C.

This extraordinary insulating capability has led to the thermal tile's use in a new spinoff application: the PYRAN™ System, manufactured by Ruska Instrument Corporation, Houston, Texas. Designed for thermal analysis of the composition of organic matter, the system employs fused quartz for infrared heating of samples up to 610°C.

"To achieve precise control and repeatability at high temperatures, we needed a special material to insulate the heating chambers," explained Douglas King, a Ruska spokesman. "None of the commercially available products met our requirements, so we turned to NASA."

After meeting with Lockheed and NASA Kennedy Space Center thermal experts, Ruska scientists decided the Shuttle ceramic tiles would solve their difficult insulation problem. "The material's temperature stability was very impressive," said Mr. King. "Also, we found the tile easy to cut into various shapes to fit around our quartz components.

"The thermal tiles have given us exactly the high performance insulation we were looking for," King added.

Initial sales of the PYRAN System were to petroleum industry laboratories for analysis of geochemical samples. The product's market has since expanded to general analytical laboratories for analysis and quality control of such items as polymers, cosmetics, pharmaceuticals, and foods. Current customers include the Philip Morris Company, using the system to analyze tobacco samples, and Louisiana State University's Institute for Environmental Studies, utilizing PYRAN for hazardous waste analysis.

While Ruska's successful reapplication of the silica tile has sparked further industry interest, mass marketing the tile will "only be feasible if major changes are made in the manufacturing process," according to Dr. John Cleland, Manager of Industrial Applications at NASA's North Carolina Science and Technology Research Center. Because each tile is precision-machined, he explained, "the production cost is simply too expensive for many potential applications." How expensive? A single six inch square tile, depending upon its thickness, can cost up to $7000.

One possible solution is injection-molding. "Pumping the ceramic material into a mold would help increase production while at the same time significantly lowering costs," Cleland said.

Dr. Cleland also recommends relaxing stringent quality control methods for commercial production. "There are currently about 180 steps in the manufacturing process, due to the high level of purity and homogeneity required for space use," he said. "Many of these steps could be eliminated in mass production and you'd still have a superior high-temperature insulating material."

Fragility is yet another barrier to commercialization. "In their present form, the tiles are too brittle for widespread application," stated Cleland, who recommends densification of the fibers for the commercial market. The material could then be molded into such items as aprons, beakers, and protective gloves.

"There's a whole untapped market out there," said Cleland. "Though there are numerous low-cost silica insulation products available, they don't go to nearly as high a temperature (as the tile). The thermal tile is a unique item." □

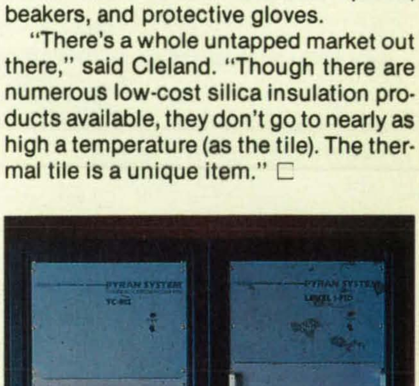

The PYRAN System consists of two independent instruments: the Thermal Chromatograph™—Mass Spectrometer analyzer (left), and the Level 1—FID (Flame Ionization Detector) analyzer (right); both precisely heat solid materials in order to rapidly quantify, separate, and identify thermally evolved organic compounds. The system is controlled by an IBM PC/AT or compatible.

New Product Ideas

New Product Ideas are just a few of the many innovations described in this issue of *NASA Tech Briefs* and having promising commercial applications. Each is discussed further on the referenced page in the appropriate section in this issue. If you are interested in developing a product from these or other NASA innovations, you can receive further technical information by requesting the TSP referenced at the end of the full-length article or by writing the Technology Utilization Office of the sponsoring NASA center (see page 16). NASA's patent-licensing program to encourage commercial development is described on page 16.

Rotation Control in a Cylindrical Acoustic Levitator

Containerless processing is enhanced by the addition of a second acoustical transducer to a single-mode, cylindrical acoustic levitator that can now rotate a levitated sample in a controlled manner. The torque is increased simply by increasing the amplitude in the second transducer. (See page 67).

Carboranylmethylene-Substituted Cyclophosphazene Polymers

A new class of polymers is based on cyclophosphazene monomers substituted with carboranylmethylene groups. This synthesis opens up a development of such new products as thermally stable coatings, catalysts, fibers, films, moldings, and solvent-swelled gels. (See page 46).

Tool Protects Internal Threads During Rework

A tool that fits into a threaded hole protects useful thread from damage while unwanted thread is ground or machined. The tool also prevents contamination by collecting the machining debris. (See page 68).

Flexible Protective Shield for Newly Welded Joints

A simple device promotes defect-free welds in oxidation-prone metals. Built to trail a welding torch, the shield follows the contours of the weld joint and protects hot-metals from oxygen of the surrounding air until the weld bead has cooled. (See page 69).

Real-Time X-Ray Inspection

An x-ray imaging instrument adapted to continuous scanning is based on the Lixiscope, a low-intensity x-ray imaging scope that converts the pattern of x rays transmitted through the specimen into a visible-light image. This image is intensified and can be viewed directly, photographed, recorded on videotape, or coupled to other imaging devices. (See page 70).

Fixture for Polishing Optical-Fiber Ends

A new fixture simplifies precise shaping and polishing of optical fiber ends needed for efficient coupling between the injected laser and the fiber. This fixture assures precise cutting of end-polished fibers into specific depths and angles and provides accurate repeatability during the polishing process. (See page 70).

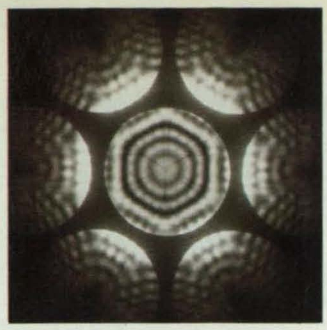

Boeing hired Dr. Hari Narayanan to do some of its most demanding materials analysis work.

So can you.

Dr. Narayanan ranks among the leading experts in his field. And the 62,000-square-foot Boeing Materials Technology Laboratory where he works is among the best anywhere.

This level of talent and these facilities are available to you through Boeing Technology Services. Our job is to help other companies and research organizations make profitable use of Boeing resources.

When it comes to materials engineering, we have a full range of services including prototype and process development, testing, and detailed materials analysis. Typical projects include manufacturing and repair process development, specification development, materials qualification, failure analysis and project research and development.

We have experience in a broad range of materials — metals, composites, finishes, sealants, fluids, lubricants, textiles and more.

For more information, call Paula Royalty, Marketing Manager at (206) 277-4600. Or write to Boeing Technology Services, P.O. Box 3707, M/S 9R-28, Seattle, WA 98124-2207.

BOEING

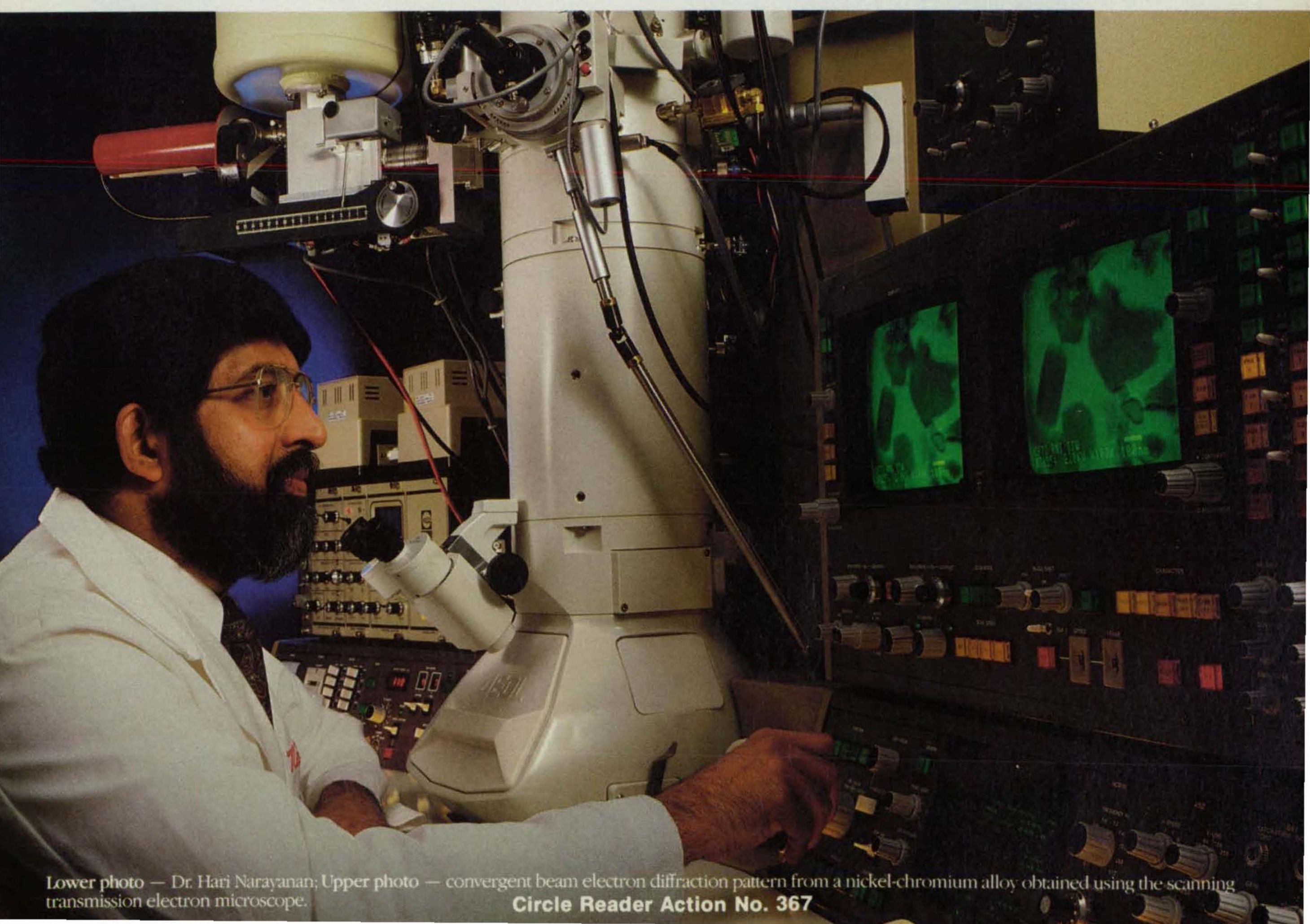

Lower photo — Dr. Hari Narayanan; Upper photo — convergent beam electron diffraction pattern from a nickel-chromium alloy obtained using the scanning transmission electron microscope.

HOW YOU CAN BENEFIT FROM NASA's TECHNOLOGY UTILIZATION SERVICES

If you're a regular reader of TECH BRIEFS, then you're already making use of one of the low- and no-cost services provided by NASA's Technology Utilization (TU) Network. But a TECH BRIEFS subscription represents only a fraction of the technical information and applications/engineering services offered by the TU Network as a whole. In fact, when all of the components of NASA's Technology Utilization Network are considered, TECH BRIEFS represents the proverbial tip of the iceberg.

We've outlined below NASA's TU Network—named the participants, described their services, and listed the individuals you can contact for more information relating to your specific needs. We encourage you to make use of the information, access, and applications services offered by NASA's Technology Utilization Network.

How You Can Utilize **NASA's Industrial Applications Centers**—A nationwide network offering a broad range of technical services, including computerized access to over 100 million documents worldwide.

You can contact NASA's network of Industrial Applications Centers (IACs) for assistance in solving a specific technical problem or meeting your information needs. The "user friendly" IACs are staffed by technology transfer experts who provide computerized information retrieval from one of the world's largest banks of technical data. Nearly 500 computerized data bases, ranging from NASA's own data base to Chemical Abstracts and INSPEC, are accessible through the nine IACs located throughout the nation. The IACs also offer technical consultation services and/or linkage with other experts in the field. You can obtain more information about these services by calling or writing the nearest IAC. User fees are charged for IAC information services.

Aerospace Research Applications Center (ARAC)
Indianapolis Center for Advanced Research
611 N. Capitol Avenue
Indianapolis, IN 46204
Dr. F. Timothy Janis, Director
(317) 262-5036

Central Industrial Applications Center/NASA (CIAC)
Southeastern Oklahoma State U.
Station A, Box 2584
Durant, OK 74701
Dr. Dickie Deel, Director
(405) 924-6822

North Carolina Science and Technology Research Center (NC/STRC)
Post Office Box 12235
Research Triangle Park, NC 27709
J. Graves Vann, Jr., Director
(919) 549-0671

NASA Industrial Applications Ctr. 823 William Pitt Union
University of Pittsburgh
Pittsburgh, PA 15260
Dr. Paul A. McWilliams, Exec. Director
(412) 648-7000

NASA/Southern Technology Applications Center
P. O. Box 24
Progress Ctr., One Progress Blvd.
Alachua, FL 32615
J. Ronald Thornton, Director
(904) 462-3913
(800) 354-4832 (FL only)
(800) 225-0308 (toll-free US)

NASA/UK Technology Applications Center
University of Kentucky
109 Kinkead Hall
Lexington, KY 40506-0057
William R. Strong, Director
(606) 257-6322

NERAC, Inc.
One Technology Drive
Tolland, CT 06084
Dr. Daniel U. Wilde, President
(203) 872-7000

Technology Application Center (TAC)
University of New Mexico
Albuquerque, NM 87131
Dr. Stanley A. Morain, Director
(505) 277-3622

NASA Industrial Applications Center (WESRAC)
University of Southern California Research Annex
3716 South Hope Street, Room 200
Los Angeles, CA 90007
Radford G. King, Exec. Director
(213) 743-8988
(800) 642-2872 (CA only)
(800) 872-7477 (toll-free US)

NASA/SU Industrial Applications Center
Southern University Department of Computer Science
Baton Rouge, LA 70813
Dr. John Hubbell, Director
(504) 771-2060

If you represent a public sector organization with a particular need, you can contact NASA's Application Team for technology matching and problem solving assistance. Staffed by professional engineers from a variety of disciplines, the Application Team works with public sector organizations to identify and solve critical problems with existing NASA technology. **Technology Application Team, Research Triangle Institute, P.O. Box 12194, Research Triangle Park, NC 27709. *Doris Rouse, Director*, (919) 541-6980**

How You Can Access Technology Transfer Services At NASA Field Centers: **Technology Utilization Officers & Patent Counsels**—Each NASA Field Center has a Technology Utilization Officer (TUO) and a Patent Counsel to facilitate technology transfer between NASA and the private sector.

If you need further information about new technologies presented in *NASA Tech Briefs*, request the Technical Support Package (TSP). If a TSP is not available, you can contact the Technology Utilization Officer at the NASA Field Center that sponsored the research. He can arrange for assistance in applying the technology by putting you in touch with the people who developed it. If you want information about the patent status of a technology or are interested in licensing a NASA invention, contact the Patent Counsel at the NASA Field Center that sponsored the research. Refer to the NASA reference number at the end of the Tech Brief.

Ames Research Ctr.
Technology Utilization Officer: Laurance Milov
Mail Code 223-3
Moffett Field, CA 94035
(415) 694-6471
Patent Counsel: Darrell G. Brekke
Mail Code 200-11
Moffett Field, CA 94035
(415) 694-5104

Lewis Research Center
Technology Utilization Officer: Daniel G. Soltis
Mail Stop 7-3
21000 Brookpark Road
Cleveland, OH 44135
(216) 433-5567
Patent Counsel: Gene E. Shook
Mail Code 301-6
21000 Brookpark Road
Cleveland, OH 44135
(216) 433-5753

National Space Technology Laboratories
Technology Utilization Officer: Robert M. Barlow
Code GA-00
NSTL Station, MS 39529
(601) 688-1929

John F. Kennedy Space Center
Technology Utilization Officer: Thomas M. Hammond
Mail Stop PT-TPO-A
Kennedy Space Center, FL 32899
(305) 867-3017
Patent Counsel: James O. Harrell
Mail Code PT-PAT
Kennedy Space Center, FL 32899
(305) 867-2544

Langley Research Ctr.
Technology Utilization Officer: John Samos
Mail Stop 139A
Hampton, VA 23665
(804) 865-3281
Patent Counsel: George F. Helfrich
Mail Code 279
Hampton, VA 23665
(804) 865-3725

Goddard Space Flight Center
Technology Utilization Officer: Donald S. Friedman
Mail Code 702
Greenbelt, MD 20771
(301) 286-6242
Patent Counsel: R. Dennis Marchant
Mail Code 204
Greenbelt, MD 20771
(301) 286-7351

Jet Propulsion Lab.
NASA Resident Office
Technology Utilization Officer: Gordon S. Chapman
Mail Stop 180-801
4800 Oak Grove Drive
Pasadena, CA 91109
(818) 354-4849
Patent Counsel: Paul F. McCaul
Mail Code 180-801
4800 Oak Grove Drive
Pasadena, CA 91109
(818) 354-2734
Technology Utilization Mgr. for JPL: Norman L. Chalfin
Mail Stop 156-211
4800 Oak Grove Drive
Pasadena, CA 91109
(818) 354-2240

George C. Marshall Space Flight Center
Technology Utilization Officer: Ismail Akbay
Code AT01
Marshall Space Flight Center, AL 35812
(205) 544-2223
Patent Counsel: Leon D. Wofford, Jr.
Mail Code CC01
Marshall Space Flight Center, AL 35812
(205) 544-0024

Lyndon B. Johnson Space Center
Technology Utilization Officer: Dean C. Glenn
Mail Code EA4
Houston, TX 77058
(713) 483-3809
Patent Counsel: Edward K. Fein
Mail Code AL3
Houston, TX 77058
(713) 483-4871

NASA Headquarters
Technology Utilization Officer: Leonard A. Ault
Code CU
Washington, DC 20546
(202) 453-2119
Assistant General Counsel for Patent Matters: Robert F. Kempf, Code GP
Washington, DC 20546
(202) 453-2424

A Shortcut To Software: **COSMIC®**—For software developed with NASA funding, contact COSMIC, NASA's Computer Software Management and Information Center. New and updated programs are announced in the Computer Programs section. COSMIC publishes an annual software catalog. For more information call or write: **COSMIC®**, 382 East Broad Street, Athens, GA 30602 *John A. Gibson, Dir.*, (404) 542-3265

If You Have a Question... **NASA Scientific & Technical Information Facility** can answer questions about NASA's Technology Utilization Network and its services and documents. The STI staff supplies documents and provides referrals. Call, write or use the feedback card in this issue to contact: **NASA Scientific and Technical Information Facility,** Technology Utilization Office, P.O. Box 8757, Baltimore, MD 21240-0757. *Walter M. Heiland, Manager,* (301) 859-5300, Ext. 242, 243


Never out of uniform.
GAF CARBONYL IRON POWDERS
GAF's Carbonyl Iron Powder particles are spherical in shape and, within any given group, uniform in size distribution, from 2 microns to 10 microns.
The only ones that are domestically manufactured, GAF's Carbonyl Iron Powders find ready and broad utility in the aerospace industry in coatings and advanced composites. In addition, their wide range of uniform particle sizes, excellent high frequency absorption, and electromagnetic interference properties recommend them for use in other aerospace applications as well.
GAF's Carbonyl Iron Powders get along famously with plastic resins, and other metals & alloys, too, like tungsten, copper and bronze. Composites with improved properties are made more easily and economically, usually with no need for additional pre-processing.
If you think GAF's Carbonyl Iron Powders may fit into your plans, our Advanced Technology and Materials Group is available for developmental work on customers' aerospace applications.
All iron powders may look the same. But GAF Carbonyl Iron Powders are always in uniform.
See for yourself. For a free sample and literature, call or write: GAF Chemicals Corporation, Organometallics and Metals Group, 1361 Alps Road, Wayne, NJ 07470. (201) 628-3000.
©Copyright 1987 GAF Chemicals Corporation
GAF®
Where specialties are on the move
Circle Reader Action No. 404

Electronic Components & Circuits

Hardware Techniques, and Processes

Pulse Coil Tester

A set of relays can be tested easily and repeatedly.

Marshall Space Flight Center, Alabama

A testing circuit helps to identify short circuits in relay coils or similar inductors. The tester (see figure) applies a gradual current pulse to each coil, then suddenly turns it off; this causes the coil to emit a transient high voltage, the waveform of which can be viewed on an oscilloscope or recorded. The waveform of the tested coil can then be analyzed and compared with the waveform of a reference coil or with a previous waveform from the tested coil, to determine whether the tested coil has developed any shorted turns.

Under the overall control of a timing circuit, the current pulses are applied at a repetition rate of 7.14 Hz. Just before each pulse, a relay switch in the tester connects the tester to the coil. After a 5.25-ms delay that allows for the closure of the relay, an integrating circuit generates a voltage that ramps to −6.2 V in 21.8 ms and is then held at −6.2 V by a Zener diode: this voltage waveform controls a current-generating circuit that applies to the coil a similar current waveform that ramps up and is held steady at 35 mA.

Next, the relay switch is disconnected from the coil. The resulting inductive transient voltage is fed through a 100:1 attenuator and a buffer amplifier to the oscilloscope or other suitable monitor. After a delay of 5.25 ms that allows for the opening of the relay, the integrating circuit is reset for the next current pulse.

The tester can accommodate an assembly of up to four coils at a time. One pole of a double-pole, quadruple-throw rotary switch selects one of four relays,

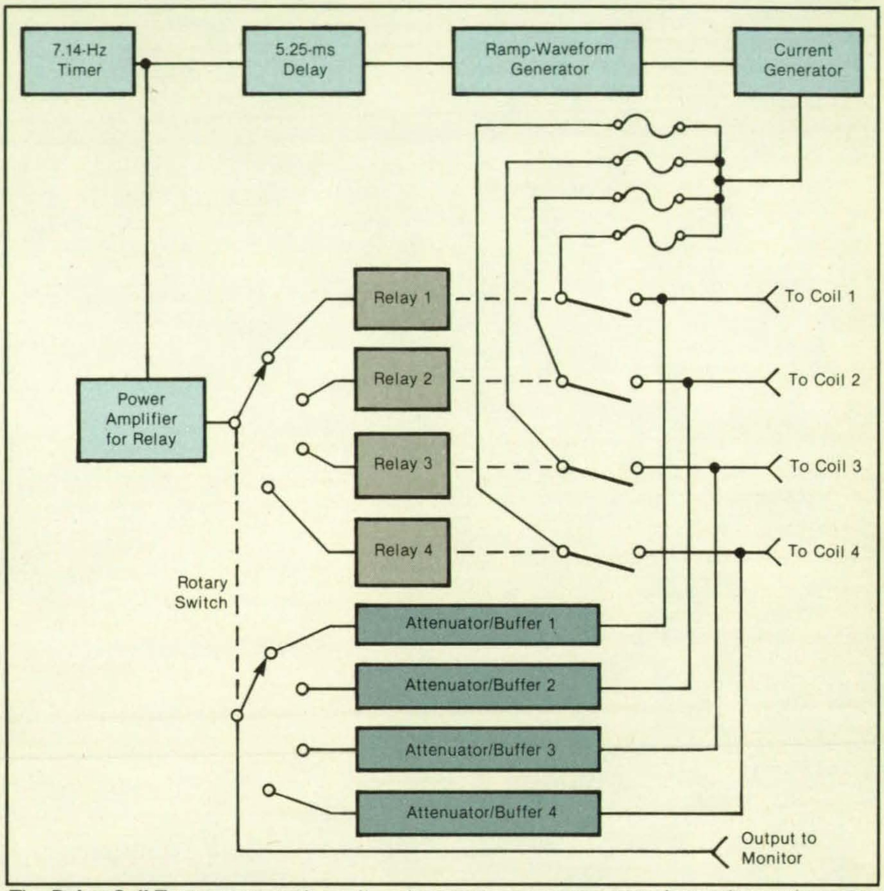

The **Pulse Coil Tester** causes the coil under test to generate a transient voltage, the waveform of which indicates the condition of the coil.

each of which is connected to one of the coils to be tested. The other pole connects the attenuator/buffer for that coil to the output connector.

A total short circuit across a coil does not harm the tester: the current generator is designed to supply the current at the regulated 35-mA value while dissipating the excess power. Additional "fallback" protection against overcurrent in the coil is supplied by resistors in the current generator, by the power supply, and by a 100-mA fast-blow fuse in series with each tested coil.

This work was done by Richard A. Simon of Rockwell International Corp. for **Marshall Space Flight Center**. *For further information, Circle 151 on the TSP Request Card.*

Inquiries concerning rights for the commercial use of this invention should be addressed to the Patent Counsel. Marshall Space Flight Center [see page 16]. Refer to MFS-29301.

MOSFET Electric-Charge Sensor

A charged-particle probe would be compact and would consume little power.

NASA's Jet Propulsion Laboratory, Pasadena, California

A proposed modification would enable a metal oxide/semiconductor field-effect transistor (MOSFET) to act as a detector of static electric charges or energetic charged particles. Because MOSFET's are smaller than conventional electrostatic probes and consume less power, a MOSFET probe of the new type might be useful in compact, lightweight equipment

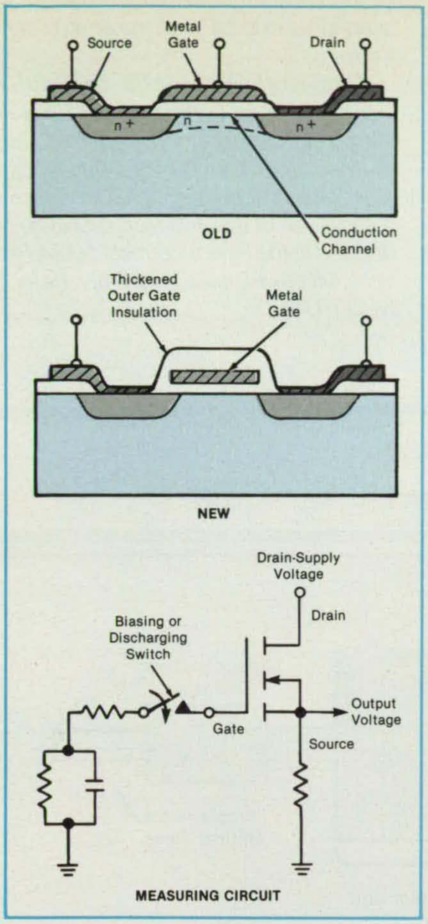

Figure 1. In the **Modified MOSFET**, the thickened gate insulation would act as the control structure. During measurements the metal gate would be allowed to "float" (in an electrostatic sense) to the potential of the charge accumulated in the insulation.

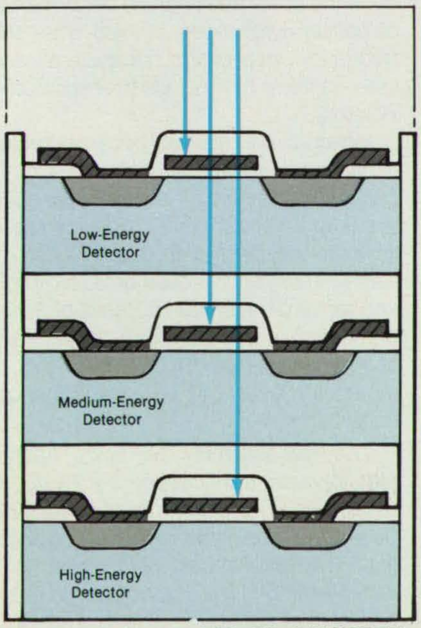

Figure 2. A **Stack of Modified MOSFET's** would constitute a detector of energetic charged particles. Each gate would "float" to the potential induced by the charged-particle beam that would penetrate its layer.

for monitoring charges on the surfaces and in the interiors of dielectrics, mapping strong electrostatic fields, or measuring the penetration of ionizing radiation through material layers.

The modification (see Figure 1) is a thickening of the insulating, passivating layer over the gate from the conventional depth of about 1 μm to a new depth (typically, 2 to 20 μm) that favors the accumulation of electric charges. Either permanently or during measurement periods, the gate would be electrically isolated so that it would float to a potential determined by the accumulated charge.

The gate potential would affect the electric field in the MOSFET conduction channel and could therefore be used to control the drain and source currents. With the source and drain connected in the source-follower configuration, the voltage at the source terminal would provide a convenient, low-impedance signal indicative of the accumulated charge.

By the choice of the initial gate bias, the MOSFET can be placed in the enhancement or the depletion mode. The voltage superimposed on the bias by the subsequent accumulation of charge could thus be made to increase or decrease the conductivity of the channel. The polarities can also be reversed: instead of the negative-channel MOSFET shown here, a positive-channel MOSFET can be formed by interchanging the positive and negative doping.

At the end of the measuring interval, the metal gate could be reconnected to the bias-voltage source or to ground to remove the accumulated measured charge. The gate could also be connected to a voltage source for calibration or checking.

A MOSFET of the new type could be placed inside a larger insulator to measure the internal electrostatic field or the density or flux of charged particles. The MOSFET could be embedded in a dielectric object with its gate structure acting as a sampling area of the surface to measure the surface charge.

A spectrometer for energetic charged particles could be built by stacking several of the new MOSFET's. In the example of Figure 2, the top transistor would be made with an aluminum gate to trap low-energy charges. Medium-energy charges would penetrate to the middle transistor, which would have an iron gate. Charges of higher energy would penetrate to the gold gate in the bottom transistor. Stacks with more or fewer transistors and different gate metals could be constructed, depending on the required transparency or opacity to particles of various energies and the resolution desired in various parts of the energy spectrum.

This work was done by Paul A. Robinson, Jr., of Caltech for **NASA's Jet Propulsion Laboratory**. *For further information, Circle 93 on the TSP Request Card.*

Inquiries concerning rights for the commercial use of this invention should be addressed to the Patent Counsel, NASA Resident Office-JPL [see page 16]. Refer to NPO-16045.

Optical Isolator for Use With Single-Mode Fiber

Unusually-low forward-transmission loss and high reverse-transmission loss are achieved.

NASA's Jet Propulsion Laboratory, Pasadena, California

An assembly of commercially available components acts as a signal isolator for a single-mode optical fiber. The degree of isolation (that is, the attenuation of signals traveling in the opposite of the intended direction along the fiber) is approximately that of two previously-commercially-available optical isolators in series. Because such isolators cost about $3,000 apiece (1986 prices), the new design should reduce the costs and improve performance of optical gyroscopes, precise time- and frequency-signal-distribution systems, and other systems that include fiber optics and isolators.

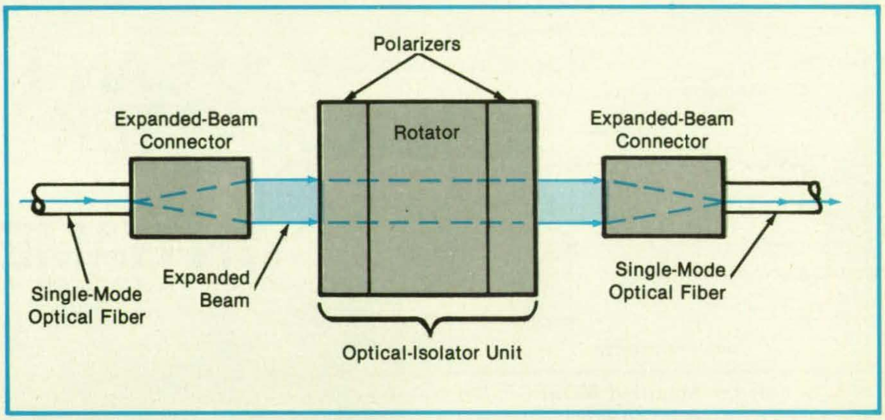

The **Assembly of Commercially Available Components** acts as a single-mode fiber-optic isolator with lower forward-transmision loss and higher attenuation of reverse transmission than were previously achieved in a single such unit.

Isolators are needed because reflections cause intolerable instabilities (e.g., changes in frequency) in some fiber-optic systems. The best single-mode fiber-optic isolators previously available exhibited reverse-transmission losses of 30 to 40 dB and forward-transmission losses of 3 to 4 dB per unit. It was necessary to place two such units in series to obtain the isolation of more than 60 dB required in some fiber-optic systems.

The new assembly (see figure) attenuates reverse transmission by 70 dB or more, while imposing a loss of only 2.6 dB on signals transmitted in the forward direction. The single-mode input signal, at a wavelength of 1.3 μm, is coupled in along one of two fiber-optic pigtails. The input light beam is expanded by lenses in an expanded-beam single-mode fiber-optic connector. The expanded beam passes through a 4-mm-aperture optical-isolator unit that contains two polarizers and a rota-

A CALL TO ACTION
SPACE CHALLENGE '88
SUMMIT MEETING ON SPACE
THE FOURTH NATIONAL SPACE SYMPOSIUM
April 12-15, 1988
BROADMOOR HOTEL
COLORADO SPRINGS, CO
Attend the Space Technology Hall of Fame Dinner, Wednesday, April 13. Call today: (719) 550-1000
We . . . know the price of being a world leader includes a willingness to live and work at the cutting edge of technology; to create new scientific economic and personal opportunities for growth. For this generation, that cutting edge is in space.
From "Open Letter to the Nation" by Astronauts Alan Shepard, Deke Slayton, Gene Cernan, Walter Cunningham, Alan Bean and Joseph Allen
Our Space Program is a shambles. We have got to be responsible for that, because ultimately we are the people who must impress the politicians that the Space Program not only deserves more and deserves better, but is vital to the future development and orientation of this nation.
Dr. David Webb, National Commission on Space, in an address to the Third National Space Symposium, January 1987
With our future as a great nation at stake, this country cannot continue its present course for space development. We must regain the space stimulus to technology advancement—to national productivity—to international competitiveness.
THE CHALLENGE DEMANDS YOUR PARTICIPATION.
Join the key space policy makers at the 4th National Space Symposium, April 12-15, 1988.
Art Direction, Design and Illustration donated by Howard E. Cook, dba Airworks, 7500 Shadow Bay Drive, Callaway, Florida 32404 904/871-4428. Airworks offers complete services from concept to final product in design, illustration and fine art for the Space/Aerospace Industry. ©1988
UNITED STATES SPACE FOUNDATION
P.O. BOX 1838
COLORADO SPRINGS, CO 80901
303/550-1000
Circle Reader Action No. 586

tor, then passes out into the other pigtail through a fiber-optical connector like that at the input end.

The degree of isolation would ordinarily be limited by scattering due to internal reflections in the isolator unit because the polarization of scattered light is not in the direction required for high attenuation. The nonuniformity of the polarizers across their diameters would also ordinarily reduce the degree of isolation. However, both effects are counteracted by the expanded-beam fiber-optical connectors, which have a small aperture (expanded-beam diameter of 1.5 mm) and strongly attenuate scattered light more than a few milliradians off axis.

This work was done by George F. Lutes of Caltech for **NASA's Jet Propulsion Laboratory**. *For further information, Circle 16 on the TSP Request Card.*

This invention is owned by NASA, and a patent application has been filed. Inquiries concerning nonexclusive or exclusive license for its commercial development should be addressed to the Patent Counsel, NASA Resident Office-JPL [see page 16]. Refer to NPO-17207.

"Thumball" Auxiliary Data-Input Device

A track-ball-type device is mounted on a joystick and operated by a thumb.

Langley Research Center, Hampton, Virginia

The Thumball is designed to enable the precise input of data about two different axes to an autopilot, avionics computer, or other electronic device without the need for the operator to remove his or her hands from the joystick or other vehicle control levers.

The Thumball mechanism (see figure) includes a ball retained in a socket in the end of the control handle in such a way that it is free to rotate. Two rollers are pressed by spring-loaded bearings against the ball at points 90° apart about its circumference. As the ball is turned by the operator's thumb, friction drives the two rollers and their respective disks through angles proportional to the rotation of the ball about its x and y axes. This well-known mechanism, called a spherical integrator, simply resolves the motion of the ball into its components about the x and y axes.

The two disks are made of transparent material and have a pattern of dark and transparent sectors printed on their surfaces. A pair of light sources and a pair of photodetectors are mounted on opposite sides of each disk in such a way that, as the disk rotates, light is alternately transmitted to and cut off from the photodetectors. As the disk rotates, the outputs of its two photodetectors produce two square waves, displaced from each other by 90°. The direction of the displacement is an indication of the direction of rotation of the disk, and the number of pulses produced is a measure of the amount of rotation of the disk. The square waves are passed through suitable decoding logic that converts them into a series of clockwise or counterclockwise pulses that can be fed directly to the autopilot or avionics computer to effect a change in heading and/or pitch trim, to reposition a cursor on the screen of a cathode-ray tube, or to make any other precise adjustment required.

This work was done by H. Douglas Garner, Anthony M. Busquets, Thomas W. Hogge, and Russell V. Parrish of **Langley Research Center**. *For further information, Circle 24 on the TSP Request Card.*

This invention is owned by NASA, and a patent application has been filed. Inquiries concerning nonexclusive or exclusive license for its commercial development should be addressed to the Patent Counsel, Langley Research Center [see page 16]. Refer to LAR-13626.

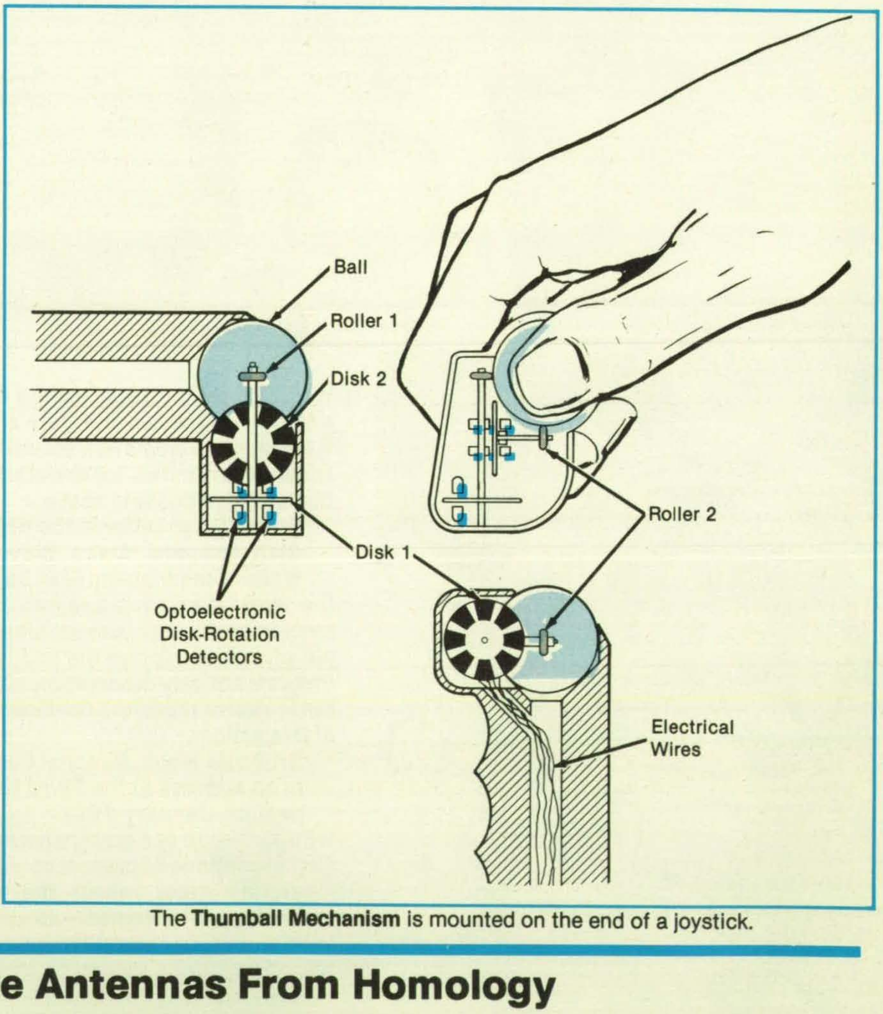

The **Thumball Mechanism** is mounted on the end of a joystick.

Deviations of Microwave Antennas From Homology

Surface distortions are quantified over a range of tilt angles.

NASA's Jet Propulsion Laboratory, Pasadena, California

A formula has been advanced to quantify the deviation of a paraboloidal antenna reflector from the intended homologous shape, over a range of tilt angles. As used here, "homology" and its derivatives denote a concept in antenna design that

compensates for the primary distortions of the reflector surface caused by such variable loads as those of tilt, wind gusts, and temperature: The antenna is designed so that when tilted, the paraboloidal reflector deforms as nearly as possible to another paraboloid (called the homologous paraboloid) that may have a focal length, focal point, and axial direction different from those of the original paraboloid.

In practice, the surface of the reflector has ripples. The rippled surface can be characterized in part by a best-fit paraboloid, about which the root-mean-square (rms) ripple is a minimum. This best-fit paraboloid differs from the theoretical paraboloid required by antenna theory (see figure); but to the degree to which the design is successful, it conforms to the homologous paraboloid.

In quantifying the deviation of the best-fit surface of a real reflector from the homologous surface, the new formula gives a measure of the success of the design. The best-fit surface is characterized at a tilt angle, α, for a given vector, **h**, of homology parameters given by

$$\mathbf{h} = (u_o, v_o, w_o, k, \beta, \gamma)$$

where u_o, v_o, and w_o denote the translation of the vertex in the orthogonal directions x, y, and z, respectively; k denotes the change in focal length; and β and γ denote rotations about the x and y axes, respectively. The rms deviation of the surface from the best-fit paraboloid specified by **h** is then given by

$$rms(\alpha) = \min\{\tfrac{1}{2}[\textstyle\int \delta^2(S)dS/\int dS]^{1/2}\}_{\mathbf{h}}$$

where $\delta(S)$ is the local deviation at point S on the surface and the integrals are taken over the surface.

If the antenna has a perfect paraboloidal surface at all tilt angles, then $\mathrm{rms}(\alpha) = 0$. However, because there is an irreducible amount of ripple even in the absence of mechanical loads, a more-practical homologous-design strategy is to strive for $\mathrm{rms}(\alpha) =$ a constant. The new formula expresses the deviation, H, from homology as follows:

$$H = \{(\alpha_2 - \alpha_1)^{-1} \int_{\alpha_1}^{\alpha_2} [\mathrm{rms}(\alpha) - \overline{\mathrm{rms}}]^2 d\alpha\}^{1/2}$$

where the measurements are made at all tilt angles between α_1 and α_2 and

$$\overline{\mathrm{rms}} = (\alpha_2 - \alpha_1)^{-1} \int_{\alpha_1}^{\alpha_2} \mathrm{rms}(\alpha) d\alpha =$$

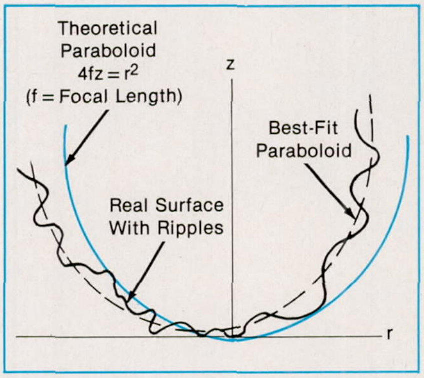

A **Reflector Surface** has ripples. The paraboloid that makes the best rms fit to the rippled surface does not necessarily conform to the paraboloid called for in the theoretical antenna design. Here, the best-fit paraboloid is tilted with respect to the theoretical paraboloid.

the average of $\mathrm{rms}(\alpha)$ for angles betweeen α_1 and α_2. For a homologous antenna, $\mathrm{rms}(\alpha) = \overline{\mathrm{rms}}$ for all α, resulting in $H = 0$.

Because the antenna gain decreases with $\mathrm{rms}(\alpha)$, H is a measure of the variability of the antenna gain with changes in tilt angle. Measurements of gain on two large microwave antennas confirm the correlation between the variability of gain and the deviation from homology.

This work was done by Krystyna Kiedron of Caltech for **NASA's Jet Propulsion Laboratory**. *For further information, Circle 140 on the TSP Request Card.* *NPO-17008*

Electronic Systems

Handling Flight-Research Data in Real Time

Researchers at widely separated locations will be able to participate in tests and analyze data immediately.

Ames Research Center, Moffett Field, California

Real-time data-handling facilities play a growing role at the NASA Western Aeronautical Test Range. The facilities perform the vital functions of data acquisition, communication (video, audio, and data), data processing, display, and tracking.

The amount of data acquired and telemetered to ground-based experimental support facilities has increased dramatically in recent years. If the facilities can handle the data in real time, the cost and time of flight research are greatly reduced, and productivity is greatly increased.

Although specific requirements vary widely among programs, certain basic data-handling needs are common:

- To communicate with the vehicle, pilot, and test team;
- To acquire, compute, and display data; and
- To know the exact location of the research vehicle at all times.

The continuing challenge for the designers and operators of ground support facilities is to perform these tasks in real time and to present the integrated results to the research team in real time. The paper presents several approaches to satisfaction of the requirements of representative types of aircraft research programs at the NASA Western Aeronautical Test Range of Ames Research Center.

Probably the most-important data-handling technique employed by the test range is the transmission of data in real time to sites across the North American Continent via satellite (see figure). Such links have been used on all Space Shuttle landings at Edwards Air Force Base in California. In addition, data acquired at Edwards on the Harrier aircraft have been sent by satellite and microwave land link to the Naval Air Test Center in Maryland. Data from flight tests of the X-29A aircraft are sent by a secure satellite link to the Grumman Aerospace Corp. in Calverton, New York, so that the research team there can participate in flight tests as they occur.

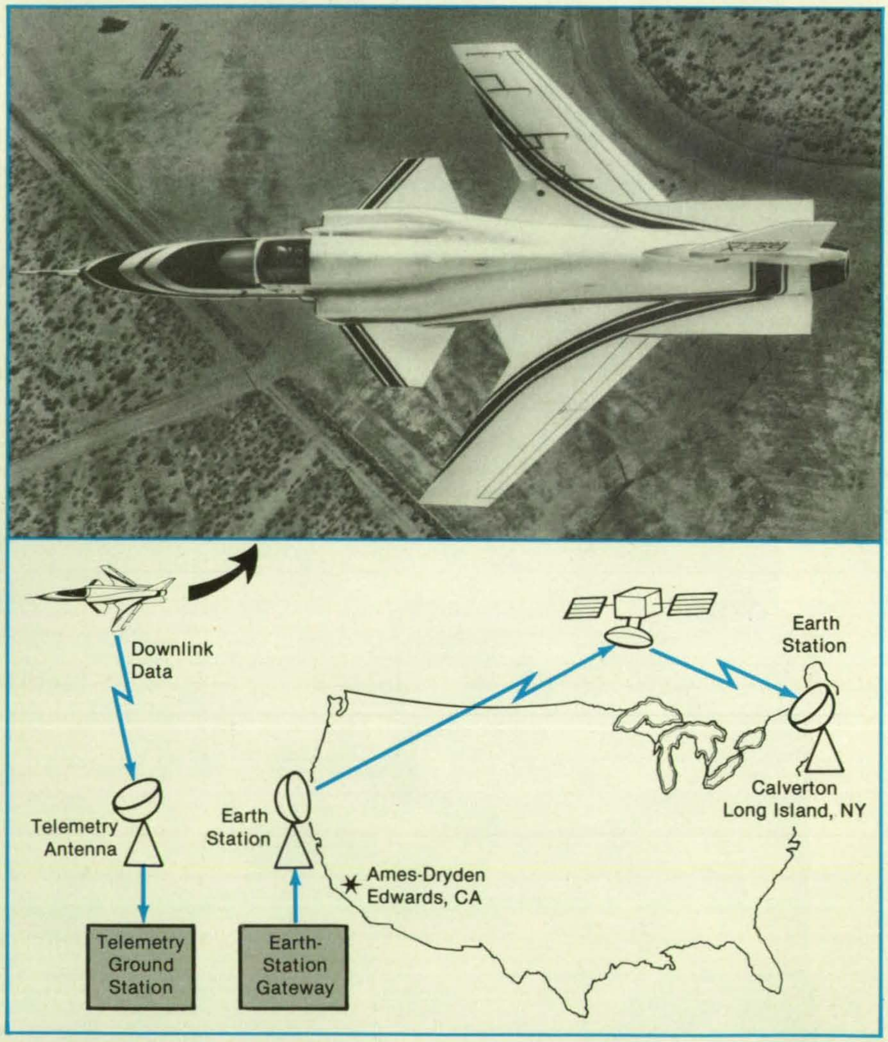

Data are Transmitted from a flight test of the X-29 airplane across the continent via satellite communication links.

This work was done by Archie L. Moore of **Ames Research Center**. *Further information may be found in NASA TM-86805 [N86-19330/NSP], "The Role of a Real-Time Flight Support Facility in Flight Research Programs."*

Copies may be purchased [prepayment required] from the National Technical Information Service, Springfield, Virginia 22161, Telephone No. (703) 487-4650. Rush orders may be placed for an extra fee by calling (800) 336-4700.

Inquiries concerning rights for the commercial use of this invention should be addressed to the Patent Counsel. Ames Research Center [see page 16]. Refer to ARC-11746.

The NEW Alsys Cross-Development System

AdaNow

Real-Time Embedded, Bare-Board Ada Now Targeted To Entire iAPX86 Family.

Efficient, compact, production quality Ada code. Efficient, application-tailored Run Time system. On an 8 MHz 286, a pure synchronization rendezvous in 250 microseconds.

Real-time Ada has come of age.

The new Alsys cross-development system is now available. And, of course, validated. It is hosted on an IBM PC AT or compatible, and targets every member of the Intel iAPX86 family.

The system contains two compilers and a toolset. First, a validated Ada cross-compiler to bare 8086, 80186, 80286, 80386 and other boards. Second, a validated self-hosted Ada compiler on the AT that allows you to generate code for the target that can be tested on the host.

And the tools. First, AdaProbe, Alsys' unique debugger and program viewer for the host, and Cross-AdaProbe for the target. And then, a complete and uniquely powerful multi-library system, binder, AdaReformat, AdaXref, AdaMake, downloading utilities, configurability interface, and utilities supporting PROM-burning.

The new cross-development system is based on the new Alsys Version 3 "root" representing a quantum leap forward in Ada technology. If you thought Ada wasn't ready for real-time, you owe it to yourself to call.

alsys

In the US: Alsys Inc., 1432 Main St., Waltham, MA 02154 Tel: (617) 890-0030
In the UK: Alsys Ltd., Partridge House, Newtown Rd., Henley-on-Thames, Oxon RG9 1EN Tel: 44 (491) 579090
In the rest of the world: Alsys SA, 29 Avenue de Versailles, 78170 La Celle St. Cloud, France Tel: 33 (1) 3918.12.44

Send me: ______New Brochure on Ada Real-Time

______Data Sheet on Cross-Compiling to the iAPX86

______New Brochure on V. 3 "Quality"

Name____________________

Company____________________

Address____________________

City________State______Zip______

Phone____________________

Alsys, Inc. • 1432 Main Street • Waltham, MA 02154

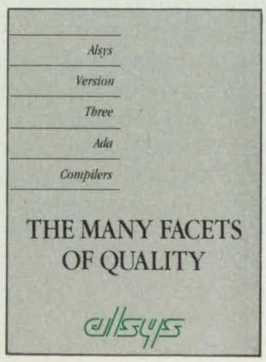

Circle Reader Action No. 341

*Ada is a registered trademark of the U.S. Government (AJPO).

NTB 3/88

Digital-Difference Processing for Collision Avoidance

The difference in frequency between two signals is tracked digitally.

Lyndon B. Johnson Space Center, Houston, Texas

A digital system for automotive crash avoidance measures and displays the difference in frequency between two sinusoidal input signals of slightly different frequencies. The system was designed for use with Doppler radars. In a single-transmitter system like a law-enforcement highway speed detector, the two inputs are the transmitted and returned signals, which may differ in frequency by the Doppler shift caused by the target path. In a two-transmitter system, the inputs are the two return signals with two different Doppler shifts.

The system (see Figure 1) can be characterized as a digital mixer coupled to a frequency counter that measures the difference frequency in the mixer output. First, the sinusoidal inputs are amplified, tracking filtered, and converted by phase-lock loop to square waves. When a positive-going edge of the squared version of waveform B occurs while squared A is in the low state, the latch output is set high. When a positive-going edge of squared A occurs while squared B is low, the latch output is then set low (see Figure 2).

Thus, the latch output alternates between the high and low states as frequently as the occurrence of the positive-going edge of squared A alternates between the high and low states of squared B. The frequency of this alternation, averaged over a large number of cycles, is just the difference in frequency between signals A and B. By use of two more basic digital circuits shown in Figure 1, the digital-difference processor can detect if A> B or A< B. This indicates target path, and a low Doppler difference indicates a target collision path.

The number of cycles in the latch output is counted during 2^{13} cycles of signal B, which serves as the frequency-and-time reference. The count thus equals 2^{13} times the ratio of the difference (or Doppler) frequency to the frequency of signal B. The count is displayed, and the counter is reset every 2^{13} cycles for repeated updating. By measuring digital difference for distance traveled, the same difference readout is obtained for all speeds.

Other uses for the digital-difference processor are for frequency discrimination in frequency demodulation, digital phase detection, frequency-shift-keying demodu-

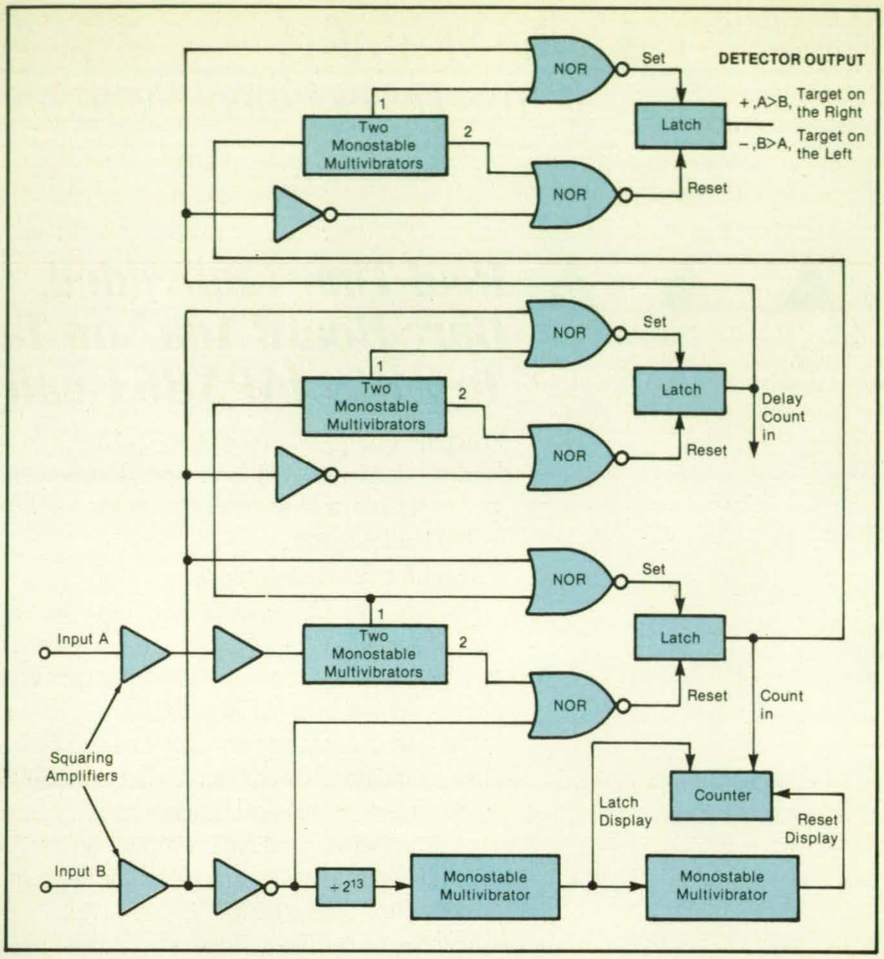

Figure 1. This **Digital Frequency-Difference Counter** measures and displays the difference in frequency between sinusoidal inputs 1 and 2, using signal 2 as a time-and-frequency reference.

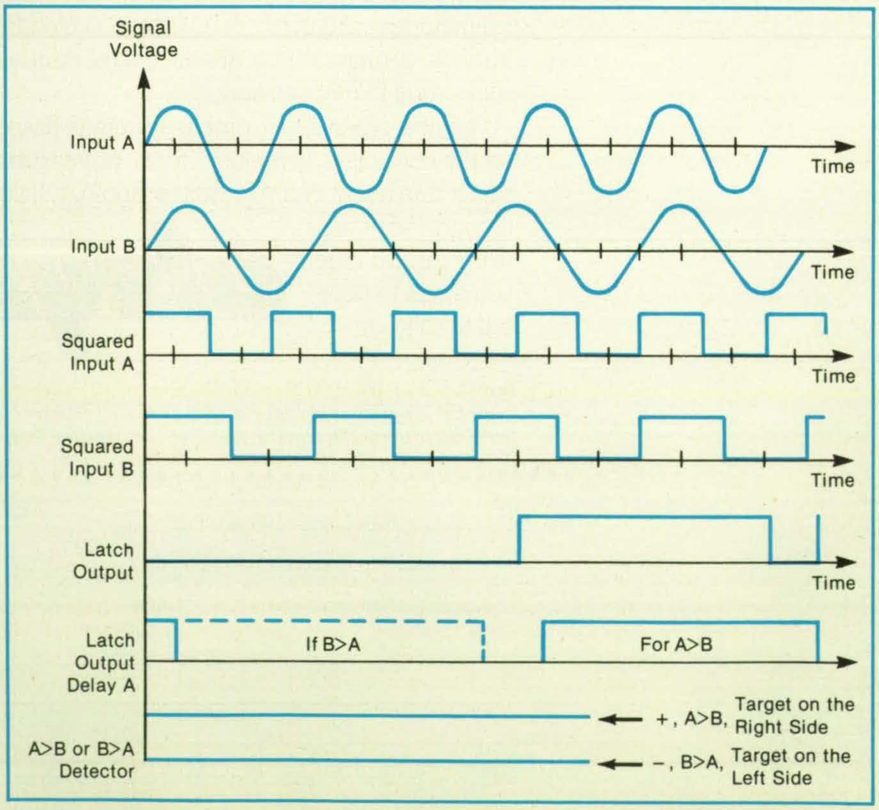

Figure 2. This **Timing Diagram** shows the relationships between the inputs and the key digital waveforms in the counter. The positive (negative) transitions of the latch output occur when the positive transitions of squared B occur during the upper (lower) states of squared A.

lation, and the like. The technique determines the target path mathematically, which makes its response faster than that of the tracking antenna. The technique therefore, can be used for tracking cars, missiles, bullets, baseballs, and other fast-moving objects.

This work was done by Paul Shores, Chris Lichtenberg, Herbert S. Kobayashi, and Allen R. Cunningham of **Johnson Space Center**. *For further information, Circle 38 on the TSP Request Card.*

This invention is owned by NASA, and a patent application has been filed. Inquiries concerning nonexclusive or exclusive license for its commercial development should be addressed to the Patent Counsel, Johnson Space Center [see page 16]. Refer to MSC-20865.

Data-Acquisition System for Rotor Vibrations

A new system trades hardware for software to reduce cost.

Lewis Research Center, Cleveland, Ohio

An optical data-acquisition system measures the vibrations of rotor blades. The system records raw data — a set of blade-arrival times — in memory and processes the data after the run. This approach yields a simple and inexpensive system with the least possible hardware.

The system replaces a more complex system in which a set of fixed optical probes sensed blade passages, a microcomputer received and processed data from the probes, and a control computer sorted the data into usable form. The older system was costly and was difficult to maintain and repair. The new system requires fewer circuit boards. Because it is simpler, it is more reliable; and self-testing circuitry can be eliminated as well.

The new system, nevertheless, retains the important performance characteristics. Its maximum allowable deflection, deflection resolution, maximum (unaliased) frequency, and frequency resolution are equal to or better than those of the older system.

There are 16 probes equally spaced about the circumference of the chamber that contains the rotor. Each probe contains three high-resolution optical reflective sensors and associated electronics. The sensors are focused light-emitting diodes (LED's) and matched photodetectors in unitary packages. A visible light beam from each LED is focused at the blade-tip path.

As a blade passes by the probe at high speed, the event is detected, converted to a signal compatible with logic circuitry, and sent to one of four data-acquisition boards. The probes variously measure the start of a revolution and the positions of the leading edge of the blade tip, the tip midchord, and the tip trailing edge at four different locations.

Because four optical probes share a single memory (see figure), the address size of the memory on each board had to be increased from 4K to 16K to obtain the same number of data points per probe as in the original system. However, the total address sizes of the memories for all the probes remain unchanged.

One penalty for the simplicity of the new system is that the size of a memory word must increase. The 8-bit memory-word size of the original system is not adequate when a high-speed wraparound clock counter is used to measure time. Although counter wraparound can be handled by software, the counter must not wrap around before the next blade arrives if it is to produce meaningful, unscrambled timing records. A 16-bit word size satisfies this racing limitation at clock speeds as high as 20 MHz for the worst case of a two-bladed rotor at 3,000 r/min.

Additional measures were taken to simplify the data-acquisition boards and to reduce the number of components. The interval of time incorporated into the equipment design to correct for missing or extraneous blade signals was eliminated and replaced by an equivalent interval generated by a controlling computer program. This offers the further advantage of easy modification of the interval as needed.

The master clock and wraparound clock counter are located on a separate

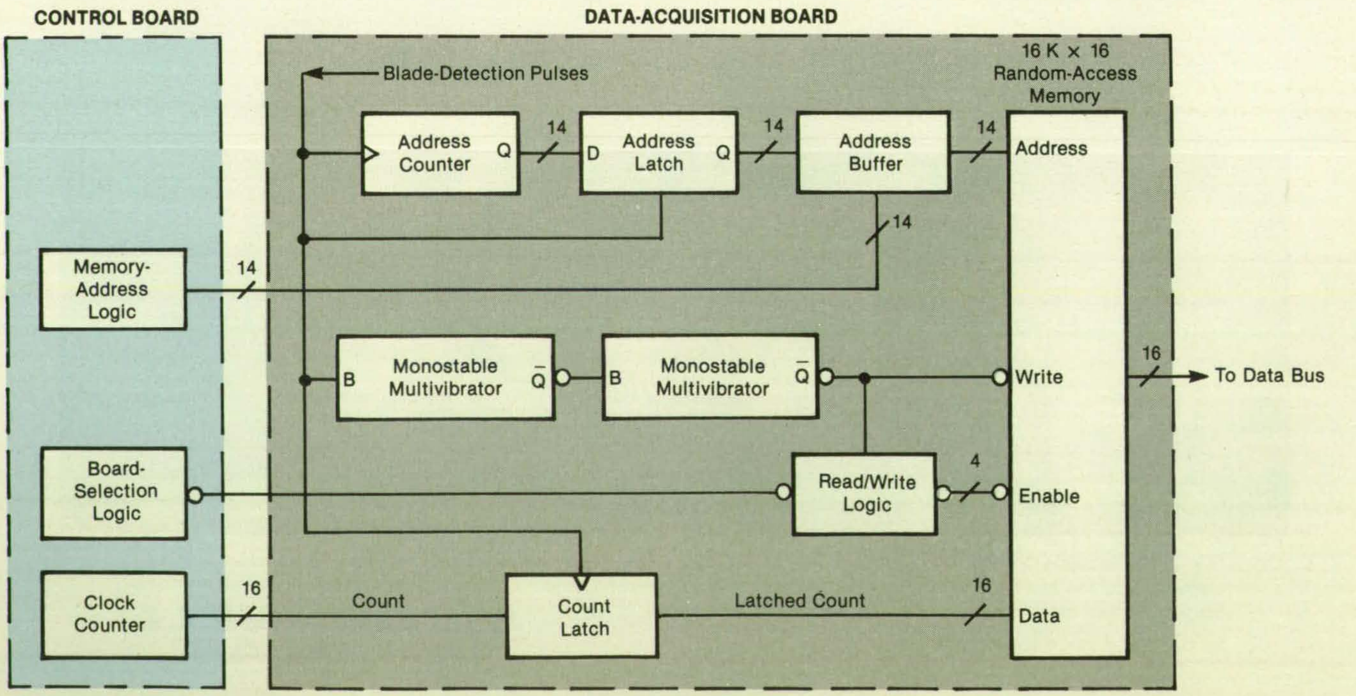

A **Composite Train of Interspersed Blade-Detection Pulses** is produced by gates at the four probe ports on a data-acquisition board. The pulses latch the count from a high-speed wraparound clock counter and initiate the writing of the count into the current address of memory. As a result, a time corresponding to each blade passage is stamped into memory.

control board, which also has control circuits for connection to an external computer. During the acquisition, storage, and retrieval phases of a data-collection run, the control circuits enable or disable control lines to the data-acquisition boards, as called upon by software.

This work was done by Stephen J. Posta and Gerald V. Brown of **Lewis Research Center**. *Further information may be found in NASA TM-88907 [N87-14730/NSP], "A Low-Cost Optical Data Acquisition System for Vibration Measurement."*

Copies may be purchased [prepayment required] from the National Technical Information Service, Springfield, Virginia 22161, Telephone No. (703) 487-4650. Rush orders may be placed for an extra fee by calling (800) 336-4700.
LEW-14557

Signal Generator Compensates for Phase Shift in Cable

A stabilized reference signal is delivered to a remote unit.

NASA's Jet Propulsion Laboratory, Pasadena, California

A signal-generating subsystem delivers a stabilized 5/N-MHz (where N is an integer) pulse and a stabilized 20-MHz tone to a receiver at one end of a cable. Intended for use in a system that generates precise time and frequency signals, the signal-generating subsystem compensates for the phase shift in the cable.

The system is capable of transferring a hydrogen-maser atomic-clock reference over a 1,000-ft (305-m) cable with no significant loss of stability. The transmitter generates the 5/N-MHz signal and an auxiliary 20-MHz signal from a 5-MHz reference oscillator. The 20-MHz signal is passed through a voltage-controlled phase shifter, and the two signals are sent through the cable to the receiver where they are separated by filters and fed to a double balanced mixer. The mixer output — a 20-MHz carrier amplitude-modulated at 5/N-MHz — is sent back through the cable to the transmitter. Because the receiver input impedance at 5/N MHz is higher than the 50-Ω characteristic impedance of the cable, a portion of the 5/N-MHz signal is also reflected back through the cable to the transmitter.

In the transmitter, a hybrid transmission-line junction separates the returning from the outgoing 5/N-MHz signal. The returning 5/N-MHz-modulated 20-MHz signal, which contains the two-way cable delay, is sent back through the phase shifter and mixed with the original 20-MHz signal. The mixer output is passed through a 3-MHz low-pass filter to obtain the low-frequency component of the mixer output, which is a 5/N-MHz signal of amplitude proportional to the cosine of ϕ_1, the sum of the two-way cable phase delay and the two-way voltage-controlled phase delay at 20 MHz. This signal is mixed with the returned 5/N-MHz signal and low-pass filtered to obtain a dc signal proportional to $\cos\phi_1 \cos\delta$, where δ is a small phase error introduced into the returned 5/N-MHz signal by dispersion in the cable and by imperfections in the hybrid junction.

The $\cos\phi_1 \cos\delta$ signal is integrated by a feedback-loop filter to generate the control signal for the voltage-controlled phase shifter. This completes the feedback loop, which continually strives to make $\cos\phi_1 = 0$, regardless of the 5/N-MHz phase error. In this way, the system acts to maintain the total 20-MHz delay through the voltage-controlled phase shifter and the cable constant at $\pi/2 + 2n\pi$ radians (where n is an integer).

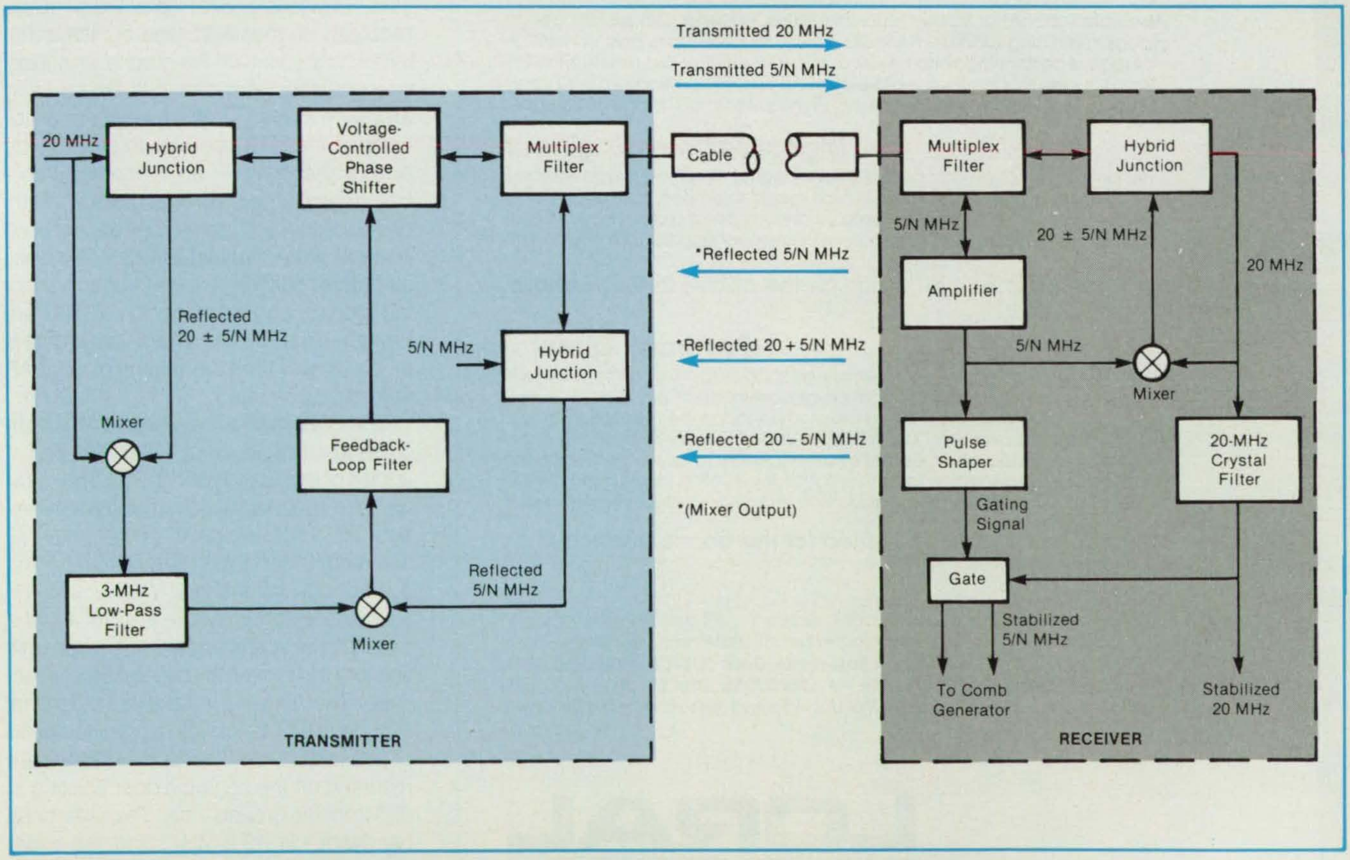

Signals at Two Different Frequencies are transmitted back and forth along a cable and mixed to measure the propagation delay in the cable. The delay-measuring circuitry is part of a feedback loop that constrains the overall delay at a stable value.

Thus, the 20-MHz signal arriving at the receiver is stabilized in phase. The 5/N-MHz signal arriving at the receiver is not stabilized, but it serves as a gate for individual cycles of the stabilized 20-MHz signal to obtain stabilized pulses at 5/N MHz. In the original application, the stabilized 5/N-MHz pulses drive a "comb" generator, which puts out microwave tones at all harmonics of the stabilized signal.

This work was done by E. H. Sigman of Caltech for **NASA's Jet Propulsion Laboratory**. *For further information, Circle 58 on the TSP Request Card. NPO-17001*

Real-Time Processor for Synthetic-Aperture Radar

Images are formed aboard the airplane.

NASA's Jet Propulsion Laboratory, Pasadena, California

A data processor for a synthetic-aperture radar (SAR) operates aboard the airplane with the radar equipment to produce images of the scanned terrain in real time. Previously, SAR data were either recorded on magnetic tape or else transmitted to stations on the ground for subsequent processing into images. By providing an image immediately, the new processor enables the SAR operator to monitor the scanning activity — an advantage especially when targets are obscured by weather. The processed images can be recorded on tape or transmitted to ground stations as before, but the required capacities for the storage and transmission of data are lower because the volume of image data is much smaller than the volume of raw SAR data.

The SAR operates aboard a CV-990 airplane at a frequency of 1.225 GHz and at angles of incidence of 0° to 60°. The radar has one horizontally polarized (H) antenna and one vertically polarized (V) antenna. The radar is capable of simultaneously acquiring data for the HH, VV, HV, and VH polarization states, where the first and the second characters represent the transmitting and the receiving polarization, respectively. The airplane is flown at a nominal altitude of 6 to 12 km with a nominal speed of 200 to 250 m/s. The radar antennas are mounted on the baggage door pointing at 90° from the ground track. The radar chirp bandwidth is 19.8 MHz, and the radar pulse width is 4.9 μs. The peak transmitter power is 4 kW. The radar pulse-repetition

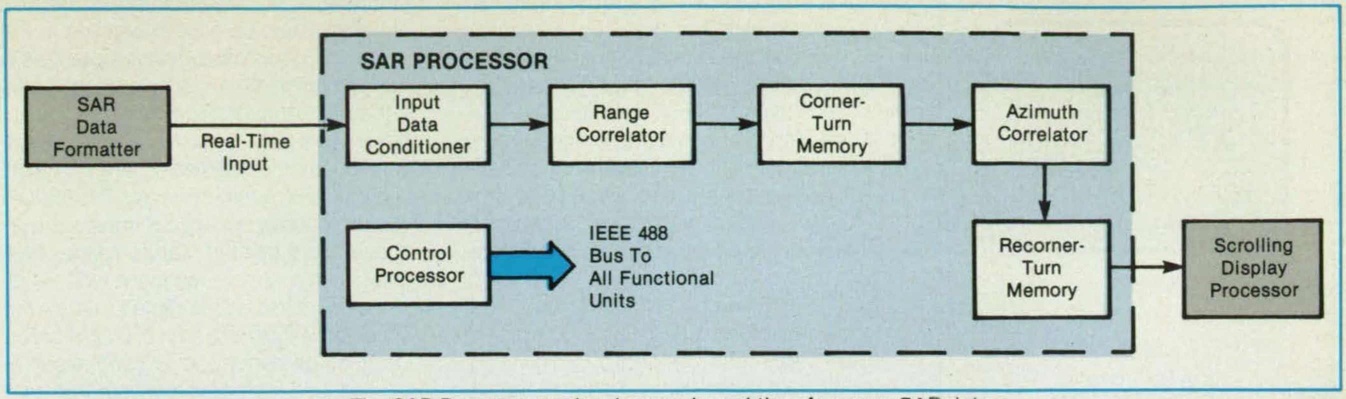

The **SAR Processor** makes images in real time from raw SAR data.

frequency is proportional to the aircraft speed and is 750 Hz at 250 m/s.

Radar echo signals are received by the antennas, amplified, and heterodyned to video frequencies. The video signals are sent to an optical recorder and to analog-to-digital converters (ADC's). The ADC outputs are merged in a formatter with the radar header information, which is supplied by the radar-control computer and the inertial-navigation system. The merged digital data are then sent to the processor and to a digital tape recorder. The output of the processor is displayed on a scrolling display device and recorded on videotape.

In the processor (see figure) the input signal is received by the input data conditioner from the SAR data formatter. The received echo data are reduced in rate by the input data conditioner before being processed in both range and azimuth dimensions to generate images. The range correlator performs a frequency-domain fast-Fourier-transform algorithm, including a correction for range curvature. The output of the range correlator is sent to the corner-turn memory. Data from the range-correlator output flow along the range direction. The corner-turn memory rotates the flow of data to the azimuth direction.

The azimuth correlator also performs a fast-Fourier-transform algorithm. However, the azimuth correlation involves only azimuth compression, with correction for range curvature. The data from the azimuth correlator flow along the azimuth direction. The recorner-turn memory rotates the flow direction to the range axis for a line-by-line display along the flight track by the scrolling display device.

This work was done by Kuang Y. Liu of Caltech for **NASA's Jet Propulsion Laboratory**. *For further information, Circle 127 on the TSP Request Card.*

This invention is owned by NASA, and a patent application has been filed. Inquiries concerning nonexclusive or exclusive license for its commercial development should be addressed to the Patent Counsel, NASA Resident Office-JPL [see page 16]. Refer to NPO-17188.

Books and Reports

These reports, studies, handbooks are available from NASA as Technical Support Packages (TSP's) when a Request Card number is cited; otherwise they are available from the National Technical Information Service.

Landing-Time-Controlled Management of Air Traffic

A conceptual system would control aircraft with old and new guidance equipment.

A report describes a concept for air-traffic management that promises to increase efficiency at busy airports. The concept is based on controlling the landing time of all aircraft entering the terminal area — aircraft with only conventional guidance equipment as well as aircraft with advanced four-dimensional (space and time) guidance systems.

The report begins with an overview of the concept, then reviews controller-interactive simulations. It describes a fuel-conservative-trajectory algorithm, based on the equations of motion for controlling the landing time. Finally, it presents the results of piloted simulations.

The two major ground-based elements in the concept are (1) an electronic scheduler, which assigns conflict-free landing times to aircraft and (2) an electronic profile-descent advisor, which generates trajectory commands for aircraft without four-dimensional guidance. Assigned landing times are transmitted by data links to four-dimensional-equipped aircraft and are translated by the on-board flight-management system into trajectory commands. Meanwhile, a human controller relays descent advisories by voice link to unequipped aircraft.

Such a system would handle a range of aircraft, from high-performance jets to low-performance general-aviation airplanes. It would also give full authority to the human controller, who would monitor the time assignments of the scheduler on a graphics terminal and could override its decisions by using a small, but flexible, set of commands. For example, a controller could delay traffic feeding into the terminal area or increase the time separation between aircraft if there were landing delays at the airport. The controller could also overrule the built-in first-come, first-served rule to give landing priority to an aircraft that had missed an approach or was in an emergency.

The simulations of trajectories flown by pilots in a training apparatus have demonstrated that profile-descent advisories can control the descent time of unequipped aircraft. A landing-time accuracy of ±20 seconds, which a time-based system needs to be effective, appears attainable.

This work was done by Heinz Erzberger and Leonard Tobias of **Ames Research Center**. *Further information may be found in NASA TM-88243 [N86-28049/NSP], "A Time-Based Concept for Terminal-Area Traffic Management."*

Copies may be purchased [prepayment required] from the National Technical Information Service, Springfield, Virginia 22161, Telephone No. (703) 487-4650. Rush orders may be placed for an extra fee by calling (800) 336-4700.

Inquiries concerning rights for the commercial use of this invention should be addressed to the Patent Counsel, Ames Research Center [see page 16]. Refer to ARC-11713.

Sensor-Failure Simulator

Outputs of defective sensors are simulated for studies of reliability of control systems.

A real-time sensor-failure simulator (SFS) was designed and built for use with the Advance Detection, Isolation, and Accommodation (ADIA) program. The equipment consists of an IBM PC/XT computer and associated analog circuitry. The user defines failure scenarios to determine which sensor signals fail and the method(s) used to simulate failure.

The user interface is entirely menu-driven and allows one to define, save, retrieve, and edit failure scenarios. The analog circuitry has five separate signal paths, with independent digital-to-analog conversion (D/A) equipment for each path. The D/A equipment, controlled by the computer, modifies the analog signals to simulate failures of sensors. The SFS was designed to be programmable, reliable, flexible, and to provide for repeatable failure scenarios. Given these characteristics, it can be used for efficient evaluation and demonstration of sensor-failure-detection logic.

The SFS has been tested in a closed loop with a controls interface and monitoring unit, the ADIA control, and a real-time hybrid simulation of the F100 engine. As a first application, the SFS will be used to simulate sensor failures of a full-scale F100 engine in conjunction with the ADIA test program.

This work was done by Kevin J. Melcher, John C. Delaat, Walter C. Merrill, Lawrence G. Oberle, and Gerald G. Sadler of **Lewis Research Center** *and Joseph H. Schaefer of the U.S. Army. Further information may be found in NASA TM-87271 [N86-31792/NSP], "A Sensor Failure Simulator for Control System Reliability Studies."*

Copies may be purchased [prepayment required] from the National Technical Information Service, Springfield, Virginia 22161, Telephone No. (703) 487-4650. Rush orders may be placed for an extra fee by calling (800) 336-4700.
LEW-14533

Research in Optical Processing of Data

Potential advantages include high speed and low cost.

A report describes current research in the optical processing of data at NASA's Ames Research Center. The research is prompted by plans for automation systems for use on the proposed Space Station; in particular, an optical pattern-recognition system that can be developed into robotic-vision and spectral-analysis systems and an optical processor for control of the wave front of an adaptive-mirror experiment. If successfully developed, these optical processors will offer several advantages over electronic systems with similar capabilities, including an optimum match for optical input; low power consumption; and reduced cost, size, and weight.

The classifier type of pattern-recognition system performs three operations: extraction of features, reduction of dimensionality, and classification. A feature extractor must be able to function in the presence of such distortions as changes in scale, rotation, changes in focus, and blur. A feature extractor might organize a set of descriptors (e.g., color, curvature, elongation, geometric moments, length, width, and area) into a feature vector. The feature vector is useful because it transforms an image into a point in feature space. Typically, such a space has more than 50 dimensions, and it is preferable to reduce the dimensionality to less than 5. Classification can then be performed by comparison of the reduced feature vector with test data for identification of the object.

The report describes an advanced optical feature extractor that would perform the Fourier-Mellin transform to generate a feature vector that is invariant under changes of scale and position and that responds to rotation with a simple translation. The Fourier-Mellin feature vector facilitates the reduction of dimensionality by means of the Fourier transform and variation of the resolution of the detector array in the processor. Classification must still be performed electronically by symbolic and digital processors.

A proposed correlator type of pattern-recognition system would involve (a) synthetic discriminant functions that can be made invariant under distortions of scale, translation, rotation, and class and (b) matched spatial filters that insert the reference images corresponding to the discriminant functions, for correlation with the scene. The matched spatial filters are Fourier-transform images generated by computer and written to a magneto-optic spatial light modulator. The system would have to be "trained" by a human operator, who would develop a library of recognizable patterns.

The mirror/wave-front-control problem has elements in common with efforts to control other high-dimensional dynamic systems. The report discusses candidate digital and analog architectures for the optical execution of state-estimation algorithms that arise in such problems. The system chosen for demonstration includes a segmented, adaptive mirror and a wave-front sensor consisting of a point-diffraction interferometer. The interferogram is sensed by a video camera and processed to yield the state estimate and control signals.

This work was done by David Ennis of **Ames Research Center** *and David Jared of Sterling Software. To obtain a copy of the report, "Optical Processing and Space Station Automation," Circle 52 on the TSP Request Card.*

Inquiries concerning rights for the commercial use of this invention should be addressed to the Patent Counsel, Ames Research Center *[see page 16]*. *Refer to ARC-11758.*

Improved Tracking of Square-Wave Subcarrier

The variance of the phase error is reduced.

A report discusses the application of a "windowing" concept to improve the ability of a telemetry receiver to track the phase of a square-wave phase-modulation subcarrier signal. The concept is based on setting the phase-tracking signal at zero outside narrow time "windows," thereby reducing the noise energy in the processed signal. The result is an increase in the signal-to-noise ratio in the tracking loop with a consequent increase in the accuracy of tracking and a reduction in the number of errors in the telemetric data.

In a telemetry system of the type considered, data are transmitted as binary modulation of the subcarrier. For correct reception of data, the receiver must track the carrier and subcarrier phases. In the conceptual receiver, the subcarrier-phase-tracking system is an all-digital Costas loop in which nominally the subcarrier-phase quadrature reference signal is zero except during the small fraction W/4 of each subcarrier cycle immediately preceding and following each zero crossing of the subcarrier.

Errors in the reception of data are treated as noise, and the phase-tracking performance is quantified in terms of the variance of the phase-tracking error. The report develops equations that describe the operation of the subcarrier-phase-tracking loop and are used to predict the performance. This analysis is based on the assumption of synchronization of the receiver with the received signals, ignoring such complications as quantization errors, nonzero data-signal rise time, and filtering distortions.

A linear treatment (valid for small phase-tracking errors and for W not too close to zero) shows that the variance of the phase-tracking error can be reduced to about $W\sigma_0^2$, where σ_0^2 is the value without "windowing." A computer simulation verifies this result and extends the prediction to regions of nonlinear response, yielding plots of variance of the phase-tracking error as a function of W, with the signal-to-noise ratio of the subcarrier-phase-tracking loop as a parameter. From these plots one can find the optimum W; in a typical case, the window can be made so narrow that the phase-error variance is reduced to $1.5\sigma_0^4$.

This work was done by William J. Hurd and Sergio Aguirre of Caltech for **NASA's Jet Propulsion Laboratory**. *To obtain a copy of the report, "A Method To Dramatically Improve Subcarrier Tracking," Circle 119 on the TSP Request Card.*
NPO-17135

Checking Fits With Digital Image Processing

Computer-aided video inspection of mechanical and electrical connectors is feasible.

A report discusses work done on digital image processing for computer-aided interface verification (CAIV). The goal was to develop ways to assure that a component at any level of assembly will fit the mating part(s) of its intended interface. Two kinds of components were examined: a mechanical mating flange and an electrical plug.

The work encompassed the following tasks:

- Identification of ground rules and guidelines;
- Definition of CAIV requirements;
- Choice of a technological approach;
- Formulation of a technology implementation;
- Demonstration of the concept; and
- Delivery of equipment, computer programs, and documents.

The reference-image/image-subtraction method was selected for pattern recognition. In this technique, a reference image of the interface in question stored in memory is subtracted, one picture element at a time, from the image of the interface being viewed. The absolute values of the differences between the two images are retained. If the interfaces are identical, there will be no differences. If the interfaces are dissimilar, the differences will be highlighted.

One of the major components of the image-processing system is a charge-coupled photodiode array in a solid-state digital camera. The unit produces digital image-intensity values. A special sample-and-hold processing filter was developed to preserve the light-intensity values in the output video signal. In contrast, most charge-coupled-device cameras include filters that average intensity values across groups of picture elements. The averaging introduces an error of 10 to 12 percent into the light-intensity values.

The work showed that a CAIV system can be built with a resolution of 0.001 inch (25 μm) per picture element and an overall accuracy of $\pm$2 percent or $\pm$0.005 inch (127 μm). In 3 to 4 years, it should be possible to improve these performance figures to $\pm$1 percent and $\pm$0.0015 inch (38 μm), respectively.

This work was done by R. M. Davis of **Kennedy Space Center** *and W. D. Geaslen of EG&G Space Systems. To obtain a copy of the report, "Computer Aided Interface Verification," Circle 123 on the TSP Request Card.*

Inquiries concerning rights for the commercial use of this invention should be addressed to the Patent Counsel, Kennedy Space Center *[see page 16]* *Refer to KSC-11367.*

Physical Sciences

Fast Measurements of Thermal Diffusivities of Ceramics

The temperature rises of samples are compared with that of a reference sample.

Ames Research Center
Moffett Field, California

An apparatus quickly measures the thermal diffusivities of ceramics at high temperatures. The apparatus produces data on the relative thermal diffusivities of as many as six ceramic specimens per hour.

The apparatus includes a furnace box with quartz-lamp heating elements, a specimen holder, and a vacuum bell jar (see figure). The furnace box is made of blocks of fused silica and has a water-cooled aluminum floor. The specimen holder, made of rigid low-density silica, accommodates four ceramic samples, one of which is a reference sample. A hole at the center of each sample recess accommodates an aluminum calorimeter glued to the back of the sample. A thermal controller adjusts the power from a 440-V, 140-A supply to the quartz lamps according to the temperatures measured by two thermocouples at the top center of the sample holder.

The specimen holder, with its samples and calorimeters, is placed in the center of the furnace box. The tops of the holder and samples are coated with a black emittance-control coat. A bell jar is placed over the furnace box and is evacuated to a pressure of 20 millimeters of mercury (2.7 kPa).

The surfaces of the samples are heated by the lamps to 2,000 °F (1,093 °C) during 15 seconds and held at that temperature for 90 seconds. The lamps are then turned off. The temperatures of the calorimeters are measured during the last 18 seconds of the heat pulse. The apparatus records the maximum temperature and the rate of rise of temperature. The data are printed out in tables that show the rates of temperature rise or are plotted on graphs of temperature rise versus time during each heat pulse.

The ratio of the rate of temperature rise of an unknown sample to that of the reference sample, the thermal diffusivity of which is known, enables the determination of the relative thermal diffusivity of the unknown. If the densities of the unknown and reference ceramics are the same, the

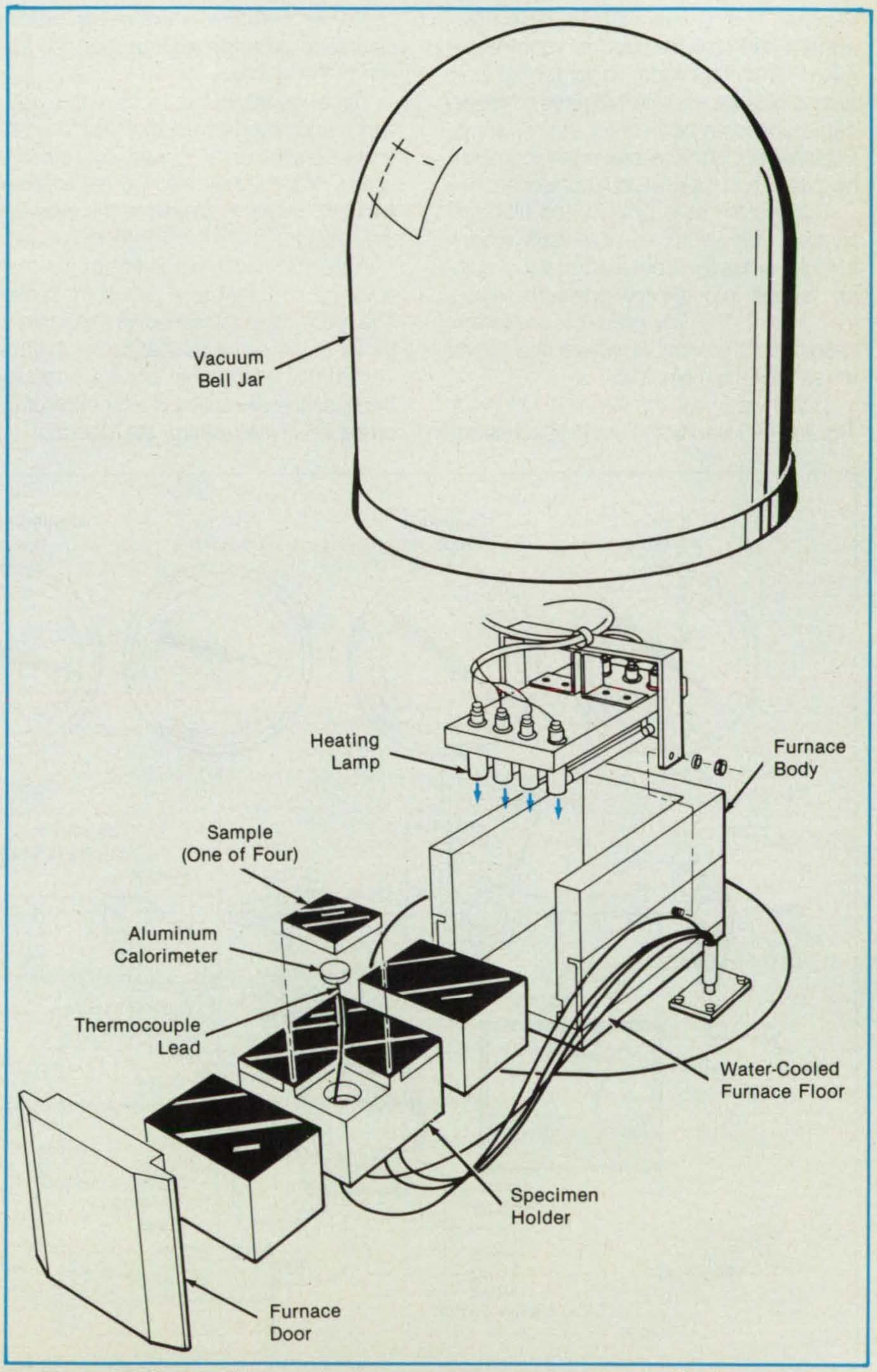

The **Thermal-Diffusivity Tester** makes it easy to determine the thermal diffusivities of ceramics. The pronounced effects of processing parameters on the thermal properties of the ceramics can therefore be evaluated quickly.

relative thermal conductivity is also obtained from the ratio.

This work was done by Marnell Smith and Howard E. Goldstein of **Ames Research Center**. *For further information, Circle 74 on the TSP Request Card.*

Inquiries concerning rights for the commercial use of this invention should be addressed to the Patent Counsel, Ames Research Center [see page 16]. Refer to ARC-11705.

Wet-Atmosphere Generator

The water content in a gas is controlled.

Marshall Space Flight Center, Alabama

A portable flow-control system generates a nitrogen/water atmosphere having a range of dew points and pressures. One use of the system is to provide wet nitrogen for the canister of a wide-field camera that requires this special atmosphere. The system can also be used to inject trace gases other than water vapor for the leak testing of large vessels. Mixtures of gases can be used as carriers for the moisture. Potential applications are in photography, hospitals, and calibration laboratories.

The system uses pressurized nitrogen to power an ejector — essentially a venturi tube with a line from a water-vapor supply tapped into the low-pressure region (see figure). The low pressure draws the vapor into the venturi, where the vapor mixes with the main flow.

Liquid water for the vapor is held in a 1-gallon (3.8-liter) bottle in the suitcaselike system housing. The line from the bottle to the ejector passes through a regulating valve that mechanically controls the flow by throttling. The pressure in the bottle is regulated by a heater; an operator sets the heater temperature to a value that yields a saturation pressure greater than the suction of the ejector.

Once mixed in the ejector, the water vapor and nitrogen are directed to an external vessel or to a vent by regulator valves. Valves may also be set to admit vacuum or return flow from the vessel to the system.

A sample line is tapped from the main flow line and sent to a dew-point sensor. The pressure at the sensor is regulated so that it is the same as that in the external vessel; this ensures an accurate reading because the dew point is a function of the pressure. If necessary, the operator adjusts the dew point by adjusting the flow of water vapor or nitrogen to the ejector.

The sensor is an automatically controlled optical device. A condensate-detector mirror is illuminated with an intense beam from a light-emitting diode. A photodetector monitors the light reflected from the mirror. The detector is fully illuminated when the mirror is clear but sees less light when dew forms on the mirror, scattering light out of the path to the detector.

The photodetector is part of a bridge circuit that produces a large output current when the mirror is dry. The bridge output is amplified and applied to a thermoelectric cooler, which reduces the temperature of the mirror. As dew begins to form on the mirror, the light to the photodetector starts to decrease, the bridge output current drops, and the thermoelectric cooling is reduced. A feedback loop in the sensor quickly stabilizes the thermoelectric cooling control so that a thin dew layer is maintained on the mirror. A precise thermometer embedded in the mirror monitors the dew-point temperature of the layer.

The sensor can reduce the temperature of the gas/vapor mixture by as much as

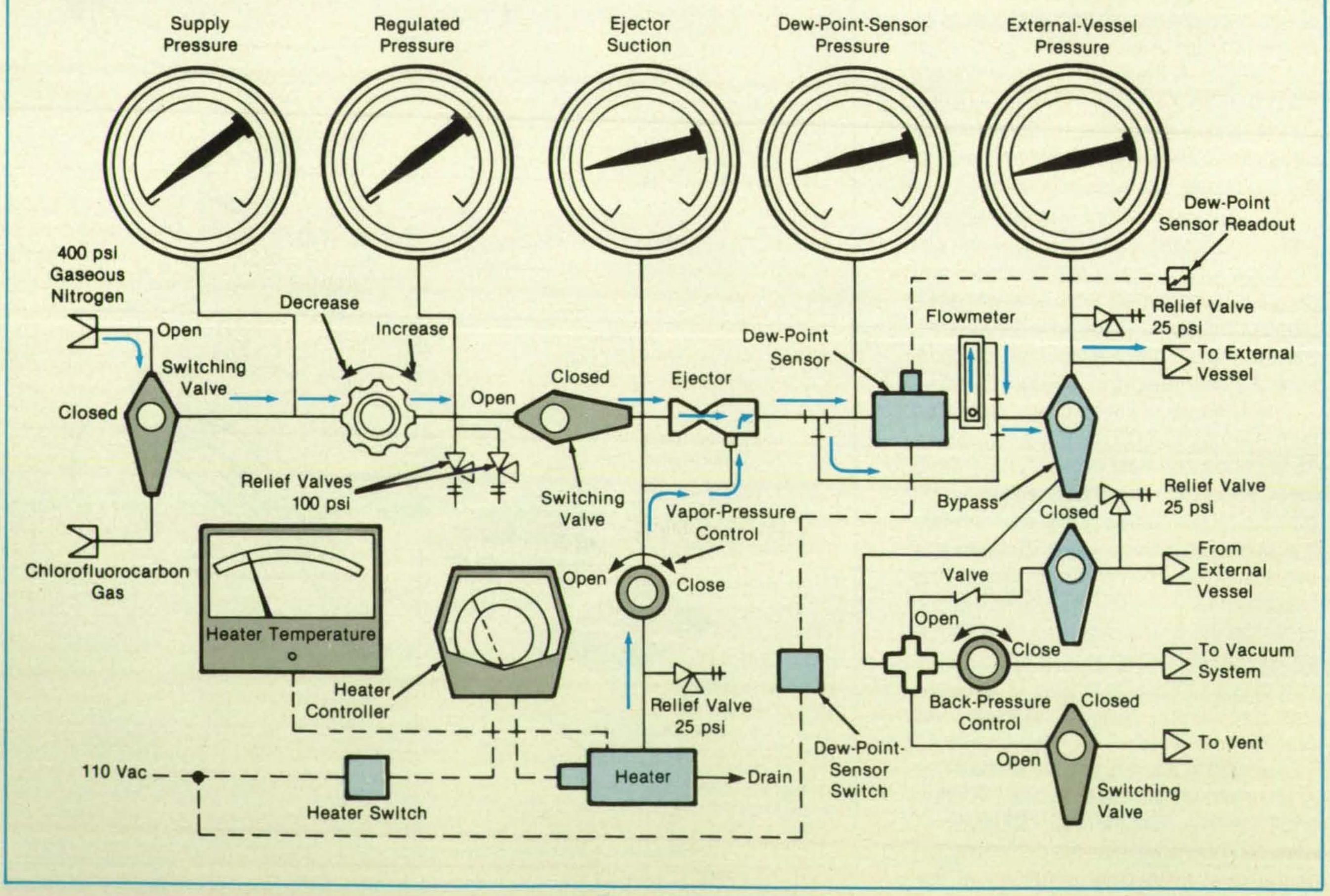

Gas-Flow Conditions in the nitrogen, water vapor, and nitrogen/vapor mixture can be set by the operator with the help of these valves, gauges, and electrical controls.

45 °C. This means, for example, that, with the system at a temperature of 25 °C, dewpoints between 25 and −20 °C can be measured.

This work was done by Richard M. Hammer and Janice K. McGuire of Teledyne Brown Engineering Corp. for **Marshall Space Flight Center**. *For further information, Circle 155 on the TSP Request Card.*

Inquiries concerning rights for the commercial use of this invention should be addressed to the Patent Counsel, Marshall Space Flight Center [see page 16]. Refer to MFS-28177.

Probing Polymer-Segment Motions by ESR

Molecular origins of mechanical properties and aging processes can be studied.

NASA's Jet Propulsion Laboratory, Pasadena, California

Electron-spin resonance (ESR) can now be used to study the motions of main-chain and side-chain segments of molecules in polymers. By enhancing the ability to determine the molecular origins of rotational and torsional relaxation modes, this extension of the ESR technique will contribute to our understanding of the degradation processes that take place as polymers age. The ESR indications of microscopic changes can be obtained long before the changes manifest themselves in changes of macroscopic physical properties.

The technique has been demonstrated in studies of poly(methyl methacrylate). For each measurement, tailored molecules of known molecular weight and size were either dispersed in the polymer to serve as spin probes or attached to the polymer to serve as spin labels. The molecular motions of the spin probes and labels were deduced from the changes in the widths and shapes of their ESR spectral lines as functions of temperature.

The motions of the main-chain and side-chain segments of the polymer were then deduced from the rotational motions of the probes and labels. From the temperature dependencies of the deduced motions, the activation energies of the motions of various molecular segments were also determined (see figure).

A correlation between the mobilities of molecular segments and the excess free volume in the polymer was found by studying the increases of the narrow components of the ESR spectra with increasing temperature. Because the sizes of the probes and labels were known, the size of the free volume was also determined as a function of temperature.

This work was done by Fun-Dow Tsay and Amitava Gupta of Caltech for **NASA's Jet Propulsion Laboratory**. *For further information, Circle 56 on the TSP Request Card.*
NPO-16970

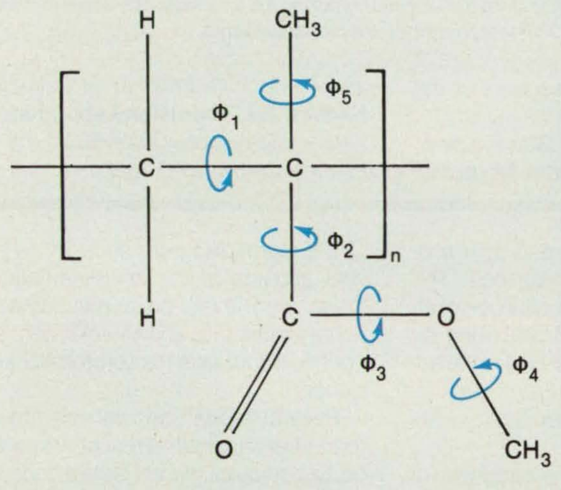

Rotation	Activation Energy, kcal/mole		
	Predicted by Theory	Measured by ESR Label	Measured by ESR Probe
Φ_1	6	6	7
Φ_2	4	5	4
Φ_3	20	18	19
Φ_4	1	1	1
Φ_5	3	2	2

Rotational Motions of Segments of poly(methyl methacrylate) molecules were studied theoretically and experimentally. The activation energies of these motions as determined from the temperature dependencies of ESR spectra agree closely with the predictions of theory.

Measuring Incorporation of Arsenic in Molecular-Beam Expitaxy

Changes in surface layers cause oscillations in RHEED measurements.

NASA's Jet Propulsion Laboratory, Pasadena, California

Reflection high-energy electron diffraction (RHEED) has been used to measure the rate of incorporation of arsenic into GaAs and InAs during growth by molecular-beam epitaxy. The measurement is sensitive only to the portion of arsenic incorporated into the growing film and not to the portion lost in splitting of the incident arsenic tetramers or by evaporation from the film. Because the measurements are independent of the characteristics of vacuum systems, pressure gauges, or flux monitors, they can be used to resolve ambiguities in the literature about absolute fluxes and flux ratios.

The measurement technique was demonstrated in a commercial molecular-beam-epitaxy system. The RHEED electron gun was operated at an energy of 8 keV and an emission current of 5 to 15 μA, aligned with the [110] axis of the growing GaAs or InAs sample. Most of the time, the samples were exposed to a flux of arsenic generated in a standard effusion cell by sublimation of As_4. The pressure of arsenic was measured by an ion gauge near the sample.

The basic measurements were made on buffer layers of GaAs that had been annealed at 600 to 620 °C and of InAs that had been annealed at 480 to 500 °C, both in the arsenic flux. Just before each measurement, the sample temperature was changed to the desired growth temperature and allowed to stabilize for 2 to 5 minutes. Typically, a burst of gallium or indium was deposited on the surface for 1.0 to 1.5 seconds at a rate of 5 to 7 monomolecular layers per second. The arsenic flux was maintained before, during, and after the deposition of metal.

The figure shows the RHEED intensities from GaAs samples at two temperatures. After the initial Ga transient, each oscillation represents the incorporation of about one monomolecular layer of arsenic into the sample from the steady arsenic flux. Once the inflowing arsenic has combined with the available deposited gallium, the oscillations stop, indicating the cessation of growth of GaAs and the return of the surface to the arsenic-stabilized condition.

The frequency of the arsenic-induced oscillations in the figure decreases with increasing temperature of the sample: this suggests that the rate of growth decreases with temperature, because of evaporation of arsenic from the sample. Except when the evaporation rate is high at high temperatures or low arsenic fluxes, the measured rate of incorporation of arsenic into GaAs follows the approximate equation

$$F = A\,P\,\exp(E/kT)$$

where F is the rate of incorporation in monomolecular layers per unit time, P is the pressure of the arsenic flux as measured by the ion gauge, A is a scale factor that depends on the particular equipment used, E is an empirical activation energy of 0.07 ± 0.02 eV, k is the ideal-gas constant, and T is the absolute temperature of the sample.

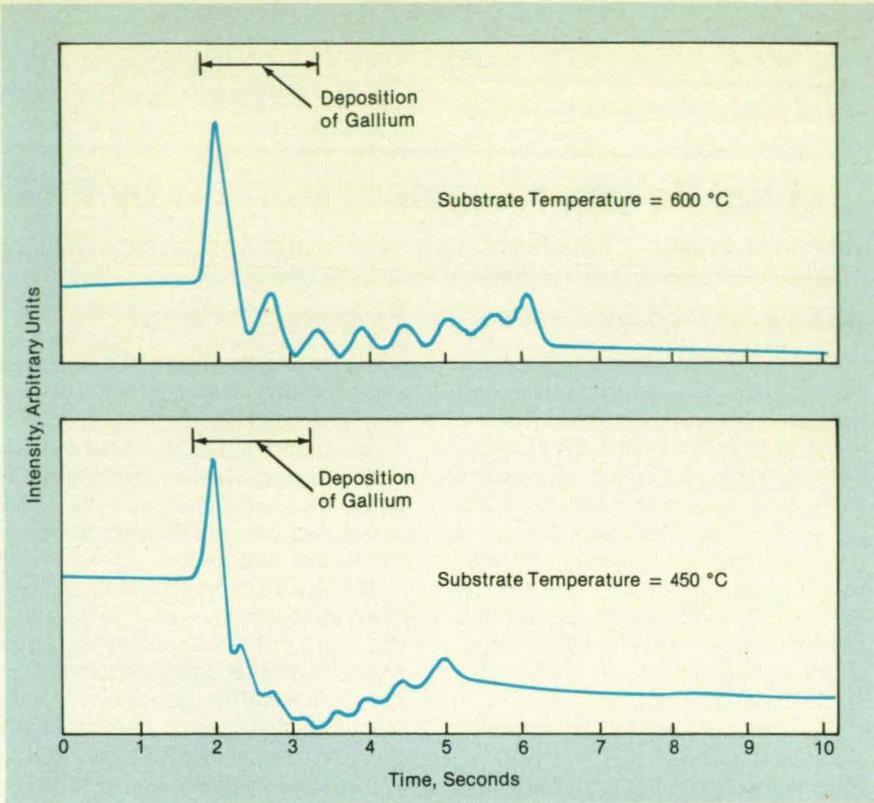

The **Specular RHEED Beam Intensity** was measured before, during, and after the deposition of seven to eight monomolecular layers of gallium during 1.5 seconds. The arsenic pressure was 1.7×10^{-7} torr (2.3×10^{-5} Pa) throughout the measurements.

This work was done by Blair F. Lewis, Rouel F. Fernandez, Anupam Madhukar, and Frank J. Grunthaner of Caltech for **NASA's Jet Propulsion Laboratory**. *For further information, Circle 63 on the TSP Request Card. NPO-16821*

Books and Reports

These reports, studies, handbooks are available from NASA as Technical Support Packages (TSP's) when a Request Card number is cited; otherwise they are available from the National Technical Information Service.

Calculating Atmospheric Effects in Satellite Imagery: Part 2

Practical computational techniques are developed.

A report discusses the practical considerations of the calculation of three-dimensional radiative transfer. It is an extension of the earlier theoretical developments described in "Calculating Atmospheric Effects in Satellite Imagery" (NPO-16373), page 82, *NASA Tech Briefs*, Vol. 9, No. 3 (Fall 1985).

The report begins with a review of the previous work. The theory is based on a model that includes a vertically inhomogeneous atmosphere bounded by a nonuniform, non-Lambertian surface. The theory takes account of the influence of atmospheric absorption and scattering on remote surface sensing. It includes the adjacency effect, in which photons originating in neighboring regions are scattered into the line of sight.

The calculation entails the separation of the total intensity field into a diffuse and direct component. The radiative-transfer equation for the diffuse field is solved by performing a two-dimensional spatial Fourier transform and solving the resulting one-dimensional equations for each of the Fourier components. The spatial-domain diffuse field is then reconstructed with the inverse transform, from which the direct field can then be obtained.

The calculations described in the present report rely on a FORTRAN radiative-transfer computer program, 'RTRAN.3D', that calculates the Fourier components of the three-dimensional diffuse intensity field. Programs were also developed for this research to specify the model atmosphere and surface parameters. Another newly developed program reconstructs the spatial-domain field from the Fourier components calculated by 'RTRAN.3D'.

The report discusses some of the practical aspects of the implementation of these algorithms on a minicomputer. Some symmetries and approximations are invoked to increase the computational efficiency.

Several model calculations are performed, and numerical results are presented. Of particular interest is the albedo-step-function problem, in which two adjoining expanses of ground have different reflectivities. The results suggest that the calculation method as a whole is practical, accurate, and versatile. The atmospheric and surface phase functions can be arbitrarily complex, and solutions are not restricted to nadir observation only. Furthermore, both internal intensity fields and radiation escaping from the top and bottom of the atmosphere can be calculated.

This work was done by David J. Diner and John V. Martonchik of Caltech for **NASA's Jet Propulsion Laboratory**. *To obtain a copy of the report, "Atmospheric Transfer of Radiation Above an Inhomogeneous Non-Lambertian Reflective Ground: Part II: Computational Considerations and Results," Circle 112 on the TSP Request Card.*
NPO-16371

Materials

Stress-and-Strain Analysis of Hot Metal/Fiber Composites

Macroscopic mechanical properties are derived from micromechanics.

Lewis Research Center, Cleveland, Ohio

Stress-and-strain equations have been developed to express the microscopic and macroscopic mechanical properties of metals reinforced by unidirectional fibers, over a range of temperatures. An object made of such a composite material can be treated mathematically by modeling the constituent materials discretely in finite-element analysis, but this treatment requires excessive computing time if the object has a complicated shape. The new equations reduce the computational load by providing approximate, closed-form expressions for the microscopic and the pseudohomogeneous anisotropic properties of a single ply reinforced by unidirectional fibers. These properties include the elastic moduli, Poisson's ratios, uniaxial strengths, thermal conductivities, coefficients of thermal expansion, heat capacities, and stresses in the microscopic constituents.

The micromechanical equations are derived by applying a mechanics-of-materials formulation to the mathematical model of the unidirectional ply, which is a planar array of square-cross-section unit cells. Each cell contains a fiber, the surrounding matrix material, and an interphase material generated by the chemical reaction between the fiber and the matrix (see Figure 1). The usual compatibility-of-displacement and equilibrium-of-forces conditions are imposed. For simplicity, it is pretended that the fibers are continuous, parallel, and equally spaced; that the fibers all have the same properties; and that the fibers, interphases, and matrix are all perfectly bonded to each other. Thermal effects are propagated by Fourier's law of heat conduction.

The resulting set of equations includes expressions for the properties of the ply as functions of the properties of the constituents. For example, the modulus of elasticity of the ply along the 1 axis is given by

$$E_{11} = k_m E_{m11} + k_f\{[1-(D/D_o)^2]\, E_{d11} + (D/D_o)^2 E_{f11}\}$$

where E denotes a modulus of elasticity; k denotes a volume fraction; the subscripts m, f, and d denote the matrix, fiber, and interphase, respectively; and D and D_o are as shown in Figure 1. The numerical results of this and the other micromechanical equations agree closely with the results of a finite-element analysis of a similar model.

Because the behavior of each constituent material is taken to be thermoviscoplastic and three-dimensionally anisotropic, the history of each constituent can be tracked independently as a function of time and represented as a state of stress and strain. A typical application of this capability would be the calculation of residual stress in a newly manufactured article (see Figure 2).

This work was done by Dale A. Hopkins and Christos C. Chamis of **Lewis Research Center**. *Further information may be found in NASA TM-87154 [N86-24757/NSP], "A Unique Set of Micromechanics Equations for High Temperature Metal Matrix Composites."*

Copies may be purchased [prepayment required] from the National Technical Information Service, Springfield, Virginia 22161, Telephone No. (703) 487-4650. Rush orders may be placed for an extra fee by calling (800) 336-4700.
LEW-14591

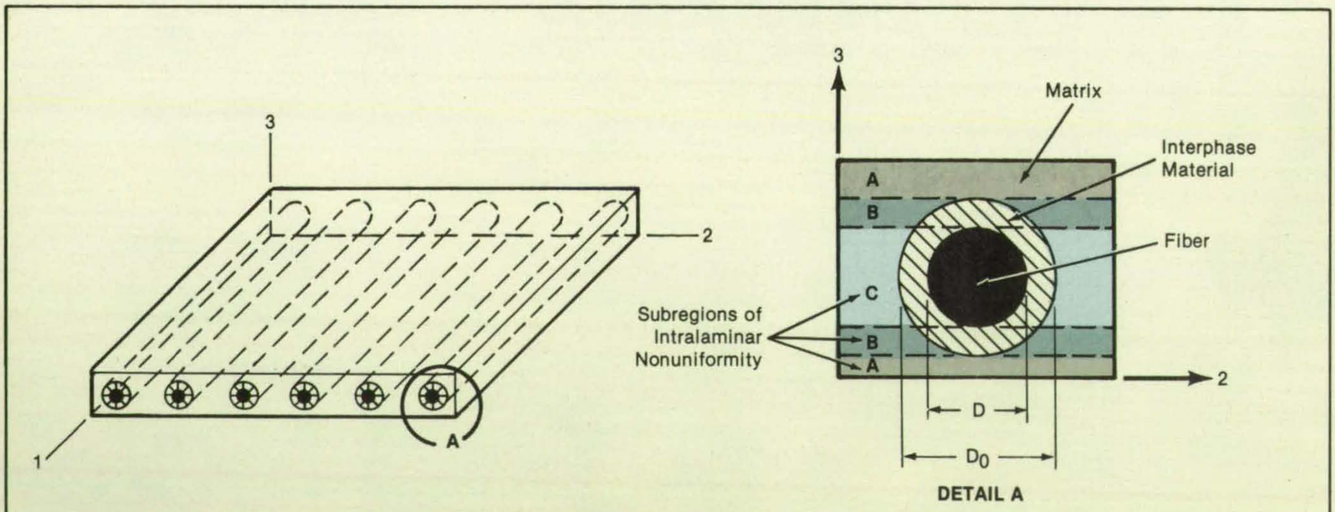

Figure 1. A **Unidirectional-Fiber Ply** in a metal/fiber composite material is modeled as an array of equally spaced fibers in square unit cells. The classical mechanics-of-materials formulation is applied to this model to obtain the micromechanical equations.

You have to work with steppers and DC servos. So should your programmable motor controller.

In developing Klinger's MC4 motor control system, our engineers' had the dilemma of choosing between steppers or DC servos, or should they design two systems, one for each type.

Considering the specific application advantages of each motor, we decided the ideal controller should work equally well with both motor types and switching from one motor to the other should be easy and inexpensive.

That's precisely what we've accomplished with the MC4 system. Where a simple plug-in power card switches the system between motor types.

The MC4 is a powerful programmable motor control system capable of controlling up to four motors, interfacing with any host computer or, with its 8K of non-volatile memory, it can stand alone to operate on the production floor. You can even store up to 99 programs and locally access any 9 programs from front panel controls.

MINI-STEPPING YIELDS HIGH RESOLUTION AND HIGH VELOCITY.

Most stepping motors rotate 1.8 degrees per full step, a relatively large motion for extremely precise work. With each motor step, a small amount of shaft rebounding is possible, thus exciting vibrational noise.

Klinger's mini-step feature divides each full step by 10 and simultaneously increases the pulse rate by 10, resulting in less shaft rebounding and settling effect, higher resolution without sacrificing speed and virtually eliminating troublesome resonance.

BUY ONE SUPERIOR CONTROLLER. NOT TWO.

You can't buy a better programmable motor controller than the Klinger MC4. And since you only have to buy one for both types of motors, you'll actually save time and money and not have to rewrite extensive software. Just slip in the modular drive card and you're ready to go.

To learn more about Klinger's programmable motor controllers, micropositioners and systems, send for our free micropositioning handbook. Write or call Klinger Scientific Corporation, 999 Stewart Avenue, Garden City, NY 11530. (516) 745-6800.

KLINGER SCIENTIFIC

Building better positioning systems, piece by perfect piece.

U.S.A. Headquarters: 999 Stewart Avenue, Garden City, NY 11530 (516) 745-6800.
Regional Offices: Northern California (415) 969-0247; Southern California (714) 999-5088. Worldwide distribution network: Contact Micro-Controle, Z.I. de St. Guenault, B.P. 144, 91005 Evry Cedex, France. Tel.33(1)64.97.98.98. FAX 33(1)60.79.45.61.

Circle Reader Action No. 368

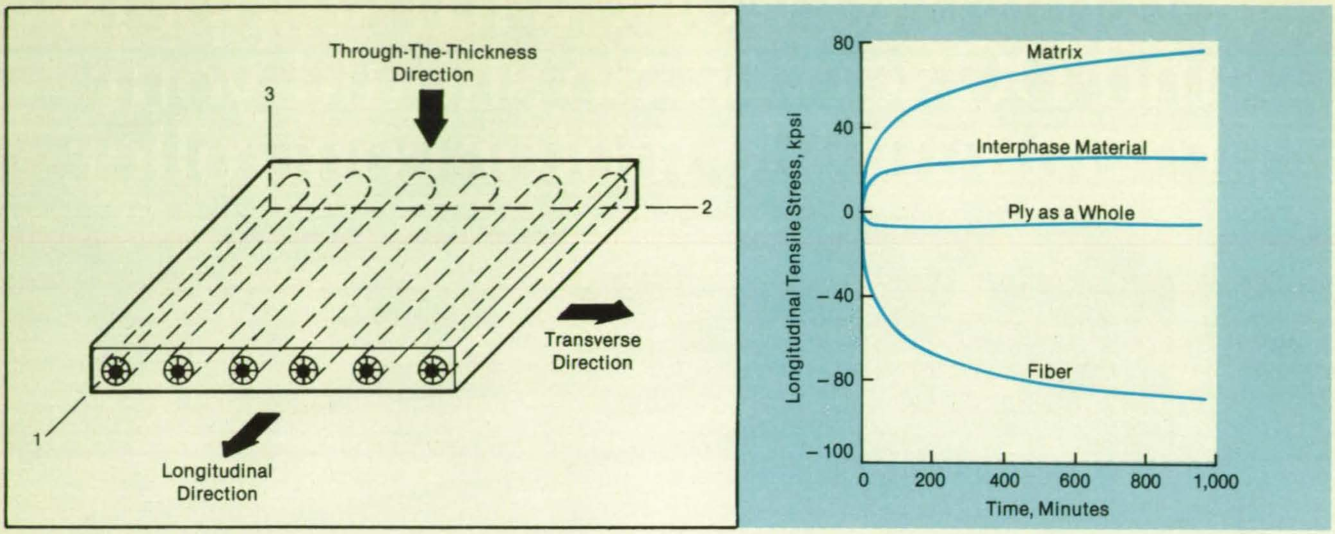

Figure 2. As a **Metal/Fiber Composite Cools** below the fabrication temperature, stresses develop in the constituents because each constituent has a different coefficient of thermal expansion.

Carboranylmethylene-Substituted Cyclophosphazene Polymers

A new synthesis produces unusual electrical and chemical properties.

Ames Research Center, Moffett Field, California

A new class of polymers is based on cyclophosphazene monomers substituted with carboranylmethylene groups. The monomers are thermally polymerizable to carboranylmethylene-substituted phosphazene polymers, which are useful as thermally stable coatings. Since these compounds act as ligands for transition metals, metallocarboranylmethylene phosphazene polymers have also been synthesized and can act as immobilized-catalyst systems. Other useful forms of the

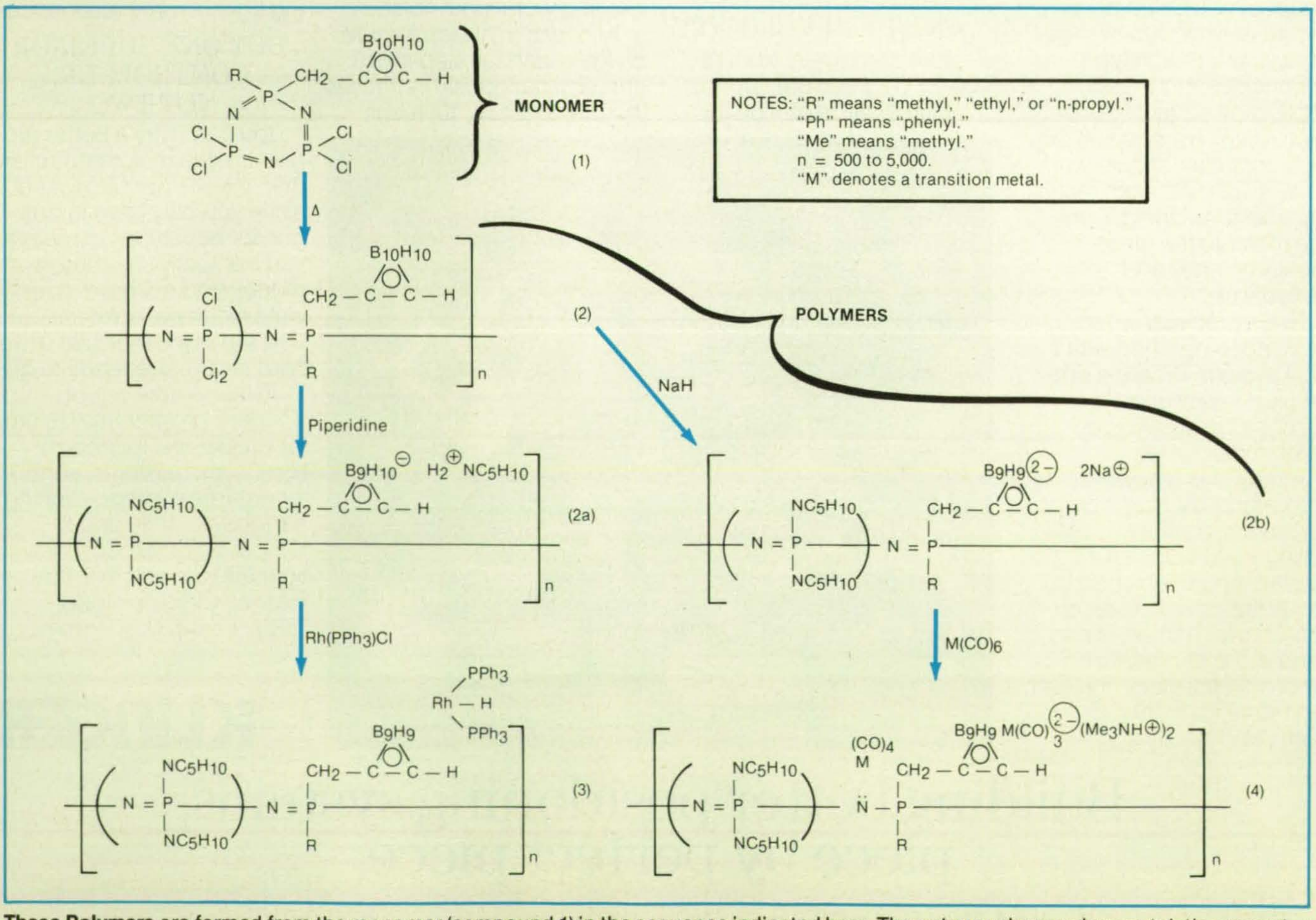

These Polymers are formed from the monomer (compound 1) in the sequence indicated here. The polymers have unique catalytic properties and are thermally stable.

GREAT BOOKS IN PHOTONICS...

EVERYTHING YOU NEED TO KNOW TO SELECT THE RIGHT PHOTOSENSITIVE DEVICES — SEND FOR THEM TODAY!

Send today for the compendium of photosensitivity knowledge. Described in detail is the world's most complete line of photosensitive devices — Hamamatsu's! You'll have at your fingertips the precise information you need to specify the right device for each application!

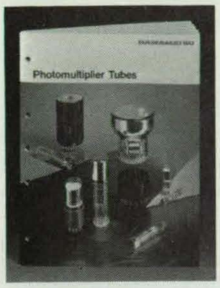

PHOTOMULTIPLIER TUBES FOR EVERY NEED This 68-page catalog details 18 PMT characteristics including spectral response, luminous sensitivity, ground polarity, dark current and hysteresis for the most complete line of head-on and side-on types, ⅜"-20 inch diameter. Selection guide with specifications and dimensional outlines help you make the best choice.

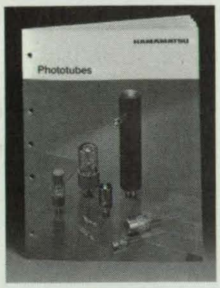

PHOTOTUBES — This 18-page catalog includes a selection guide, spectral response charts, dimensional outlines and specification charts for more than 40 head-on and side-on phototubes, UV detectors, vacuum phototubes, gas-filled and biplanar phototubes.

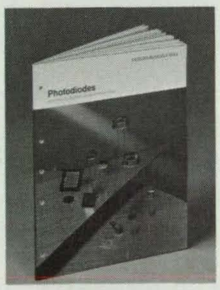

PHOTODIODES — Silicon, PIN Silicon, GaAsP, GaP, Avalanche This 44-page catalog provides spectral range, response time, temperature characteristics, linearity and specifications for UV to IR silicon, visible to IR silicon, GaAsP and GaP photodiodes.

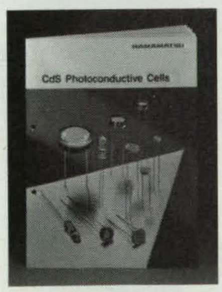

PHOTOCONDUCTIVE CELLS CdS, CdSe This 16-page catalog describes performance characteristics and specifications of various photoconductive cells used in exposure meters, auto dimmers, musical instruments, flame monitors, street light controls and other applications.

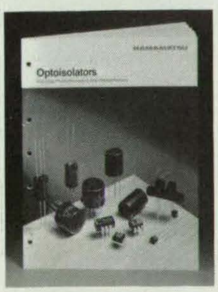

OPTOISOLATORS Single and multi-element LED-CdS optoisolators, LED phototransistors, Lamp CdS and opto-interrupters are described. Photos and diagrams illustrating physical characteristics and complete specifications are provided in this 18-page catalog.

Call or write to receive one or all ten catalogs.

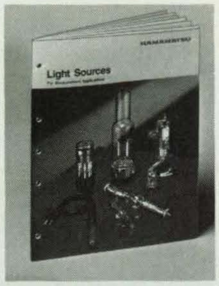

LIGHT SOURCES — Deuterium, Xenon, Mercury-Xenon, Hollow Cathode, etc. This 24-page catalog provides information about the most complete line of light sources for scientific instruments. Specifications are provided which define the high stability and dependability. Super-quiet xenon lamps are among the special light sources described.

PHOTOMULTIPLIER TUBES FOR SCINTILLATION COUNTING AND HIGH ENERGY PHYSICS This 30-page catalog provides a quick reference of PMTs with special performance characteristics. Energy resolution, pulse linearity, response time and application information are included.

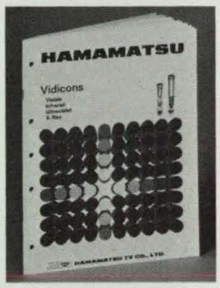

VIDICONS — Visible, IR, UV, X-Ray This 24-page catalog provides a cross-reference of vidicon types and typical applications in addition to dimensional outlines, application photos and complete specifications.

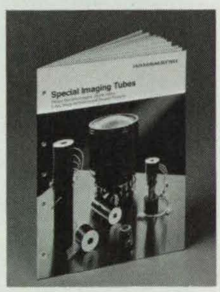

SPECIALTY IMAGING TUBES — This 25-page catalog contains a number of new types of photonic devices for capturing static and transit images. An ideal source of ideas for new types of instrumentation.

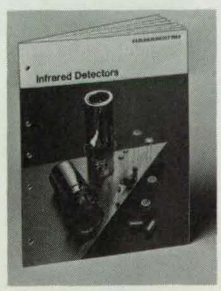

INFRARED DETECTORS — PbS, PbSe Cells; Ge, InAs, InSb Cells; Photon Drag Detector; Pyroelectric Detectors & More This 36-page catalog describes IR detectors with various elements and configurations. Extensive diagrams, characteristic graphs and glossary accompany performance specifications.

OTHER CATALOGS AVAILABLE:
Accessories for Photomultiplier Tubes, Image Intensifier Tubes, PCD Linear Image Sensors

HAMAMATSU

HAMAMATSU CORPORATION • 360 FOOTHILL ROAD, P.O. BOX 6910, BRIDGEWATER, NJ 08807 • PHONE: 201/231-0960
International Offices in Major Countries of Europe and Asia.

Circle Reader Action No. 471

polymers (both with and without metals) include fibers, films, moldings, and solvent-swelled gels.

The starting material is commercially available hexachlorocyclophosphazene. This compound is reacted with $[Bu_3 PCuI]_4$ (where "Bu" means "butyl") in the presence of RMgCl (where "R" means "methyl," "ethyl," or "n-propyl"). It is then treated with isopropyl alcohol, followed by propargyl bromide in the presence of methyllithium, followed next by decaborane in acetonitrile and benzene. The resulting compound is the carboranylmethylene-substituted cyclotriphosphazene monomer.

The figure shows the sequence in which the polymers are formed from the monomer. The first step is to thermally polymerize the monomer (compound 1) by raising it to a temperature in the range of 225 to 300 °C. The polymer thus formed (compound 2) can be used as is or converted to less-reactive compound 2a by treating it with piperidine or another cyclic amine to remove the relatively reactive chlorine atoms attached to the phosphorus atoms. When treated with a rhodium complex [for example, $Rh(PPh_3)Cl$, as in the figure], compound 2a becomes compound 3, which is useful as a catalyst for the hydrogenation of butenes to butanes at about 30 °C.

Compound 2a can also be treated with sodium hydride to produce compound 2b, which is useful as an intermediate in the production of polymers containing metallocarbonyl groups. Compound 2b is treated with the carbonyl compound of the metal to be complexed with the polymer, along with trimethylammonium chloride, while the reacting mixture is irradiated with ultraviolet light.

This work was done by Harry R. Allcock and Angelo G. Scopelianos of Pennsylvania State University for **Ames Research Center**. *For further information, Circle 128 on the TSP Request Card.*

Inquiries concerning rights for the commercial use of this invention should be addressed to the Patent Counsel, Ames Research Center [see page 16]. Refer to ARC-11370.

Electrochemical Growth of Crystals in Gels

Nucleation and growth rates are readily controlled.

Langley Research Center, Hampton, Virginia

A technique has been developed to grow crystals by controlling the rate of transfer of one component into the crystallization volume. This method involves the electrochemically controlled generation of one of the precipitation species, coupled with a diffusion barrier.

The new procedure, which can be extended to other crystals, was developed in connection with the formation of lead tin telluride by the reaction in gels of the metal ions with telluride ions. The principal difficulty in dealing with solutions of telluride ions is that the ions are easily oxidized by many impurities found in solutions. Consequently, in this new technique the telluride ions are formed in situ.

An electrically conductive gel is prepared by the use of potassium acetate in place of the usual distilled water. While still fluid, the gel is poured into the bottom of an inverted sintered-glass Gooch crucible. When the gel sets, the crucible is inverted and mounted inside a beaker (see figure). If desired, sites of nucleation and subsequent crystal growth can be established by gently pricking the gel with a very thin platinum wire or glass fiber to form small holes. A lead sheet is fitted to the inside of the outer beaker, and a piece of tellurium is mounted on the inside of the Gooch crucible. A 1-M solution of lead (II) acetate is poured into the outer beaker, and a 50-percent solution of phosphoric acid is poured into the Gooch crucible.

A constant-voltage source is applied in such a way that the tellurium is the cathode. By regulation of the voltage and current, the telluride concentration and the subsequent extent of supersaturation can be regulated to provide the conditions most suitable for crystal growth. Voltages on the order of 2 to 3 Vdc with currents of

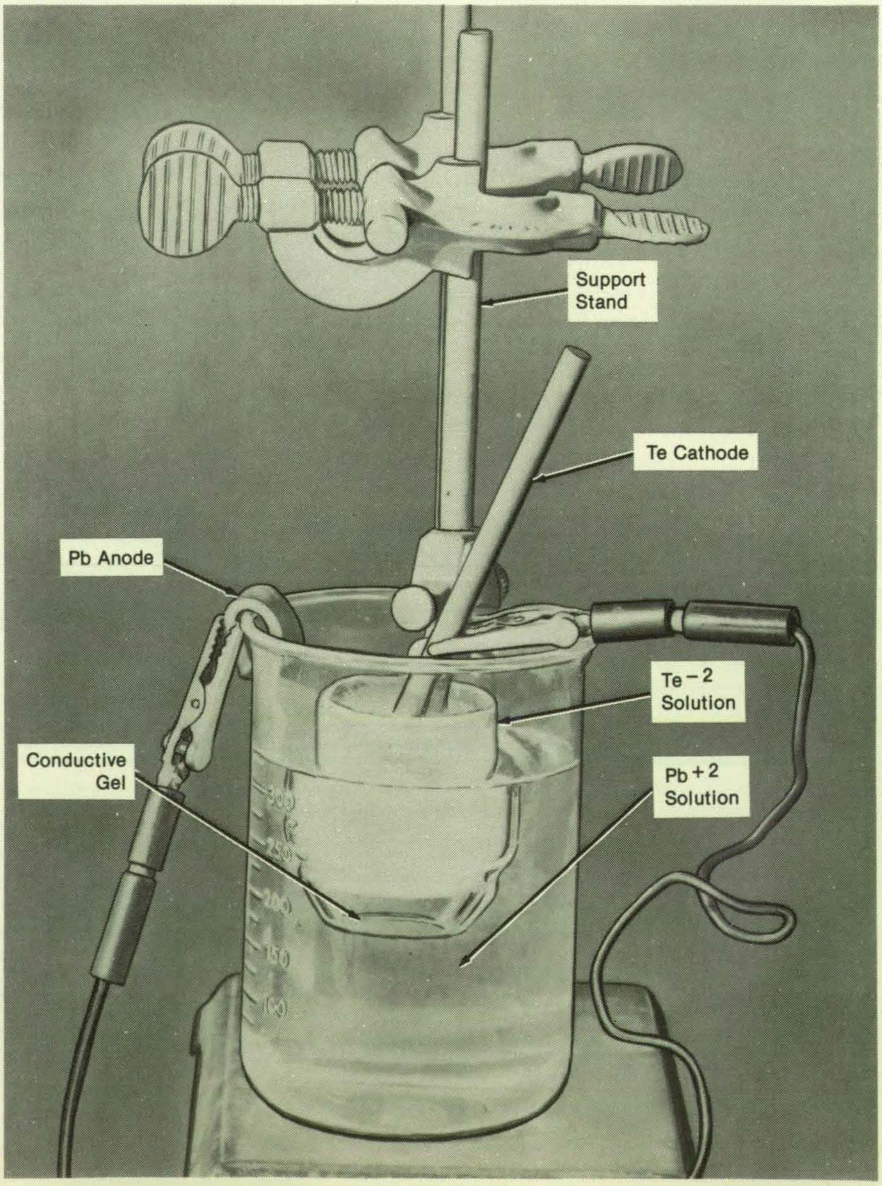

The **Electrochemical Gel Cell** is used for the control of mass flow.

10 to 15 mA have proved suitable.

Although this method was developed for lead telluride, it is generally applicable for the electrochemical growth of any crystals that are formed from the reaction of ionic species generated at cathodes and anodes. The greatest advantages of this method are the ease with which nucleation and growth rates can be controlled and the simplicity with which the concentrations of ions that are easily oxidized or reduced can be maintained.

This work was done by Patrick G. Barber and James Coleman of Longwood College for **Langley Research Center**. *For further information, Circle 91 on the TSP Request Card.*

Inquiries concerning rights for the commercial use of this invention should be addressed to the Patent Counsel, Langley Research Center *[see page 16]*. *Refer to LAR-13608.*

Contamination Barrier for Contour-Molding Material

A release agent prevents the molding compound from adhering to or contaminating the surface.

Marshall Space Flight Center, Alabama

A soap-based cleaning agent enables the making of contamination-free molds of surface contours. The cleaning agent, Turco 4215 NCLT, forms a barrier that prevents the silicone molding compound from sticking to the surface and leaving a contaminating residue [see the companion article, "Molding Compound for Inspection of Internal Contours" (MFS-29243)]. It is no longer necessary to grind or polish the surface to remove the residue.

The cleaning agent is applied to the surface and allowed to dry completely to form a film. The molding compound is applied to the surface and allowed to cure. When the molding compound has been removed, the film is easily wiped away with deionized water.

This work was done by James F. Adams of Rockwell International Corp. for **Marshall Space Flight Center**. *No further documentation is available.*
MFS-29240

Molding Compound for Inspection of Internal Contours

This material is clean, sets rapidly, and is easy to use.

Marshall Space Flight Center, Alabama

A silicone elastomer, Citrocon (or equivalent), commonly used in dentistry, in combination with a mold-release agent [see the companion article, "Contamination Barrier for Contour-Molding Materials" (MFS-29240)], speeds and facilitates the making of impressions of interior surfaces so that the surface contours can be examined. A pliable semisolid material, the elastomer does not have to be contained by temporary dams or walls as do the viscous liquid room-temperature-vulcanizing (RTV) compounds previously used to mold internal contours. The elastomer also cures faster than do the RTV compounds — in about one-fourth the time.

The elastomer can easily be moved around in a cavity until the required location is found. An impression of the surface is then made by applying a small force to the elastomer and waiting for it to cure.

This work was done by Jim Adams and Steve Ricklefs of Rockwell International Corp. for **Marshall Space Flight Center**. *No further documentation is available.*
MFS-29243

Calculating Percent Gel for Process Control

The reaction state of a thermosetting resin is tracked to assure desired properties.

Lyndon B. Johnson Space Center, Houston, Texas

The percent gel has been found to be an important parameter for monitoring the progress toward cure of thermosetting resins. The only measurement required to track the accumulated progress in a given sample is its history of temperature versus time. The percent gel is particularly useful in adjusting the process conditions to achieve desired properties in resin-impregnated laminates.

In a typical process, a laminate or other composite part is impregnated with a reacting resin in the "B stage," which is an intermediate chemical state in which the resin softens while hot, allowing the part to be molded. The reaction rate increases with temperature, and the reaction proceeds until the resin is no longer plastic while hot. This state of reaction completion is defined as 100-percent gel, and intermediate states are characterized by smaller percentages.

Because of the temperature dependence of the reaction rate, the condition of the resin at the time of processing depends on the previous temperature history. Experiments with a representative phenolic resin show that the percent gel (that is, the amount of advancement toward cure) at a given moment is simply the sum of gel percentages accumulated during previous exposures to various temperatures, and that at an absolute temperature T, the rate of gel r_g follows an Arrhenius equation of the form

$$r_g = k \exp(-E/RT)$$

where k = the specific reactivity in percent per unit time, E = the activation energy per mole of reactant, and R = the ideal-gas constant (see figure). The percent gel G reached after exposure to a series of temperatures T_i for intervals of time t_i since initial preparation is thus given by

$$G = k\Sigma t_i \exp(-E/RT_i)$$

Experiments have shown that such properties as the flexural strength, porosity, and thickness of a laminated part depend on the percent gel at the moment of application of pressure in an autoclave at the final high-pressure, high-temperature molding step. Thus the properties of the finished part can be controlled somewhat by controlling the times at various temperatures during the earlier stages of resin storage and part preparation. Since parts often arrive at the autoclave at different degrees of cure, each can be heated in the autoclave for the time needed to achieve the

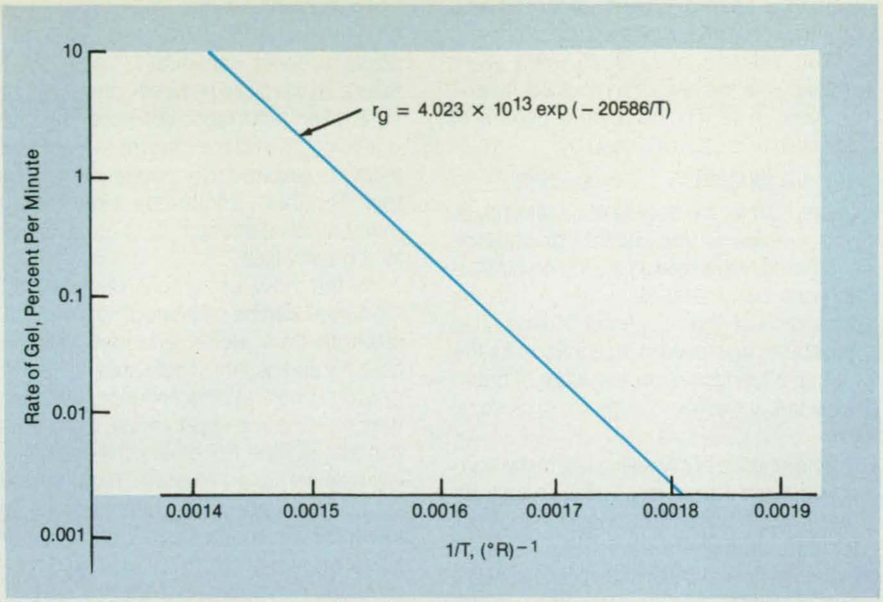

The **Rate of Gel** was determined as a function of temperature by measuring the time to gel of a part of graphite fabric impregnated with Hexcel R120 (or equivalent) phenolic resin.

specified percent gel before the application of final pressure, thereby assuring uniformity from part to part.

This work was done by Charles Neal Webster and Robert O. Scott of LTV Aerospace Corp. for **Johnson Space Center**. *For further information, Circle 111 on the TSP Request Card.*

Inquiries concerning rights for the commercial use of this invention should be addressed to the Patent Counsel, Johnson Space Center *[see page 16]*. *Refer to MSC-21169.*

Books and Reports

These reports, studies, handbooks are available from NASA as Technical Support Packages (TSP's) when a Request Card number is cited; otherwise they are available from the National Technical Information Service.

Stiffness Properties of Laminated Graphite/ Epoxy Cylinders

The dominant constituent property is the longitudinal Young's modulus of the fibers.

A report discusses the stiffnesses of cylindrical shells formed from composite graphite/epoxy laminates, as calculated from traditional composite-lamination theory. Such shells are being evaluated for use as cases for solid-fuel rocket motors. The stiffness results were compared with quasi-experimental stiffnesses developed from pressure tests of cylindrical bottles. The sensitivities of stiffnesses to variations in the constituent materials and in geometric parameters were examined with the help of two computer programs, which are included in an appendix to the report.

The macromechanics of laminated cylinders are described by a matrix constitutive equation for cylinder walls that was developed from classical lamination theory. The column matrix of the force and moment vectors is expressed in terms of the extensional-stiffness matrix, the coupling-stiffness matrix, the bending matrix, and the column matrix of the midplane strains and plate curvatures.

The properties of the graphite-fiber constituent of the composite that were varied include the longitudinal and transverse Young's moduli, E_1 and E_2, respectively, the shear modulus G_{12}, and the primary Poisson's ratio ν_{12}. Also varied were the Young's modulus, the shear modulus, and the Poisson's ratio of the epoxy matrix. The effect of variations in the helical winding angle was also studied; in forming the cylinders, the fibers in each lamination are parallel to each other but may be at different angles in different layers.

Expressions based on the rule of mixtures are used to estimate E_1 and ν_{12} of the composite from the values of the corresponding properties of the graphite fiber and the epoxy matrix. Empirical equations are used to estimate E_2 and G_{12}.

In general, it was found that the longitudinal Young's modulus of the fibers was the dominant contributor to the stiffness of the laminate. With the exception of the Poisson's ratio, the general stiffness parameters of the laminate change 82 percent of the proportion of a small change in the longitudinal Young's modulus of the fibers. On the other hand, the stiffness of the laminate is insensitive to large changes in the Poisson's ratio of either the fiber or the matrix, even though changes in these ratios cause the Poisson's ratio of the laminate to vary widely. The largest contributions of the transverse Young's and the shear moduli of the fiber to any laminate stiffness term were 8.7 and 10 percent, respectively. The contributions of the same moduli to the Poisson's ratio of the laminate were 3.4 and 15 percent, respectively.

In the simplified case of micromechanical theory of plane stress in laminates, which is adequate for thin cylinders, only the four elastic constants E_1, E_2, ν_{12}, and G_{12} are required. These can be measured experimentally by using standard laboratory tests or by a combination of micromechanical theory and pressure testing of tubes.

This work was done by R. Noel Tolbert of Tennessee Technical University for **Marshall Space Flight Center**. *To obtain a copy of the report, "Stiffness Properties for Dynamic Modeling of Composite Graphite-Epoxy Cylindrical Orthotropic Shells," Circle 6 on the TSP Request Card.*
MFS-27157

Nonisothermal Crystallization in PEEK/Fiber Composite

Several features of the crystallization process are attributable to the fibers.

A report describes experiments in the nonisothermal crystallization of poly(etheretherketone)(PEEK) in APC-2, a composite of PEEK matrix reinforced with carbon fibers. PEEK is a high-performance, semicrystalline thermoplastic with properties that make it attractive for use in composites. Such properties as toughness and resistance to impact depend on the degree of crystallinity and the microstructure, which are very sensitive to processing conditions. Consequently, to understand the relation between processing and properties, it is necessary to study the kinetics of crystallization of the neat PEEK resin and of composites. Previous studies had addressed the related issues of isothermal crystallization of the neat resin and the ultimate degree of crystallinity achieved as a function of the rate of cooling.

In the experiments, pieces of the composite weighing less than 5 mg were placed in aluminum differential-scanning-calorimeter (DSC) pans and heated to 400 ° for 10 minutes to assure complete melting. The specimens were then cooled in the DSC at various constant rates ranging from 1 to 20 °C/min. The relative degrees of crystallinity as functions of time were inferred by integration of the rates of flow of heat from the specimens measured in the DSC. The ultimate degrees of crystallinity were estimated from wide-angle x-ray scattering and from areas under DSC exotherms of similarly treated specimens.

The kinetics of crystallization were studied with the help of a modified Avrami analysis, in which the relative degree of crystallinity is approximated by

$$X_c(t)/X_c(\infty) = 1 - \exp(-Kt^N)$$

where $X_c(t)$ = the degree of crystallinity at time t, $X_c(\infty)$ = the ultimate crystallinity, and K and N are related via the crystallization-rate parameter, $K^{1/N}$, which has the dimension of the reciprocal of time. This parameter was used in an equation for the rate as a function of temperature to determine the activation energy for crystallization.

The kinetics of crystallization in the composite were found to be significantly different from those of the neat resin. Such features as higher initiation temperature, higher temperature of maximum heat flow, and greater relative conversion to crystallinity via primary processes can be attributed to the presence of the carbon fibers. The fibers act as nucleation sites, which contribute to greater overall crystallinity. The fibers initiate the crystallization earlier (at higher temperature) and thereby also decrease the rate parameter compared to that of the neat resin.

For the composite material, the change from the primary kinetics of free crystal growth to slower secondary kinetics occurred at about 50 percent relative conversion. The activation energy for the primary process of crystallization was found to be larger than that of the neat PEEK resin; the reasons for this are still under investigation.

This work was done by Peggy Cebe of Caltech for **NASA's Jet Propulsion Laboratory**. *To obtain a copy of the report, "Non-Isothermal Crystallization of Poly (etheretherketone) Aromatic Polymer Composite," Circle 62 on the TSP Request Card.*
NPO-17226

Estimating the Crack-Extension-Resistance Curve

The curve can now be obtained from residual-strength data alone.

A new analytical method enhances the capability to determine the crack-extension curve or "R-curve" of a sample. One of the most powerful techniques available to an analyst of fractures of materials, the "R-curve" can be used to predict failure loads for any initial crack size in any specimen or structure for which a stress-intensity analysis is available. For accurately predicting failure loads for stiffened-skin aircraft panels and bulkhead components, an accurate determination of the "R-curve" is necessary.

To determine the "R-curve," precracked specimens are tested with special displacements continually measured to failure. In the past, however, often the only data taken (and reported) were the initial crack length and the maximum load. New tests are required to accurately determine the "R-curve" accurately even though many residual-strength data are available in company files.

In the new analytical method, the "R-curve" can be estimated from residual-strength data alone, provided that the quantity and quality of data are sufficient to permit numerical differentiation with confidence. For some applications, the estimation may suffice. For others, the estimation will help set up an efficient "R-curve" test plan. The method has been verified by using data from the literature and by participation in a predictive blind round-robin program.

This work was done by Thomas W. Orange of **Lewis Research Center**. *Further information may be found in NASA TM-87182 [N86-18750/NSP], "Estimating the R-Curve from Residual Strength Data."*

Copies may be purchased [prepayment required] from the National Technical Information Service, Springfield, Virginia 22161, Telephone No. (703) 487-4650. Rush orders may be placed for an extra fee by calling (800) 336-4700.
LEW-14509

Investigation of Epoxy Curing

A kinetic model describes major features of the curing process.

A report describes an investigation of the curing of an epoxy resin to be used in a carbon-fiber/epoxy version of the cases of the Space Shuttle booster rockets. The purpose of the investigation was to develop a physical and chemical kinetic model of the curing reaction for use in the control, verification, and optimization of the curing process to satisfy engineering objectives.

The resin studied was a mixture of a commercial epoxy and a reactive diluent. The curing agent was a commercial mixture of aromatic amines. The rocket case is to be made by winding carbon filaments impregnated with the mixture of resin and curing agent, partially curing the epoxy at room temperature, and completing the cure in an oven.

During the cure at room temperature, the resin gels and/or vitrifies, constraining the motion of the reacting molecules and thereby decreasing the rate of reaction to a value low on the time scale of the 2 to 3 weeks required for winding. Consequently, about 30 percent of the epoxy functional groups remain unreacted after the room-temperature cure. During the subsequent cure at higher temperatures, the resin may alternately soften and harden, allowing the curing reaction to continue.

A differential scanning calorimeter was used to determine the onset and extent of hardening as a function of temperature and time. Hardening and softening were considered to occur at the same rate and temperature. The transition temperature was defined as the temperature at which hardening begins. The extent of hardening was defined as the ratio of energy absorbed at a given point in a transition during a differential-scanning-calorimetry run to the total energy absorbed during that transition. The extent of reaction of the epoxy functional groups was also studied by Fourier-transform infrared spectroscopy. The transition temperature was correlated with the number average molecular weight. The number average molecular weight of the reacting mixture was measured as a function of time by dissolving the mixture in chloroform and measuring the resulting decrease in the vapor pressure.

The experimental data were interpreted in terms of an engineering model that accounts for the chemical and physical kinetics of the curing reaction. The chemical model includes the formation of an amine/water complex that reacts with the epoxy. The formation of an amine/epoxy complex and its decomposition into linear and cross-linked polymers are the steps that determine the reaction rate in the regime controlled by chemical kinetics.

Hardening is considered a zero-order reaction that begins when the transition temperature equals the actual temperature of the reacting mixture. As determined by differential scanning calorimetry, the hardening reaction has an activation energy typical of values associated with hydrogen bonding. An empirical correlation was developed to predict the transition temperature as a logarithmic function of the number average molecular weight during the room-temperature cure, when little cross-linking occurs.

The model predicts well the conversion of epoxy during the room-temperature and oven curing stages. However, the model needs to be improved to account for any reaction that may continue in the solid state and to predict the transition temperature more accurately, especially when cross-linking occurs at high temperatures.

This work was done by D. E. Cagliostro and A. Islas of **Ames Research Center** *and Ming-Ta Hsu of H C Chem. Corp. To obtain a copy of the report, "A Cure-Rate Model for the Shuttle Filament-Wound Case," Circle 23 on the TSP Request Card.*

Inquiries concerning rights for the commercial use of this invention should be addressed to the Patent Counsel, Ames Research Center [see page 16]. Refer to ARC-11810.

Microstructure of MnBi/Bi Eutectic Alloy

The effect of convection is examined.

A collection of three reports describes studies of the directional solidification of MnBi/Bi eutectic alloy. Fibers of MnBi are formed in a Bi matrix, with fiber dimensions and spacing that depend upon the conditions at and around the advancing solidification front. Prompted by the observation that the fibers formed on Earth are coarser than fibers formed in outer space (where there is no gravitationally driven convection) under otherwise identical conditions, the authors have engaged theoretical and experimental techniques to elucidate the effect of convection and other phenomena on the MnBi/Bi microstructure.

Two of the reports, "Influence of Convection on Lamellar Spacing of Eutectics" and "Influence of Convection on Eutectic Microstructure," establish the theoretical foundation for the remaining document. These reports seek to quantify the effect of convection on the concentration field of a growing lamellar eutectic. Numerical simulations lead to a number of conclusions regarding the coarsening effect of convection, including the following:

- The lamellar spacing, λ, increases with the square of the convective mixing.
- The influence of convection on λ decreases with an increase in the speed of the solidification front.
- The maximum increase of λ occurs where the lamellae are perpendicular to the flow.
- The lamellae tend to grow in the upstream direction.
- The increase in λ depends weakly on the eutectic composition and is a maximum in a 50:50-volume-percent eutectic.
- In a cylindrical ampoule held with its axis vertical, either not rotating or in alternating rotation about the axis, and with solidification proceeding along the axis, λ should increase with radial distance from the axis, both for gravitationally driven and rotationally driven convection.

The remaining report, "Study of Eutectic Formation," begins by continuing the theoretical developments. It notes that the effect, in the foregoing theory, of gravitation/buoyancy-driven convection alone is insufficient to explain the twofold increase in λ from solidification in space to solidification on Earth. The authors advance a partial explanation by discarding a previous simplistic assumption regarding the degree of undercooling and deriving equations that take account of the effect, upon undercooling, of the decrease in the eutectic mass fraction at the solidification interface and of the curvature of the interface. They also note that, although the theory was developed for lamellar eutectics, the increase in λ might be much larger in fibrous eutectics like MnBi/Bi, especially if the MnBi fibers extend out from the Bi matrix into the melt.

In alternating-spin, directional-solidification experiments, stirring affected the microstructure profoundly, even at high freezing rates: this contradicted the theoretical prediction that the effect of convection should die out at high freezing rates. At low freezing rates with 200-r/min stirring, no MnBi was found at the center of the ingot; there is no theoretical explanation for this.

A new technique under development by one of the authors will help to reveal the three-dimensional microstructures of alloys. The alloy specimen is etched in an electrochemical cell while it is monitored by time-lapse videotaping through a zoom microscope. The best candidate etching solution to date has been a mixture of sulfuric and phosphoric acids with water. This solution remains optically clear and etches the surface uniformly.

This work was done by William R. Wilcox, G. F. Eisa, B. Baskaran, and Donald C. Richardson of Clarkson University for **Marshall Space Flight Center**. *To obtain copies of the three reports, Circle 68 on the TSP Request Card.*
MFS-27174

Computer Programs

COSMIC: Transferring NASA Software

COSMIC, NASA's Computer Software Management and Information Center, distributes software developed with NASA funding to industry, other government agencies and academia.

COSMIC's inventory is updated regularly; new programs are reported in *Tech Briefs*. For additional information on any of the programs described here, circle the appropriate TSP number.

If you don't find a program in this issue that meets your needs, call COSMIC directly for a free review of programs in your area of interest. You can also purchase the 1988 *COSMIC Software Catalog*, containing descriptions and ordering information for available software.

COSMIC is part of NASA's Technology Utilization Network.

COSMIC® — *John A. Gibson, Director,* (404) 542-3265
The University of Georgia, 382 East Broad Street, Athens, Georgia 30602

Computer Programs

These programs may be obtained at a very reasonable cost from COSMIC, a facility sponsored by NASA to make computer programs available to the public. For information on program price, size, and availability, circle the reference number on the TSP and COSMIC Request Card in this issue.

Electronic Systems

Spectrum/Orbit-Utilization Program

Interferences among geostationary satellites determine allocations.

Current and projected demands on the use of the geostationary orbit/spectrum resource require an analytical tool for determining the interferences among operating and planned communications satellite systems. Prior to development of a satellite system, a detailed analysis must be performed to determine the expected interference environment during operations. Such calculations determine the permitted spacing between satellites and the limits on the capacity of a particular orbit/spectrum segment.

The Spectrum/Orbit Utilization Program (SOUP) is an analytical computer program for determining the mutual interferences among many geostationary-satellite communication systems operating in a given scenario. The major computed outputs are the carrier-to-interference ratios at receivers at specified stations on Earth. This information enables the determination of the acceptability of planned communication systems.

SOUP has been developed during the last 14 years. In 1970, an early version was used to evaluate the general interference problem in satellite communications. In 1971, the program was adapted for the evaluation of the initial Domestic Satellite applications in the United States. Until 1981, the program underwent a series of minor modifications and improvements. In late 1981, SOUP was selected to be the analysis program used at the 1983 Regional Administrative Radio Conference for the broadcasting satellite service at 12 GHz in the Western Hemisphere. A number of major modeling changes were made, and inputs and outputs were modified to interface with other programs and the several data bases used at the conference. The current version of SOUP is SOUP 5 Version 3.10.

SOUP calculates the mutual interference among a number of communications satellite systems. The feederlink uplink carrier-to-interference ratio (C/I) is calculated at each satellite. At each Earth-station receiving point, the downlink C/I is calculated, taking into account interferences from all other satellites in the geostationary orbit. Of course, only those satellites operating at nearby frequencies are considered.

The program, as presently configured, can handle up to 300 downlink service areas and 300 feederlink service areas, where each service-area pair is associated with a satellite in the geostationary orbit. The downlink service area and the feederlink service area associated with a single satellite are not required to be the same, although in most cases they are assumed to coincide. There can be up to 1,600 feederlink transmitter sites and 4,500 Earth-station receiving sites. The dimensions of the arrays of numbers in the program can be increased at the expense of increased memory requirements and longer running times.

When the total C/I is calculated at an Earth-station receiver, account is taken of interferers operating at cochannel, adjacent-channel, and second-adjacent-channel frequencies. Downlink and feederlink interferences are mathematically combined, and the total interference is compared to a given requirement that varies with type of modulation, grade of service, and other parameters. Earth-station receivers that exceed a required C/I called the protection ratio are said to have positive margins, while those that fail to meet the requirement are said to have negative margins.

For some systems, communications performance may be specified in terms other than C/I; e.g., picowatts of noise added to a telephone channel or the bit-error rate in a digital system. In these cases, a receiver transfer constant is used to transform from a C/I to a measure of output performance.

The calculations performed for each test point have technical parameters that are variable for each service area. Attenuation by rain and other effects on propagation can be taken into account. Either circular or linear polarization can be used. Additional calculated quantities include the power flux density, received power, received carrier-to-noise ratio, and spacecraft power.

SOUP is written in FORTRAN and has been found to be easily transferable from machine to machine. It has been run on IBM 370, VAX, Amdahl 5480, Prime-400, and Siemens computers.

This program was written by Edward F. Miller of **Lewis Research Center** *and Paul Sawitz and Fred Zusman of ORI, Inc. For further information, Circle 142 on the TSP Request Card.*
LEW-14461

Mathematics and Information Sciences

Ada Linear-Algebra Program

Routines are provided for common scalar, vector, matrix, and quaternion operations.

A computer program extends the Ada programming language to include linear-algebra capabilities similar to those of the HAL/S programming language. The package is designed for such avionics applications as software for the Space Station.

In addition to the HAL/S built-in functions, the package incorporates the quaternion functions used in the Shuttle and Galileo projects and routines from LINPACK that solve systems of equations involving general square matrices. Language conventions in this package follow those of HAL/S to the maximum extent practical and minimize the effort required for writing new avionics software in Ada and translating existing software to Ada.

Valid numeric types are scalar, vector, matrix, and quaternion. (Quaternions are four-component vectors used here to represent motion between coordinate frames.) Infix operators are used instead of function calls to define dot products, cross products, quaternion products, and mixed scalar·vector, scalar·matrix, and vector·matrix products.

There are two generic packages: one for floating-point components and one for integer components. The actual component types are selectable by the user and are passed as formal parameters to the generic packages. The floating-point package is instantiated for double- and single-precision components, the integer package is instantiated for double-precision integer components, and the three instantiations are collected in a single package. Each floating-point instantiation offers 71 subprograms, and the integer instantiation offers 56.

All the common vector, matrix, and quaternion arithmetic and input/output operations are provided. HAL/S functions include ABVAL, UNIT, TRACE, DET, INVERSE, TRANSPOSE, and IDENTITY. Quaternion functions include INVERSE, CONJUGATE, and functions that convert between quaternion and matrix representations of coordinate rotations. LINPACK procedures include GEFA, GECO, GESL, and GEDI and are represented by eight procedures in each floating-point package.

This program was written by A. R. Klumpp and C. L. Lawson of Caltech for **NASA's Jet Propulsion Laboratory**. *For further information, Circle 78 on the TSP Request Card.*
NPO-17119

Analyzing Commonality in a System

Cost can be decreased by use of fewer types of parts.

The System Commonality Analysis Tool (SCAT) computer program was designed to aid managers and engineers in identifying common, potentially common, and unique components of a system. Commonality lowers the overall cost of a system through the use of the smallest variety of items or types of subsystems in the greatest number of applications. SCAT, through utilization of a comprehensive data base on parts, determines cost effectiveness by comparing the life-cycle costs of unique and standard configurations of parts. The SCAT data base reflects both engineering and financial data. SCAT was instituted for the analysis of commonality in the Space Station but is easily applicable to such other projects as commonality in software, which is used as an example in the detailed documentation.

SCAT incorporates three major functions: (1) a program for the creation and maintenance of a data base, (2) the analysis of commonality, and (3) such system utilities as host-operating-system commands and loading and unloading of the data base. The data base on parts contains "generic" attributes needed to calculate life-cycle costs, and "discriminating" attributes for engineering design data. SCAT selects parts that are similar, based on selection criteria defined by the user.

One can choose either of two algorithms for analysis. The direct algorithm uses supplied cost figures for design, development, testing, and first-product calculations. The relational algorithm estimates these costs based on a complexity factor (simple, medium, complex); the type of item (electrical, mechanical, and the like); and the percent of new development needed. SCAT also contains a software-commonality algorithm that requires the size of the package, the expected number of years of use, and whether the programs are critical to a mission, developed in-house, or dependent on equipment that is not yet available.

SCAT produces reports that tabulate maintenance, initial configurations, and expected total costs. By examining systems made of unique parts and systems made of parts having comparable functions, SCAT can help determine which parts are good candidates for commonality. SCAT is menu-driven and includes an online help facility.

SCAT is written in FORTRAN 77 for interactive execution. SCAT is available in two machine versions. The IBM PC version has been implemented on an IBM PC/XT-compatible computer operating under MS-DOS (V.2.0 and 3.0) with a central-memory requirement of approximately 640K of 8-bit bytes. The SCAT PC version requires a 10-MB hard disk, the commercial R:base 5000 (V1.0 or 1.01) data base, and the Micro-RIM data-base interface package, which is compatible with MicroSoft FORTRAN V.3.2 or 3.31. The VAX version of SCAT has been implemented on a VAX 11/780 and a VAX 8600 under VMS 4.X with a VT100 or VT220 terminal. The SCAT VAX version requires the commercial RIM-7 (UD 12) data base and the RIM-7 FORTRAN interface library. The program was developed in 1987.

This program was written by Alfred Pacheco and Kevin Pool of The Boeing Co. for **Marshall Space Flight Center**. *For further information, Circle 129 on the TSP Request Card.*
MFS-28271

Mechanics

Optical-Fiber Temperature Sensor

Temperature could be measured in rotating machinery without speed-limiting mechanical sliprings.

Marshall Space Flight Center, Alabama

Signals from a proposed fiber-optic temperature sensor would be transmitted across a rotary interface without electromechanical sliprings. The optical signal would be carried across a noncontacting optical slipring from the sensor on a rotating shaft to a stationary measuring circuit. The noncontacting optical connection would accommodate rotational speeds (in turbomachinery, for example) much higher than the limiting speeds of the contacting connections needed for electrical signals from thermocouples and other electrical temperature sensors.

In the sensor, the tip of an optical-fiber bundle would be inserted in a slotted hollow cylinder (see figure). A piston would sit in the hollow core of the cylinder with one end fixed in the cylinder and the other end — facing the fiber bundle ends — free to move longitudinally. The fluid, the temperature of which is to be measured, would enter the core through the slot and flow around the piston.

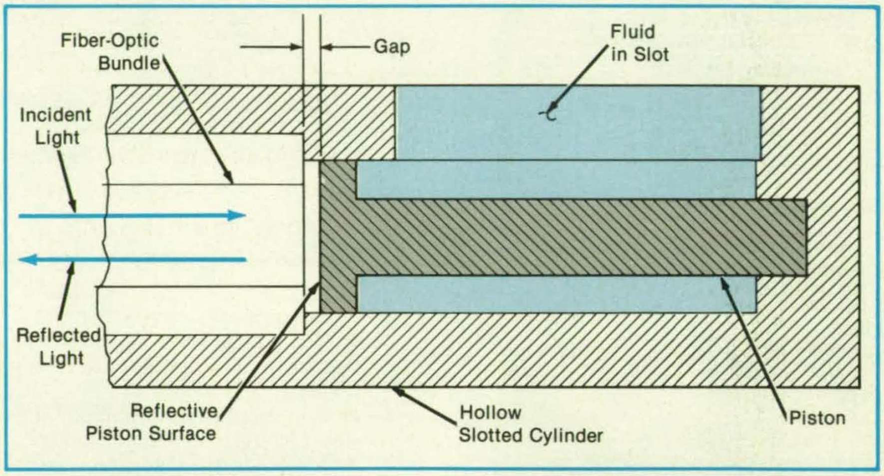

The **Gap Widens as the Temperature Rises** and narrows as the temperature falls. The light reflected from the piston face and recaptured by the fiber bundle varies accordingly.

The cylinder would be made of a material having a coefficient of thermal expansion greater than that of the piston material. Thus, when the fluid temperature rises, the gap between piston and fiber bundle would increase; and when the temperature falls, the gap would narrow. The piston would reflect less light back into the bundle when the gap is wide than when it is narrow. The amount of reflected light carried by the fiber to a light detector would therefore vary inversely with the temperature of the fluid.

This work was done by Edmund J. Roschak of Rockwell International Corp. for **Marshall Space Flight Center**. *No further documentation is available.*

Inquiries concerning rights for the commercial use of this invention should be addressed to the Patent Counsel, Marshall Space Flight Center [see page 16]. Refer to MFS-29279.

Pressure-Sealing Optical Coupling

Light signals are passed out of a high-pressure cryogenic environment.

Marshall Space Flight Center, Alabama

A design for a pressure-sealing coupling provides for the passage of optical signals between a laboratory environment and an environment filled with liquid oxygen at a pressure of 600 psi (4 MPa). In both environments, the signals are transmitted in two or more discrete light-conducting channels in fiber-optic cables. The coupling can be connected and disconnected quickly, is rugged, and resists vibration by providing a secure mount for the sensitive optical components that it contains. Designed as a feedthrough connector for a fiber-optic deflectometer in the high-pressure-oxygen turbopump of the Space Shuttle main engine, the coupling can be made in different configurations and modified to suit the requirements of other cryogenic instrumentation systems.

The coupling (see figure) maintains the alignment between an inner probe and an outer probe, both of which terminate their respective fiber-optic cables. The two probes face each other across an optical coupler, which is a rigid section of fused, coherent optical fibers. The coherent arrangement of fibers passes the discrete light channels undistorted through the coupler between the transmitting and receiving fiber ends on the facing ends of the two probes. The pressure-actuated seal around the periphery of the optical coupler constitutes the barrier to leakage between the two environments.

A nut serves as the mount for the outer probe. The outer probe is captured by a split ring at the inner end of the nut. Another split ring captures the inner probe. When the nut is threaded into the housing, the outer and inner probes are pressed against the optical coupler, spring-loaded against vibration by spring washers. The split rings enable the easy installation or removal of components and can be reached, if desired, through small access holes leading to the coupling.

The inner probe is kept from rotating by a key, slot, or half-circle shape (not shown). The outer probe is rotated in the nut until maximum signal output indicates that the optical channels in the two probes are aligned. A clamp is then tightened about the nut to fix the position of the outer probe.

This work was done by Timothy B. Irvin and Richard E. French of Rockwell International Corp. for **Marshall Space Flight Center**. *No further documentation is available.*

Inquiries concerning rights for the commercial use of this invention should be addressed to the Patent Counsel, Marshall Space Flight Center [see page 16]. Refer to MFS-29348.

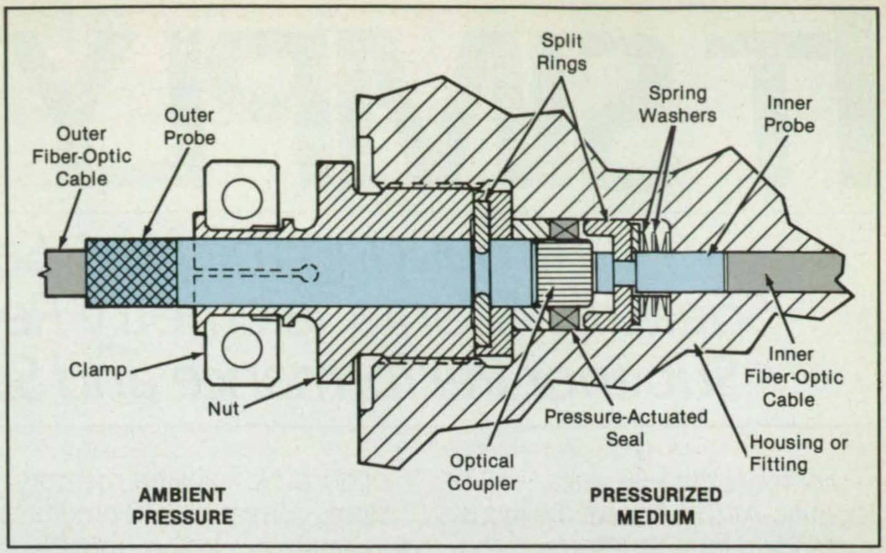

The **Optical Coupling** passes signals in fiber-optic channels across a pressure-and-temperature barrier.

Books and Reports

These reports, studies, handbooks are available from NASA as Technical Support Packages (TSP's) when a Request Card number is cited; otherwise they are available from the National Technical Information Service.

Predicting Roll Angle of a Spinning Spacecraft

Data for corrections of attitude are derived on Earth from secondary measurements.

A paper describes how the attitude of the *Pioneer 10* spacecraft has been controlled since the spacecraft lost the signal from its Sun-sensor signal in late 1983. Without the Sun-sensor signal, *Pioneer 10* cannot automatically orient itself for communication with Earth. Instead, the spacecraft must now be oriented by signals from Earth.

Launched in 1972 to study Jupiter and the properties of the interplanetary medium, *Pioneer 10* encountered Jupiter in 1973 and has since traveled on an escape trajectory away from the Sun. By 1983, *Pioneer 10* had traveled beyond the outermost known planet. It is now moving away from the Sun at a rate of almost 3 astronomical units per year.

The roll angle of the spin-stabilized spacecraft is calculated on Earth from data furnished by the imaging photopolarimeter — an instrument on the spacecraft designed to collect images of Jupiter. The roll-angle-versus-time measurements are fitted by the least-squares method with a simple parabolic curve based on the assumption of constant acceleration. The curve is then used to predict the roll angle at a specified time in the future. With calculations of the roll angle made only once a week, the roll angle of the spacecraft can be predicted more than a week ahead for timing reorientation impulses by the spacecraft thrustors.

Attitude-reorientation maneuvers based on such predictions of the roll phase have been successfully executed for several years. Predictions are made for as many as 10 days in the future from data spanning only 12 days of measurement. The average maneuver was planned by projecting the roll phase for 3 days (22,000 spacecraft revolutions) and resulted in a maneuver-execution phase error of only 11°.

Pioneer spacecraft are unique among deep-space probes in that they are spin-stabilized and are left undisturbed for periods up to several months. The roll calculations described in the paper may therefore yield insight into the environment of the solar system at great distances.

This work was done by M. A. Smith and J. W. Dyer of **Ames Research Center**. *Further information may be found in AIAA Paper No. 87-0502, "Long Term Prediction of Roll Phase for an Undisturbed Spinning Spacecraft."*

Copies may be purchased [prepayment required] from AIAA Technical Information Service Library, 555 West 57th Street, New York, New York 10019, Telephone No. (212) 247-6500.

Inquiries concerning rights for the commercial use of this invention should be addressed to the Patent Counsel, Ames Research Center [see page 16]. Refer to ARC-11788.

Evaluating Solid-Lubricant Films

The pin-on-disk tribometer provides valuable information when used properly.

A report describes experimental techniques for measuring the properties of solid-lubricant films. In addition, it discusses experimental parameters that are important in evaluating and developing new solid-lubricant materials.

The techniques are based on a pin-on-disk tribometer — a stationary, hemispherically tipped pin that slides against the flat surface of a rotating disk to which a specimen lubricant has been applied. The friction force on the pin is measured with a strain gauge. The measurement is made under varying loads. The temperature can be held constant or varied.

The report reviews the basic pin-on-disk configurations and methods of preparing disks and applying solid lubricants. Application methods range from quite simple (rubbing with a polishing cloth) to complex (plasma spraying, ion plating, and sputtering). The report describes factors that affect the performances of films; for example, the types of materials in sliding contact, sizes and shapes of the sliding parts, temperature, speed, and the presence or absence of liquids or dirt.

Techniques for constant-temperature testing, low-contact-stress testing, and temperature-versus-time testing are presented. Finally, the report suggests methods of measuring pin-wear volume and recommends ways of presenting data. In particular, plots of friction versus time and pin wear or film wear as functions of sliding distance are found useful.

This work was done by Robert L. Fusaro of **Lewis Research Center**. *Further information may be found in NASA TM-87236 [N86-19465/NSP], "How to Evaluate Solid Lubricant Films Using a Pin-on-Disk Tribometer."*

Copies may be purchased [prepayment required] from the National Technical Information Service, Springfield, Virginia 22161, Telephone No. (703) 487-4650. Rush orders may be placed for an extra fee by calling (800) 336-4700. *LEW-14610*

IT SIMPLY PERF

Introducing the New Series 930 Scientific-Atlanta Telemetry Receiving System— Superior Performance and Superior Value.

For more than 20 years, Scientific-Atlanta has set the industry standard for telemetry receiving systems. Our new microprocessor controlled Series 930 Receiver raises the standard still higher, with standard features our competitors consider options. And with greater ease of operation.

930 Receiver Performance Advantages:

- Menu-driven push button control of data entry, status displays, and options. Non-volatile memory stores current plus 10 programs.
- Internal module Spectrum Display Unit with the signal displayed on the LCD screen.
- Simultaneous operation of two front panel plug-in demodulators (FM/PM/BPSK) or one demodulator and a record translator.
- State-of-the-art low phase noise performance, stability and coherence.
- Front panel plug-in record translator and playback translator cover all standard IRIG plus any frequency between 100 kHz and 4.0 MHz.
- Space saving design simultaneously houses an SDU, tuner, demodulator, record and playback translators–all with remote control access.
- Full range of options and accessories.

Series
930
Telemetry Receiving System

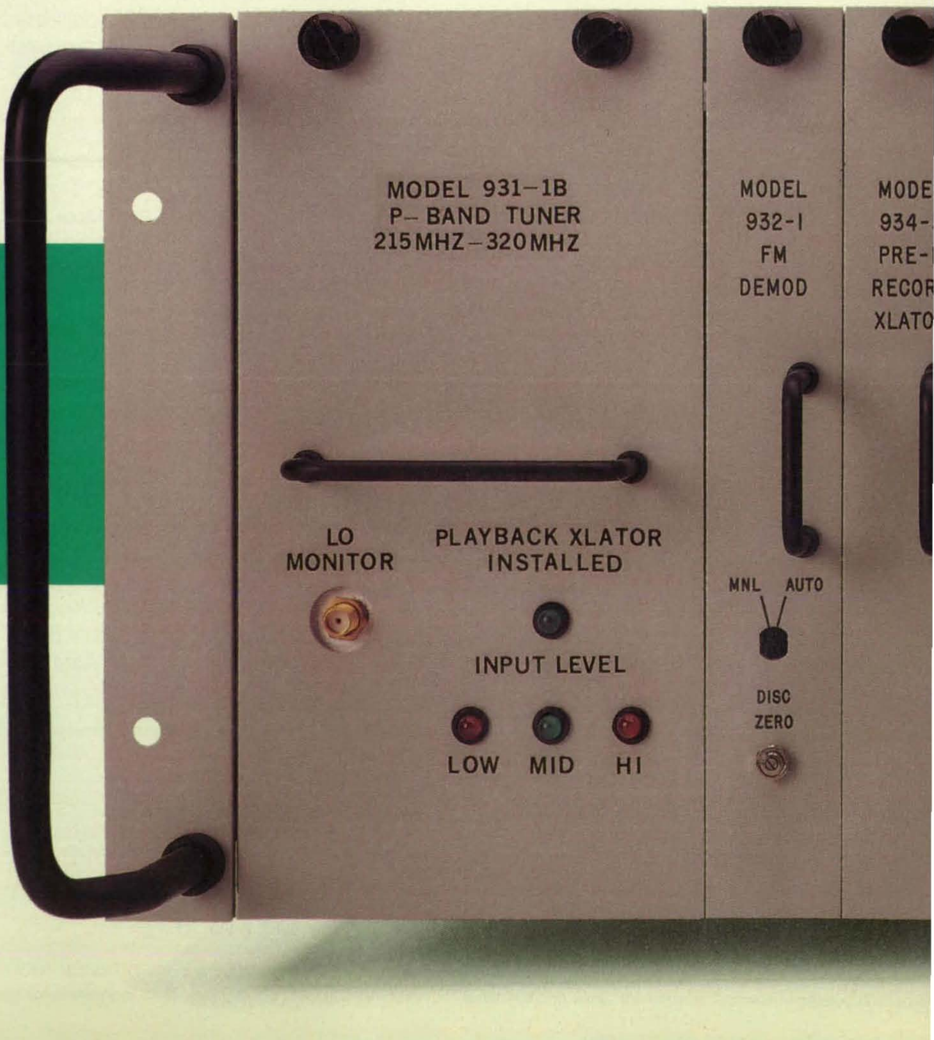

ORMS BETTER.

930 Diversity Combiner Advantages:

- Only combiner capable of maintaining data lock through signal fade or doppler shift in phase modulated telemetry.
- Phase noise performance unsurpassed in the industry.
- Real-time demodulation of the combined IF signal in the combiner.
- Processes each channel equally, eliminates a master/slave configuration and related loss of data lock.
- Wideband AM/AGC optimal weighting on both pre- and post-detection combined signals.

Add up the advantages and compare the costs, and in the end there is really *no* comparison. The Series 930 has more to offer in performance *and* value.

For additional information, call Glenn Horning at (404) 449-2338. Or write: Scientific-Atlanta, Electro-Products Division, 3845 Pleasantdale Rd., M/S ATL-10E, Atlanta, GA 30340.

Scientific Atlanta
ELECTRO-PRODUCTS DIVISION

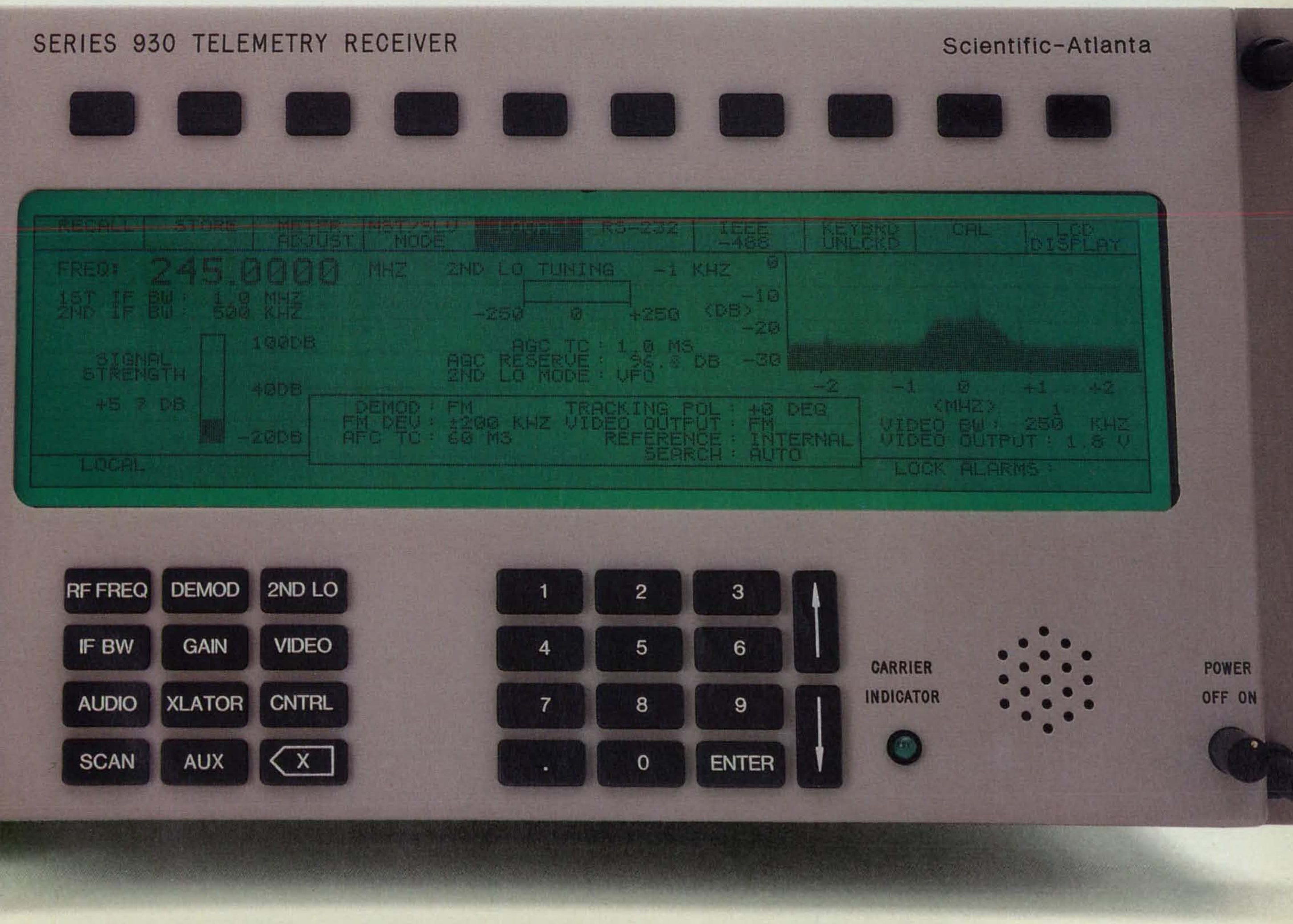

Books and Reports

Computer-Aided Design of Turbine Blades and Vanes

Analysis and design procedures lead quickly to an efficient and strong final design.

Marshall Space Flight Center, Alabama

A quasi-three-dimensional method for determining the aerothermodynamic configuration of a turbine uses computer-interactive analysis and design and computer-interactive graphics. The design procedure can be executed rapidly so that the designer can easily repeat it to arrive at the best performance, size, structural integrity, and engine life.

The engine-balance calculation establishes the overall turbine specifications, which are fed to a two-dimensional gas-path program for preliminary evaluation (see figure). This interactive program enables the designer to alter various design parameters iteratively while adhering to constraints imposed by the operating conditions of the common-shaft pump. Such parasitic losses as those of incidence, diffusion, leakage, and tip clearance are evaluated, and the overall turbine efficiency is predicted.

The designer uses the two-dimensional configuration from the gas-path program in a quasi-three-dimensional program to analyze the streamline-curvature flow field. This program establishes the meridional stream-surface locations and the characteristics of the associated velocity and pressure fields. At first, the designer enters only the inlet and outlet data for the rotor blades and stator vanes — such data as flow angles and edge thicknesses and locations — and the distributions of efficiencies or loss coefficients for the blades and vanes. The initial run gives an overall picture of the approximate flow field.

In succeeding trials, the designer enters the estimated blade-thickness distribution, axial chord, and other blade-profile parameters; the blade-stacking angles; the flow angles; the end-wall contours; and the axial locations of blades and vanes. The designer analyzes the reactions, radial loading distributions, and secondary flow effects

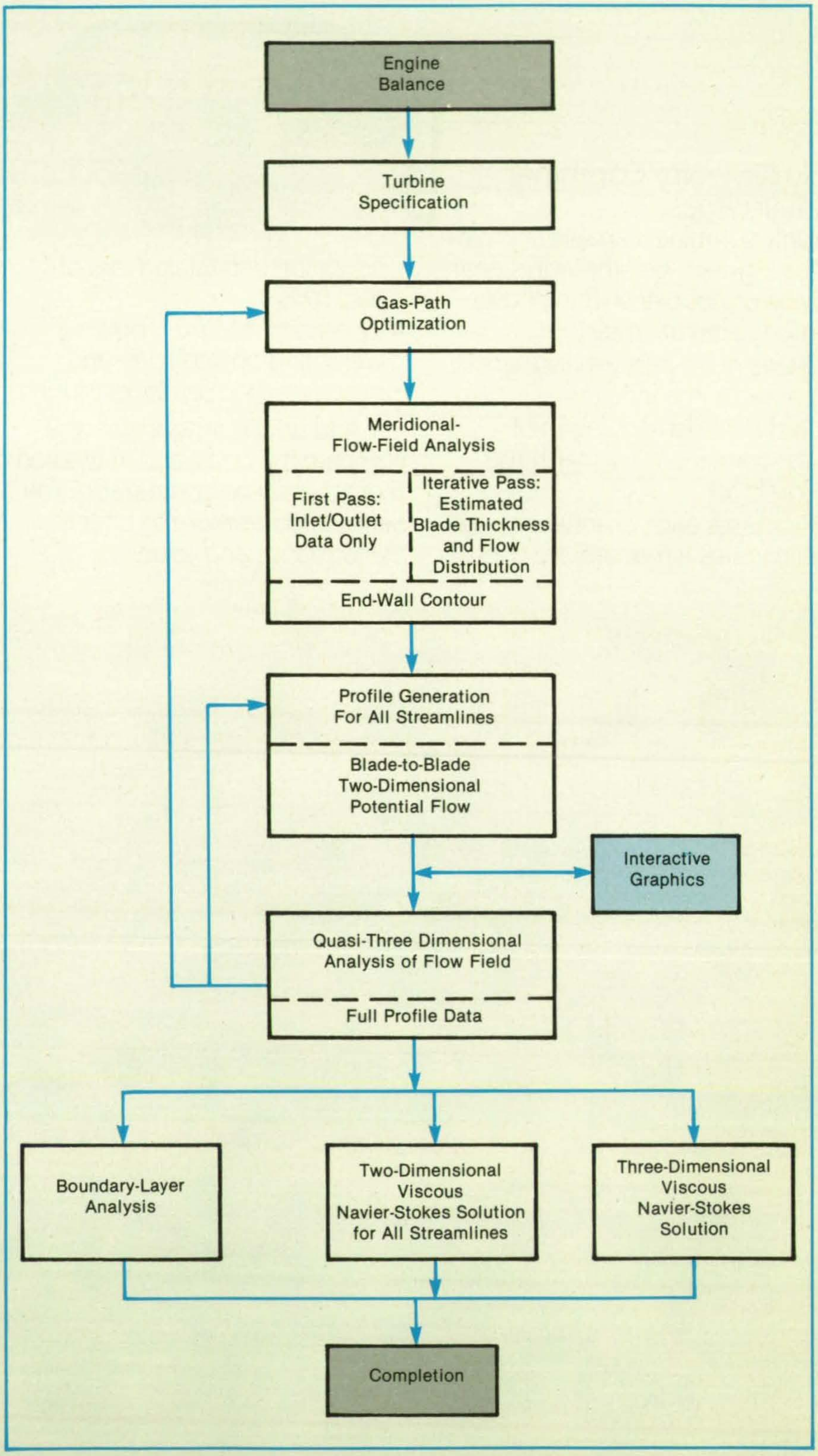

The **Sequence of Events in Aerothermodynamic Analysis and Design** starts with the engine-balance equations and ends with boundary-layer analysis and viscous-flow calculations. The analysis-and-design procedure is interactive and iterative throughout.

and eventually finds a preliminary optimized meridional configuration.

The next task is to generate the final blade profiles on various streamlines. The designer uses a program that determines the velocity and pressure distributions over the full blade profile along a streamline. By variation of the blade-coordinate distribution from the inlet to the outlet, the load distribution can be adjusted to achieve an optimum design. The results are displayed on a screen so that the designer can examine them immediately.

When all the profiles show acceptable loading characteristics, the profile data are transferred to a program for hub-to-tip analysis and another program for blade-to-blade analysis. The two programs interact to provide the quasi-three-dimensional analysis of the flow field. The blade-profile-generation and flow-field-analysis steps are repeated as many times as necessary to achieve the required blade characteristics.

Meanwhile, the designer can evaluate the blade and vane stackings with three-dimensional interactive graphics. The designer considers various stacking options and reviews the continuity of blade and vane surfaces, streamline-surface cross sections, and three-dimensional perspective views. (A stress-analysis engineer should become involved at this point to guide the choices of stacking, lean angles, and profile-thickness distribution to achieve a suitable stress distribution.)

Finally, a boundary-layer-analysis program is executed on the streamline profiles to ensure that flow is stable throughout the turbine, and viscous Navier-Stokes equations are solved — a time-consuming procedure carried out only when the design is close to completion.

This work was done by Wayne Q. Hsu of Rockwell International Corp. for **Marshall Space Flight Center**. *For further information, Circle 100 on the TSP Request Card. MFS-29265*

Portable Horizontal-Drilling and Positioning Device

This portable device drills horizontal holes in irregularly shaped objects.

Goddard Space Flight Center, Greenbelt, Maryland

A portable horizontal-drilling and positioning device (see figure), constructed mainly of off-the-shelf components, accurately drills horizontal small holes in irregularly shaped objects. With this device, holes can be precisely placed and drilled in objects that cannot conveniently be moved to a shop area.

This device was designed specifically to drill accurately, ream, and pin a series of holes in some irregularly shaped hardware in a semiclean room without using any lubricants. Because the fragility and the irregularity of shape of the hardware precluded the use of standard fixtures or guides, previous methods of locating and drilling holes relied on free-hand drilling or on specially designed fixtures. The use of handheld drills gave inconsistent results, poor hole shape, poor depth control, and angularity.

These difficulties were overcome with the new device (see figure), which provides three axes of movement while maintaining horizontal drilling. A 48 in. (122 cm) length of dual linear ball bearings provides friction-free travel in the x-direction (horizontal), and a dovetailed vertical column, at least 26 in. (66 cm) high, of anodized aluminum secured to the linear bearing base provides the required travel in the y-direction (vertical). A standard, commercially-available, variable-speed, sensitive drill press with a sensitive hand feed is secured to a standard x-y positioning table that provides the fine, graduated movements required for positioning the drill press.

Once the part to be drilled is aligned with the horizontal axis, any number of horizontal holes can be drilled. The use of the linear ball bearings provides a quick, accurate means of establishing a reference plane. A locking device secures the drill assembly prior to drilling, a quill coupled to a depth dial indicator provides accurate depth (z-axis) control, and the self-contained, variable-speed drill head enables the drilling of a variety of materials.

This work was done by Edmund Smigocki and Clarence Johnson of **Goddard Space Flight Center**. *No further documentation is available. GSC-13031*

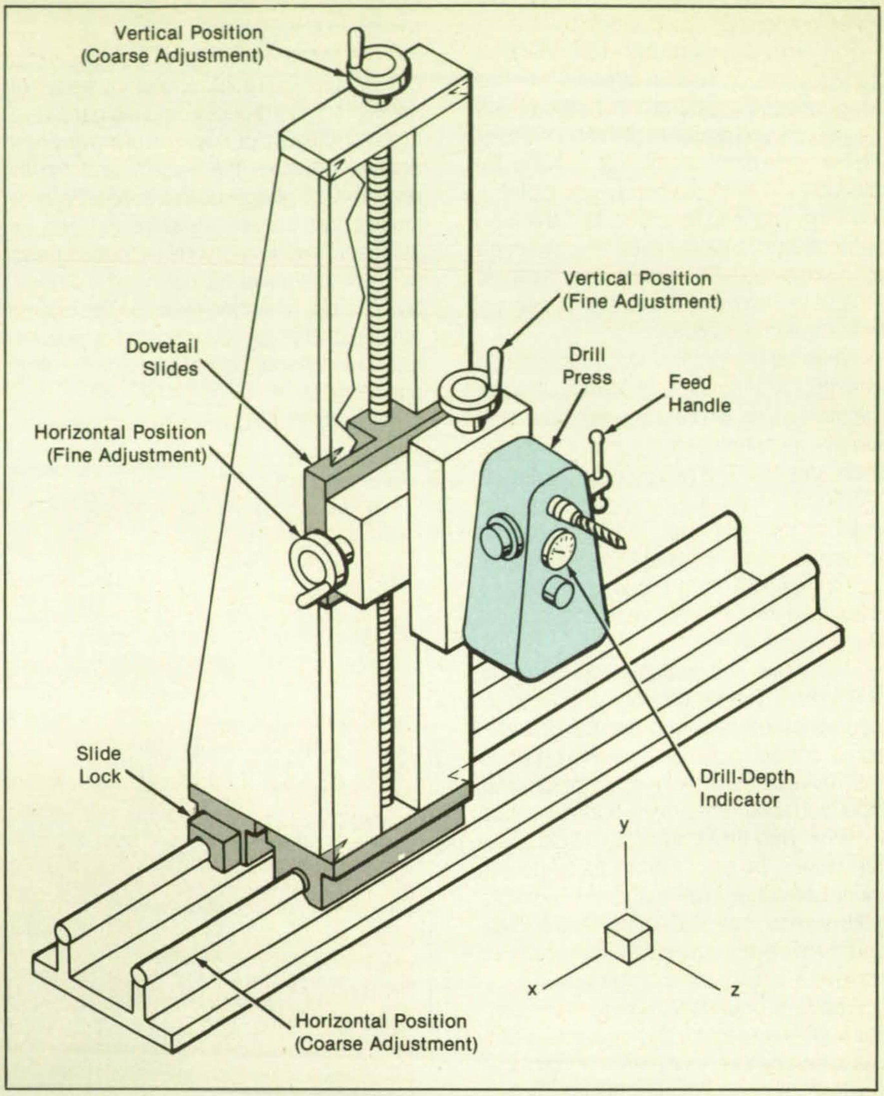

The **Portable Horizontal-Drilling Device**, constructed mainly of standard components, provides three axes of movement while maintaining the drill perpendicular to the workpiece.

Books and Reports

These reports, studies, handbooks are available from NASA as Technical Support Packages (TSP's) when a Request Card number is cited; otherwise they are available from the National Technical Information Service.

Systems Analysis of Advanced Coal-Based Power Plants

Fuel-cell technologies are evaluated and compared with advanced non-fuel-cell alternatives.

A report presents an appraisal of integrated coal-gasification/fuel-cell power plants. The report is based on a study that compared fuel-cell technologies with each other and with coal-based alternatives and recommended the most promising ones for research and development.

The study evaluated the capital cost, cost of electricity, fuel consumption, and conformance with environmental standards. It analyzed the sensitivity of the cost of electricity to changes in fuel cost, to economic assumptions, and to the level of technology.

The following seven of a total of ten types of plants were evaluated:

1. Molten-carbonate fuel cell;
2. Molten-carbonate fuel cell with hot gas cleanup;
3. Internal-reforming, molten-carbonate fuel cell with fluidized bed and hot gas cleanup (Internal reforming converts the higher fraction of methane produced by gasifiers in these plants.);
4. A version of type 3 that recirculates fuel-cell anode exhaust gas to the gasifier and eliminates the need for a separate oxygen feed to the gasifier. (This plant does not use a steam cycle.);
5. Pressurized solid-oxide fuel cell with hot gas cleanup;
6. Phosphoric acid fuel cell; and
7. A version of type 5 with a catalytic gasifier.

The three remaining types of plants, which are alternatives to fuel cells, were considered:

8. Integrated coal gasification, combined cycle, with a 2,200 °F (1,200 °C) turbine;
9. A version of the foregoing with a 2,600 °F (1,400 °C) turbine; and
10. Pulverized-coal-fired combustion with flue-gas desulfurization.

In the analyses, the plant capacity was assumed to be 675 megawatts. The levelized cost of electricity was projected for both 30-year and 10-year plant economic lives, based on a capacity factor of 65 percent.

The projected efficiencies of plants of type 3, 4, and 5 are significantly higher than the efficiencies of the other plants. Type 5 will consume 31 percent less coal than will type 8, for example.

The only fuel-cell plant that has the potential for competing with the low capital costs of the plants (8, 9, and 10), which do not use fuel cells, is type 5. The capital costs of types 2 and 6 are almost 50 percent higher than the equivalent costs for the other plants.

The report recommends further evaluation of integrated coal-gasification/fuel-cell, integrated coal-gasification/combined-cycle, and pulverized-coal-fired plants. The report concludes with appendixes detailing plant-performance models, subsystem-performance parameters, performance goals, cost bases, plant-cost data sheets, and plant sensitivity to fuel-cell performance.

This work was done by Joseph F. Ferrall, Charles N. Jennings, and Alfred W. Pappano of Caltech for **NASA's Jet Propulsion Laboratory**. *To obtain a copy of the report, "Systems Analysis of Advanced Technology Coal-Based Power Plants," Circle 17 on the TSP Request Card. NPO-16842*

Cover for Duct Expansion Joint

The size and shape of the cover reduces stress and increases strength.

Marshall Space Flight Center, Alabama

A cover for expansion joints on ductwork seals tightly while accommodating the movement of a joint. The cover provides ample bonding area on both members of a joint.

The cover (see figure) is molded from silicone resin in an omega-shaped cross section. The resin is reinforced with glass fibers or, preferably, with Kevlar (or equivalent) aromatic polyamid. The cross section allows the cover to flex readily with the contraction or expansion of the joint, without applying a peeling stress to the bonded edges — a stress mode in which the silicone adhesive is weakest.

The molding die is circular, with radius equal to that of the duct on which the cover will be installed. This ensures that the cover edges will lie flat on the duct.

The cover was developed as a replacement for a flat, glass-reinforced cover for a cryogenic fuel duct on the Space Shuttle. The tape tended to apply a peel stress to the adhesive when the joint contracted. Moreover, the tape provided a bond area only ½ in. (1.3 cm) wide on each element of the joint. The new cover not only reduces peeling stresses but provides a ¾-in. (1.9-cm) bond width on each edge.

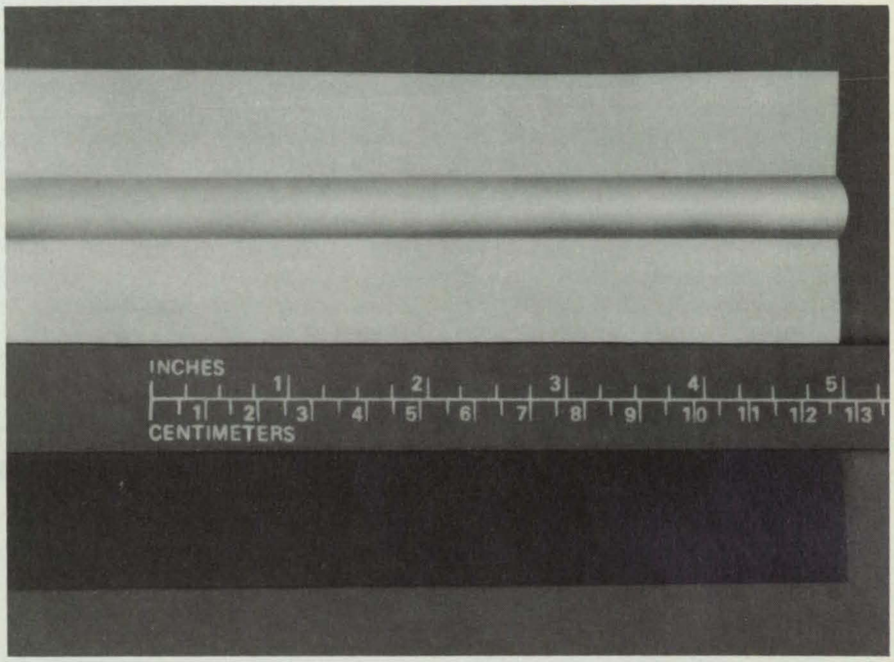

The **Edges of an Omega-Shaped Cover** fit on the opposing members of an expansion joint. The arch of the omega takes up expansion and contraction without unduly stressing the adhesive bonds on the joint members.

This work was done by A. R. Brown of Rockwell International Corp. for **Marshall Space Flight Center**. *No further documentation is available.*

Inquiries concerning rights for the commercial use of this invention should be addressed to the Patent Counsel, Marshall Space Flight Center [see page 16] Refer to MFS-29189.

Rotation Control in a Cylindrical Acoustic Levitator

A second driver introduces net circulation around the levitated sample.

NASA's Jet Propulsion Laboratory, Pasadena, California

The addition of a second acoustical transducer enables a single-mode, cylindrical acoustic levitator to rotate a levitated sample about the cylinder axis in a controlled manner. The ability to control rotation will enhance the usefulness of acoustic levitation in containerless processing, studies of the effects of rotation on fluid flows, and heating of samples by focused beams of light.

In the unmodified levitator, the sample does not rotate. The physical principle is easily visualized for a typical levitating acoustic field using the lowest-order non-plane wave made of the cylinder. In this mode, the acoustic pressure, P_1, varies about the axis and is given by

$$P_1 = a_1 \cos\phi \cos\omega t = \frac{a_1}{2}[\cos(\phi + \omega t) + \cos(\phi - \omega t)]$$

where a_1 contains the drive amplitude as well as the radial and axial dependences, ϕ is the azimuthal angle, ω is the angular frequency of the levitating sound, and t is time. The term in brackets represents two counterrotating acoustic fields that are equal and consequently impart no net torque or rotation to the sample.

In the modified levitator (see figure), a second transducer is orthogonal to the levitating transducer and excited at the same frequency but at a different amplitude or phase or both. In one scheme, the phase in the second transducer is shifted 90° from that in the first transducer, and the amplitude is different, resulting in an acoustic pressure, P_2, given by

$$P_2 = a_2 \sin\phi \sin\omega t = \frac{-a_2}{2}^2 [\cos(\phi+\omega t) - \cos(\phi-\omega t)]$$

where a_2 is an amplitude factor similar to a_1. This equation also represents two additional equal counterrotating acoustic fields. However, the total acoustic field is expressed by

$$P_1 + P_2 = ½ [(a_1 - a_2)\cos(\phi+\omega t) + (a_1 + a_2)\cos(\phi-\omega t)]$$

This represents two unequal counterrotating fields, which produce a net torque. The torque is increased by increasing the amplitude in the second transducer.

In an alternative scheme, both transducers are excited at the same amplitude. If no rotation is desired, both are excited at the same phase to produce equal counterrotating acoustic fields. The introduction of a phase shift between the two transducers makes the counterrotating fields unequal. The degree of inequality, and therefore the torque, can be increased by raising the phase shift.

In both schemes, it is necessary to apply a starting acoustic torque in excess of a critical minimum to make the sample turn; less torque is needed to keep it turning. Thus, the sample begins to turn rapidly. If slower rotation is desired, the torque must then be reduced. This behavior is analogous to the decrease in frictional force between two objects when they begin to slide on each other.

This work was done by M. B. Barmatz and J. L. Allen of Caltech for **NASA's Jet Propulsion Laboratory**. *For further information, Circle 80 on the TSP Request Card.*

Inquiries concerning rights for the commercial use of this invention should be addressed to the Patent Counsel, NASA Resident Office-JPL *[see page 16]*. *Refer to NPO-16995.*

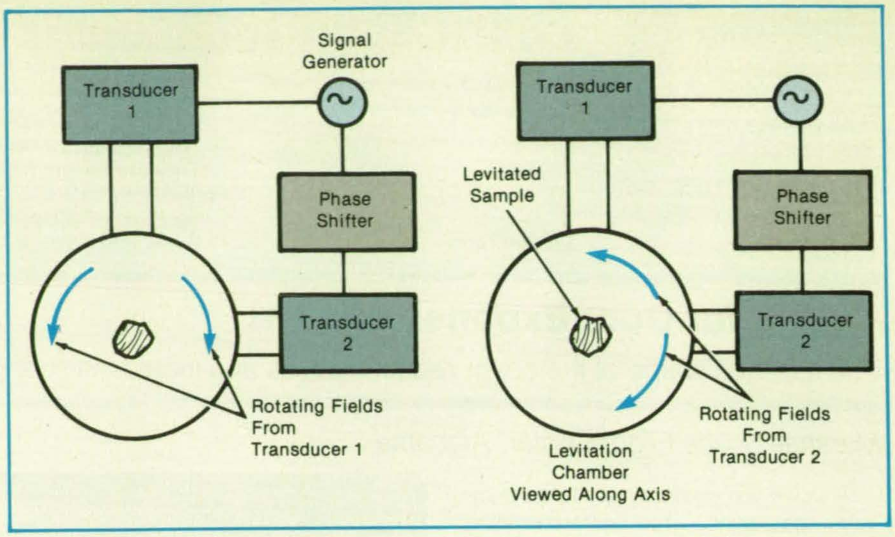

Two Transducers produce two sets of equal counterrotating acoustic fields. By appropriate adjustment of the amplitudes and phases in the two transducers, the total acoustic field can be made to consist of two unequal counterrotating fields, therefore producing a net torque on the levitated sample.

Tool Protects Internal Threads During Rework

A simple device covers some areas but exposes other areas for grinding.

Marshall Space Flight Center, Alabama

A tool protects part of an internal thread from damage while an adjacent surface is ground or machined. The tool also collects machining debris so that they do not contaminate the part.

The tool is a flanged cylinder with a window (see figure). Grinding and other operations can be done through the window while the tool masks the threaded surface to be protected. The flange positions the window precisely in the hole to be reworked. The cylinder can be rotated so that the window exposes the full circumference for machining.

The tool was developed to remove the portion of a thread that had been extended to too great a depth in a hole. With the tool, the thread extending below a depth of 0.87 ± 0.06 in. (2.21 ± 0.15 cm) could be ground away without damage to the thread above that depth. The grinding chips and dust fell to the bottom of the tool and were removed with the tool at the completion of grinding.

This work was done by Gary E. Deese of Rockwell International Corp. for **Marshall Space Flight Center**. *No further documentation is available.*
MFS-29234

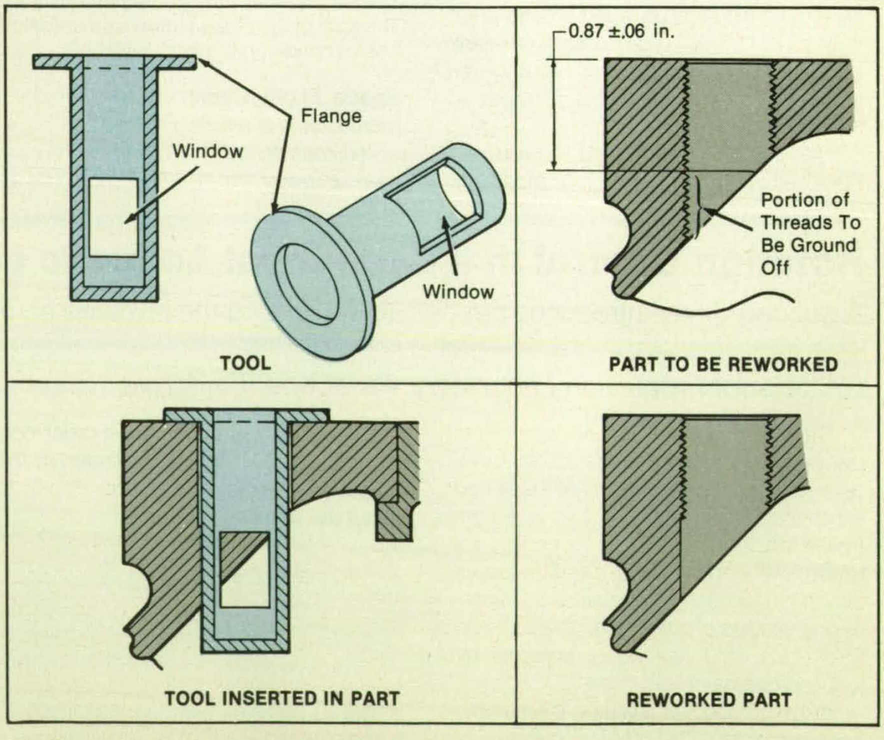

The **Protective Tool** fits into a threaded hole. The wall of the hole can be machined through the window without damage to the portion of the thread hidden by the tool.

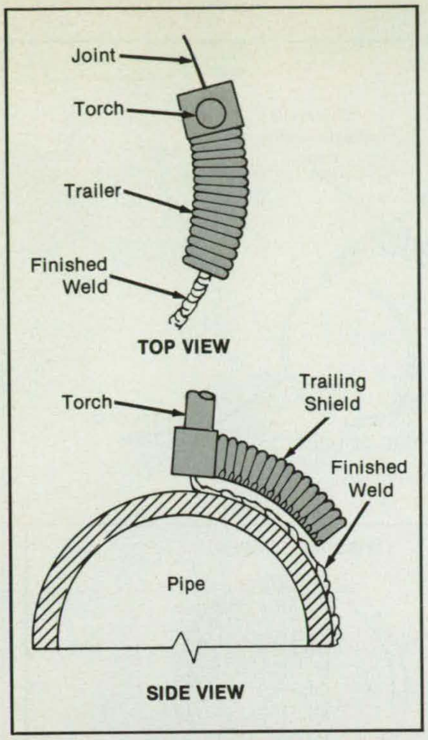

Figure 1. The **Welding Torch Pulls a Trailing Shield** behind it to provide a protective shield of argon gas over the hot weld bead. A guide at the front of the torch holder feeds welding wire to the joint.

Flexible Protective Shield for Newly Welded Joints

A simple device promotes defect-free welds in oxidation-prone metals.

Marshall Space Flight Center, Alabama

A flexible trailing shield for a welding torch protects hot metals from oxygen of the surrounding air until the weld bead has cooled. The shield bends to follow the contours of the weld joint and protects such metals as titanium, which oxidizes easily when it is hot.

The trailer flexes to fit the contours of the welded surfaces. It can follow a curved or straight joint on a curved or flat surface; for example, a straight joint on a curved surface like a pipe (see Figure 1). The flexible trailer makes it unnecessary to build a special trailer to match the joint, as has been done with the rigid trailers of the past.

A thin stainless-steel bellows forms the body of the trailer (see Figure 2). It is packed with steel wool, which distributes argon over the newly welded bead. The trailer also blows a jet of argon slightly forward of the torch to shield the hot metal before it is welded. A copper-tube manifold extends like a spine along the length of the trailer, supplying argon to the steel-wool distributor.

This work was done by Gerald E. Dyer of Rockwell International Corp. for **Marshall Space Flight Center**. *For further information, Circle 69 on the TSP Request Card.*

Inquiries concerning rights for the commercial use of this invention should be addressed to the Patent Counsel, Marshall Space Flight Center [see page 16]. Refer to MFS-29260.

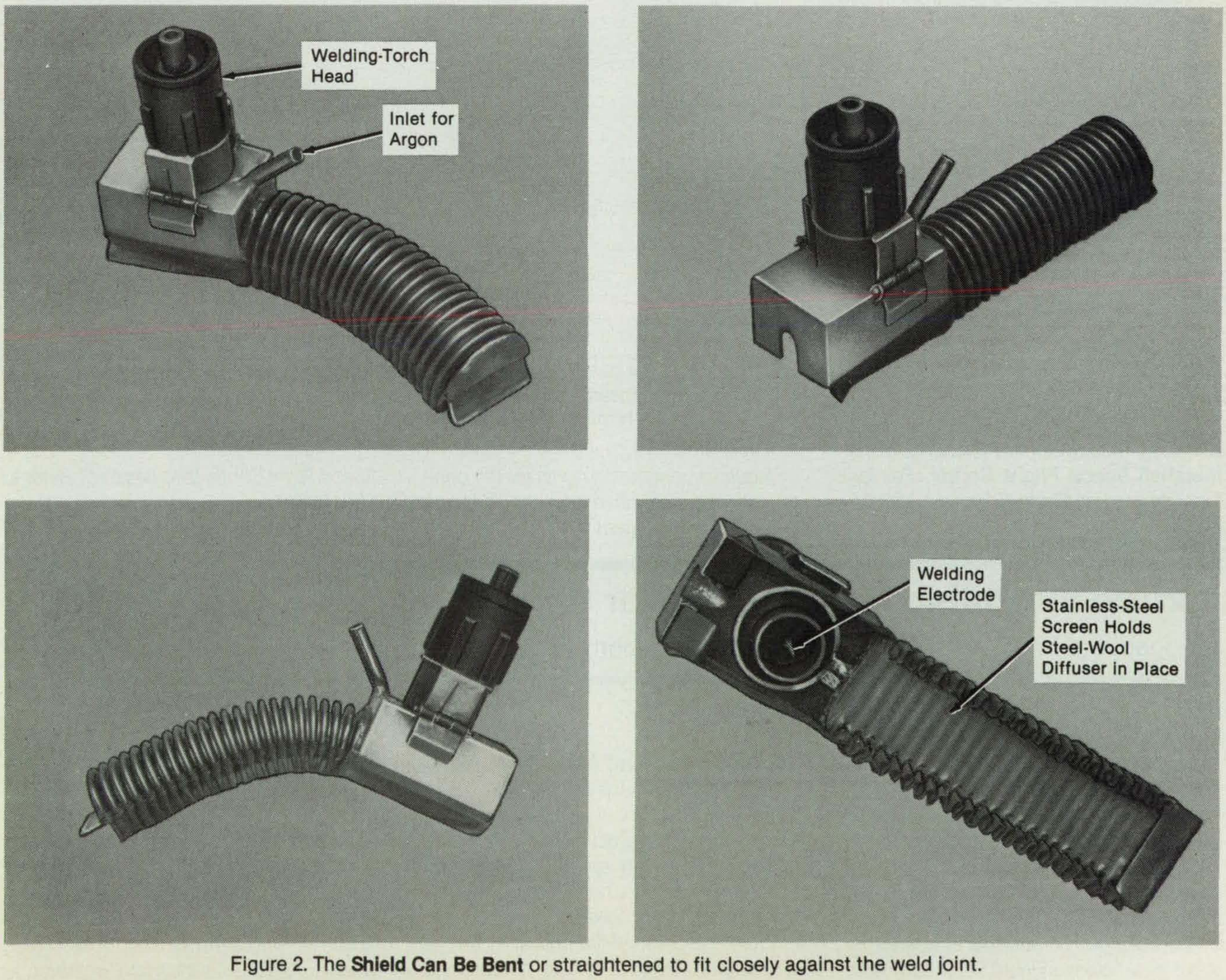

Figure 2. The **Shield Can Be Bent** or straightened to fit closely against the weld joint.

Real-Time X-Ray Inspection

An x-ray imaging instrument is adapted to continuous scanning.

Marshall Space Flight Center, Alabama

A modern version of the fluoroscope enables the rapid x-ray inspection of parts. The instrument was developed for the detection of buckling in insulated ducts. It replaced a large 160-kV x-ray machine that required time-consuming exposures of many small sections of a duct with the aid of cumbersome positioning fixtures and slow film-processing facilities.

The fluoroscope uses radiation from a radioactive gadolinium or thallium source. The instrument weighs only 6½ lb (2.9 kg). It can be quickly scanned by hand along the duct surface, providing a real-time image.

The instrument is based on the Lixiscope, a low-intensity x-ray imaging scope developed at Goddard Space Flight Center. In the Lixiscope, the pattern of x rays transmitted through the specimen is converted into a visible-light image in a scintillator. This image is intensified by a factor of 10^5 or more in a microchannel-plate device. The intensified image can be viewed directly, photographed, recorded on videotape, or coupled to other imaging devices.

The standard Lixiscope was modified so that it can be placed around the cylindrical duct. More shielding was added to the source holder so that a radioactive source with higher-than-usual energy could be used to penetrate the duct layers. The resulting image clearly shows buckled parts of the inner wall (see figure).

This work was done by Ronald V. Bulthuis of Rockwell International Corp. for **Marshall Space Flight Center**. *For further information, Circle 102 on the TSP Request Card.*

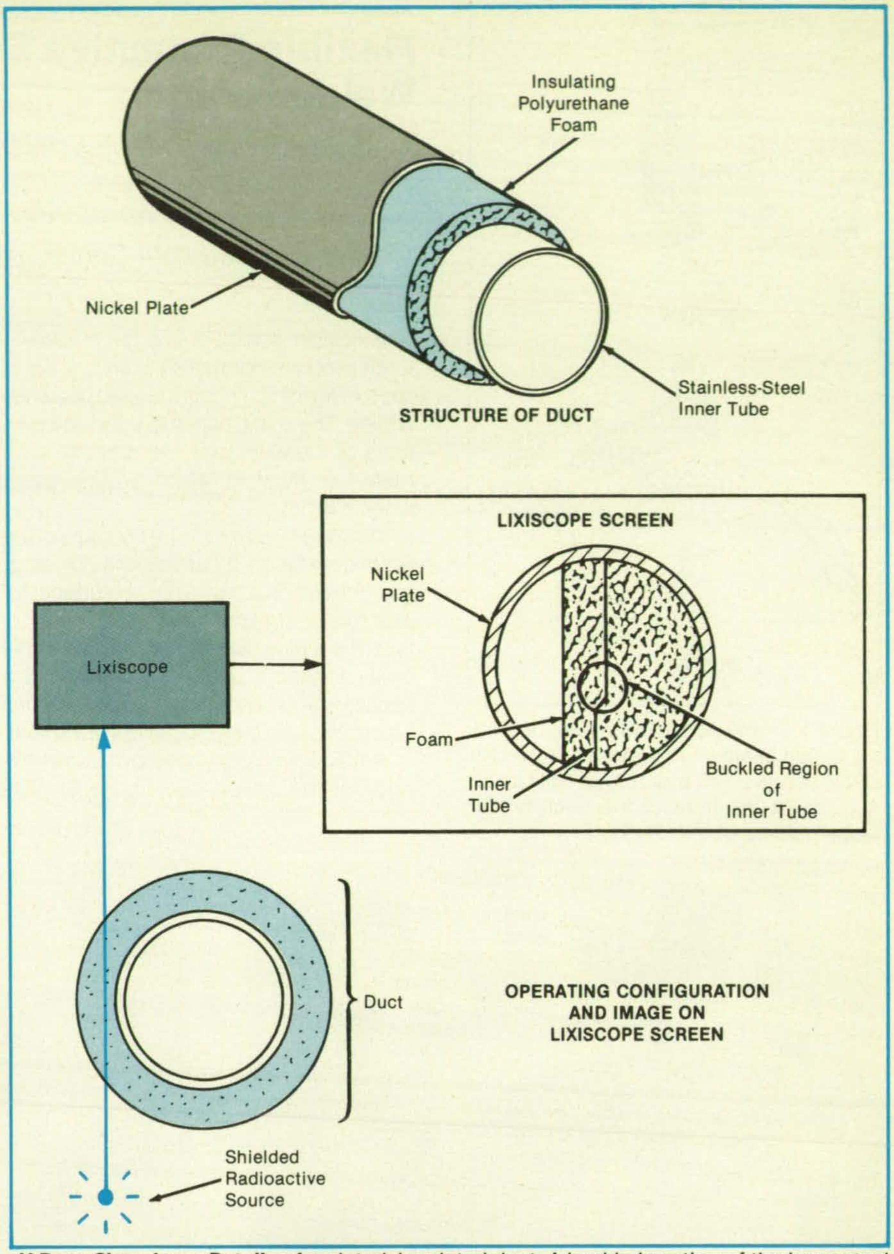

X Rays Show Inner Details of a plated, insulated duct. A buckled section of the inner steel wall of the duct appears as a bump on the vertical line at the center of the display. In an inspection, the duct is rotated and translated past the x-ray source so that it can be inspected completely.

Inquiries concerning rights for the commercial use of this invention should be addressed to the Patent Counsel, Marshall Space Flight Center [see page 16]. Refer to MFS-29217.

Fixture for Polishing Optical-Fiber Ends

Wedged and beveled ends are lapped with precision for laser applications.

Langley Research Center, Hampton, Virginia

When an injected laser is coupled into an optical fiber, emission instabilities arise because of optical feedback losses from the fiber into the laser. However, high coupling efficiency and feedback suppression can be achieved by shaping the input end of a multimode fiber into a wedge and by beveling the output end at a suitable angle [see "Wedge Fibers Suppress Feedback of Laser Beam" (LAR-13074), pages 94 and 95, *NASA Tech Briefs*, Vol. 9, No. 4 (Winter 1985)]. A fixture that has been designed for the precise cutting of end-polished fibers into specific depths and angles provides accurate repeatability during the polishing process.

Each end-polished fiber requires an obtuse-angled wedge or roof configuration at one end and a bevel at the other. These requirements posed problems in ensuring accuracy of the angles, repeatability of the angles (both from one side of the obtuse angle to the other and from fiber to fiber), and precise splitting of the core [0.001 in. (0.025 mm) or less] in the center of the fiber [0.005 in. (0.13 mm)] for the obtuse-angled wedge. A fixture allows the operator to overcome all of these problems and to accomplish precise work. This fixture holds the fiber accurately, adjusts to the correct angle, controls the amount of stock removed from one side of the fiber to the other, supports the fiber as the angle is polished, controls the finish on the fiber, and allows the fiber to be removed for inspection and to be accurately repositioned to continue polishing.

The holding block (see figure) is grooved to hold the fiber in the exact position required for polishing. The fiber is locked in position with a retaining strap and cannot rotate or slide back during polishing. A base fixture for the holding block has an adjustable angle stop, which is set at the desired angle, and a micrometer feed that allows the operator control over the inward pressure on the fiber. The holding block is set on the base fixture and aligned with the angle stop. Anchored to the side of the block is the fiber support. Once the fiber is in position for polishing, the fiber support is slid out from its holder and locked into position near the tip of the fiber. This component supports the fiber, not allowing it to bend or bow under pressure during polishing and thus change the angle. The fiber is slowly moved into position using the micrometer feed and accurately beveled to the proper angle. This fixture also has a stop adjustment that allows the operator to remove the holding block for inspection of the fiber and to replace it accurately.

The ends that require the obtuse-angled wedge require two polishing steps. The first step is similar to the beveled-edge polishing, except that the angle is polished only half way through the fiber, then the holding block is removed. The fiber support is removed from the polished side of the holding block and placed on the opposite side. The holding block then is turned over and accurately replaced on the base fixture. The second half of the fiber is polished to obtain the proper obtuse-angled wedge.

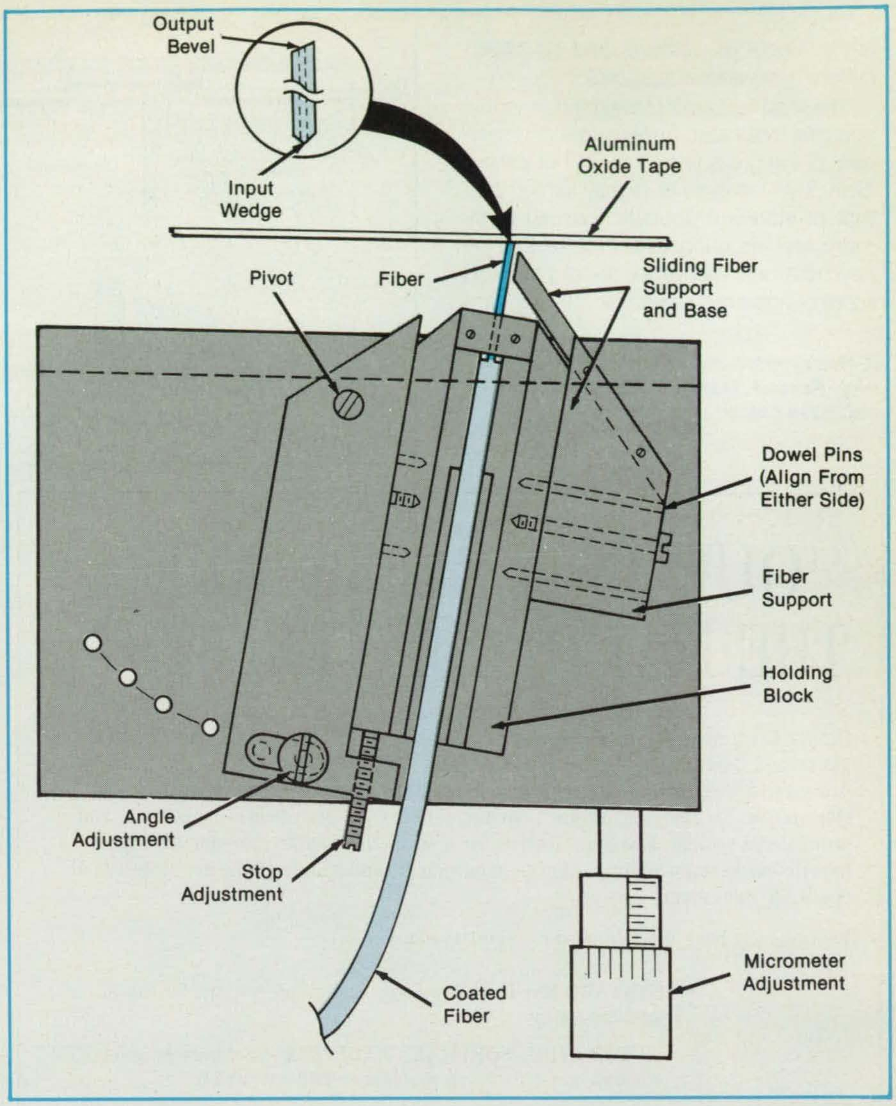

For an Obtuse-Angled Wedge End, both sides of the fiber are polished similarly. After one side of the fiber is lapped, the fiber support is removed. The holding block with the fiber is turned over, and the fiber support is replaced. The second side of the fiber is then lapped.

This work was done by Leroy H. Barlow and Vincent A. Pirone of RCA Corp. for **Langley Research Center**. *No further documentation is available.*

Inquiries concerning rights for the commercial use of this invention should be addressed to the Patent Counsel, Langley Research Center [see page 16]. Refer to LAR-13510.

New Acoustic Treatment for Aircraft Sidewalls

Cabin noise is reduced with minimal addition of weight.

Langley Research Center, Hampton, Virginia

There is a continuing need in the aircraft industry to control and reduce cabin noise and vibration. Conventional noise-reduction treatments are essentially additions of multilayered porous acoustic materials, impervious separating layers, and trim panels to the cabin walls. Additional noise reduction is usually achieved by increasing the weights of these layers. However, such increases in weight require more fuel and/or larger engines. The new aircraft-sidewall acoustic treatment reduces interior noise to acceptable levels and minimizes the addition of weight to an aircraft.

With the new technique, the transmission of noise through the aircraft sidewall is reduced by a stiffening device attached to the interior side of the aircraft skin, constrained-layer damping tape attached to the stiffening device, porous acoustic materials of high resistivity, and a relatively-soft trim panel isolated from the vibrations of the main fuselage structure.

The stiffening device is an aluminum honeycomb panel or an equivalent honeycomb panel made from other materials; the constrained-layer damping tape is effective at low temperatures; the resistivity factor of the porous acoustic material is significantly higher than that of present conventional acoustic/thermal materials used in the soundproofing of aircraft; and the trim panel is a relatively soft and impervious septum. To minimize the transmission of vibrations from the fuselage to the trim panel, soft isolators are installed when the trim panel is attached to the main frame of the fuselage. This treatment requires an increase in thickness of the exterior sheets of windows and increased stiffening of window supports.

The total increase of weight due to this acoustic treatment is approximately 2 percent of the gross takeoff weight of the aircraft. This increase is slightly lighter than that of standard acoustic/thermal treatment, and laboratory tests indicate that the new treatment will provide about 4 to 10 dB more of noise reduction than the standard treatment does. The average calculated overall noise levels of the untreated cabin will be reduced by about 17 dB with the new acoustic treatment.

This work was done by Rimas Vaicaitis of Columbia University for **Langley Research Center**. *Further information may be found in:*

NASA CR-172245 [N85-30771/NSP], "Design of Sidewall Treatments for Cabin Noise Control of a Twin Engine Turboprop Aircraft," and

NASA CR-17218 [N84-11884/NSP], "Study of Noise Transmission through Double Wall Aircraft Windows."

Copies may be purchased [prepayment required] from the National Technical Information Service, Springfield, Virginia 22161, Telephone No. (703) 487-4650. Rush orders may be placed for an extra fee by calling (800) 336-4700.

Further information may be found in AIAA Paper 84-2329 [A85-10873], "Noise Transmission through an Acoustically Treated and Honeycomb Stiffened Aircraft Sidewall."

Copies may be purchased [prepayment required] from AIAA Technical Information Service Library, 555 West 57th Street, New York, New York 10019, Telephone No. (212) 247-6500.

LAR-13545

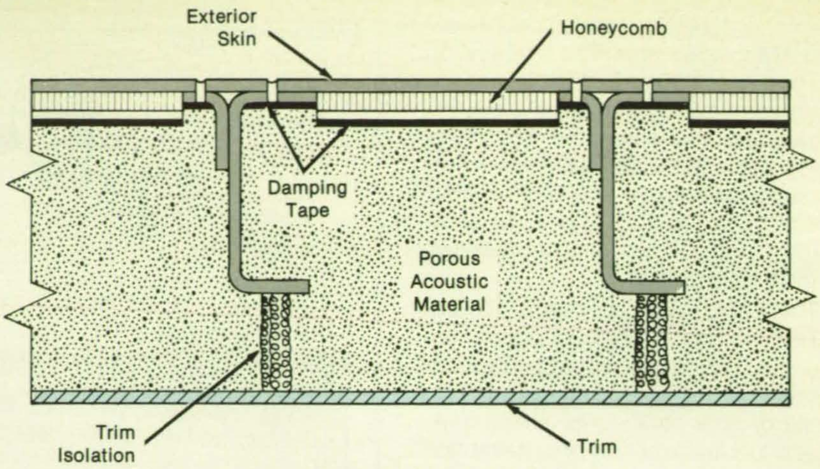

A ***Honeycomb Panel and a High-Resistivity Porous Material*** *are combined to decrease overall noise levels.*

Mathematics and Information Sciences

Coding Strategy for Critical Data

Repetition preserves the most critical data during severe attenuation.

NASA's Jet Propulsion Laboratory, Pasadena, California

Repetition coding can be used to protect a small but critical portion of a Reed-Solomon/convolutionally-encoded (RS/CE) data stream against loss during periods of signal attenuation due to bad weather. Each bit in the portion of the RS/CE data stream containing the critical data is repeated a number of times that depends on the degree of protection required. The noncritical majority of data is transmitted normally, without repetition.

The signal-to-noise ratios of some types of data channels, particularly those using radio links, vary with the transmission media fluctuations. Often the reliable reception of some portion of the data stream has a higher priority than does the reception of the remainder. When the available channel capacity is inadequate for reliable reception of all data under the worst transmission conditions, it is desirable to use an encoding strategy that reflects the relative importance of different types of data. The reception of the higher-priority (critical) data can then be assured even under poor transmission conditions, while exacting only a small penalty in the overall data rate under good conditions. The new repetitive coding scheme represents one such strategy. This scheme is superior to two other well-known low-rate codes (orthogonal and biorthogonal codes) at comparable rates and signal-to-noise ratios. Furthermore, only simple additional equipment is required to add repetition encoding to existing RS/CE equipment (see figure).

Without repetition, the RS/CE bit error rate deteriorates abruptly as the symbol signal-to-noise ratio decreases below a certain point. For example, the bit error rate rises from 10^{-5} to 10^{-2} as the bit signal-to-noise ratio drops from 2.3 to 1.9 dB; thus, a mere 0.4 dB can be the difference between successful data transmission and failure. In contrast, if the critical RS/CE data are transmitted five times in succession, the bit error rate for these data is less than 10^{-5} at a signal-to-noise ratio of -8.3 dB. If, for example, only 1 percent of the data is critical, then the overall loss in channel capacity due to the use of this repetitive scheme is only 0.18 dB.

This work was done by Laif Swanson and Joseph H. Yuen of Caltech for **NASA's Jet Propulsion Laboratory**. *For further information, Circle 39 on the TSP Request Card.* *NPO-16630*

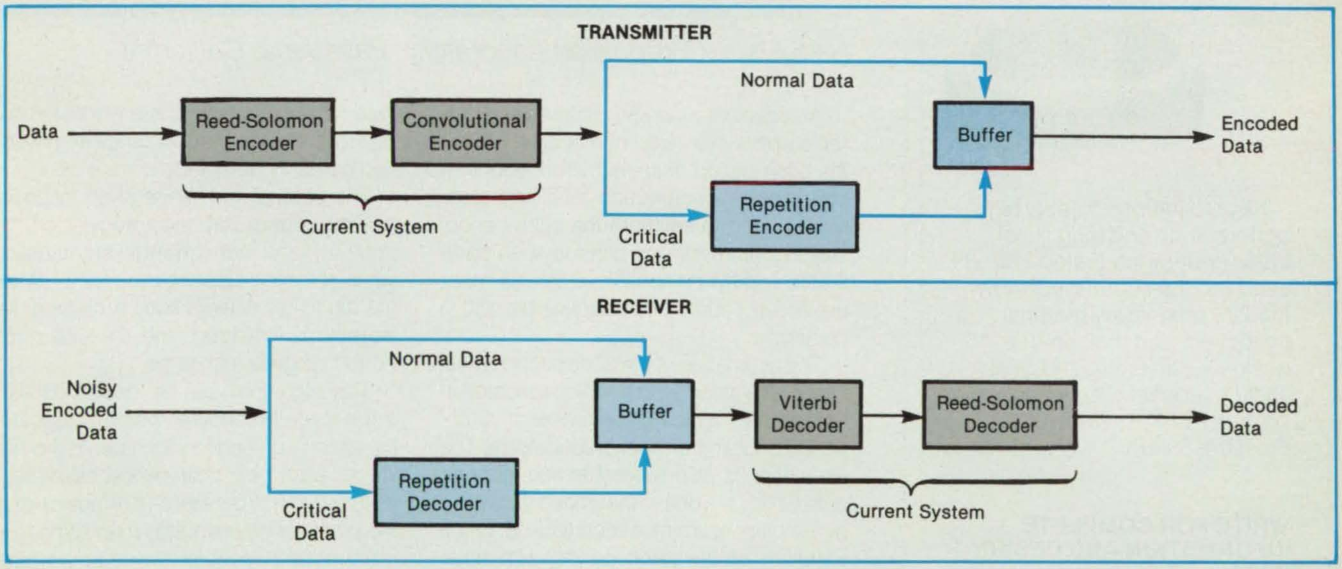

Repetition can be added to an existing system that uses Reed-Solomon and convolutional encoding by additional components shown in color.

Failure-Time Distribution of an *m*-Out-of-*n* System

Formulas for reliability are extended to more general cases.

NASA's Jet Propulsion Laboratory, Pasadena, California

Formulas have been derived for the probabilities of failure and survival and for the probability distribution of the time to failure of $n+1-m$ components of a system that initially contains n good components. The formulas should be useful in analyses of the reliabilities of practical systems and structures, especially of redundant systems of identical components,

 Update your NASA Tech Briefs qualification form every six months.

among which operating loads may be distributed equally.

The theory applies to a system that survives as long as at least m components survive and for which the failure rate of each of the $1-i$ components that remain at a given time is λ_i. Because increased stress is often placed on the surviving components, the failure rates tend to increase with each component failure; that is, $\lambda_0 \leqslant \lambda_1 \leqslant \ldots \leqslant \lambda^{n-m}$. However, the theory is valid even where this inequality does not hold.

The problem is to find the probability distribution of the time T to failure of the system, assuming that the intervals between the $n-m+1$ component failures in the sequence leading to system failure are independent and exponentially distributed with overall failure rates $\alpha_i = (n+1-i)\lambda_i$. The probability distribution can then be used to calculate the system reliability function $R(t)$, which is the probability of survival to time t; that is, the probability that T will exceed t.

Previous workers had developed probability distributions for the case in which all the α_i have the same value α, and for the case in which all the α, are different. In the first case, T has a gamma distribution with shape parameter $n-m+1$ and scale parameter α. In the second case, the formula for $R(t)$ requires an individual, exponentially distributed term for each α_i. This study adapts the previous formulas to the intermediate case in which there are some equalities among the α_i. In this case, T can be expressed as the sum of independent gamma-distributed variables, one for each distinct overall failure rate β_i. The result is that

$$R(t) = \left\{ B \sum_{k=1}^{a} \sum_{\ell=1}^{r_k} [\Phi_{k\ell}(-\beta_k)]/(\ell-1)!\beta^{r_k-\ell+1} \sum_{j=0}^{r_k-\ell} [(\beta_k t)^j \exp(-\beta_k t)]/j! \right\}$$

where $B = \prod_{j=1}^{a} \beta_j^{r_j}$,

$$\Phi_{k\ell}(t) = \frac{d^{\ell-1}}{dt^{\ell-1}} \prod_{\substack{j=1 \\ j \neq i}}^{a} (\beta_j + t)^{-r_j},$$

r_j is the number of overall failure rates having the same distinct value β_j, and a is the number of such rates.

This work was done by Ernest M. Scheuer of Caltech for **NASA's Jet Propulsion Laboratory**. *For further information, Circle 2 on the TSP Request Card. NPO-17069*

Pitch-Learning Algorithm for Speech Encoders

Gross pitch errors are detected and corrected.

NASA's Jet Propulsion Laboratory, Pasadena, California

An adaptive algorithm detects and corrects errors in a sequence of estimates of the pitch period of speech. The algorithm operates in conjunction with the techniques used to estimate the pitch period. The algorithm can be used in such parametric and hybrid speech coders as linear predictive coders and adaptive predictive coders.

The estimation of the pitch period is susceptible to gross errors, which are large in magnitude, typically because of pitch-period doubling or background noise. The estimation is also subject to fine pitch errors, which are due to the limited resolution of the pitch-estimation technique or to the variation of the pitch period with time. Gross errors result in distorted encoded speech spurts that are subjectively very objectionable. Fine pitch errors are more tolerable but reduce the natural-sounding quality of the encoded speech.

The algorithm is based on the observation that the range of pitch periods for a given speaker is narrower than that for all speakers: in the general speaker population, pitch periods range between 2 ms and 20 ms, whereas the pitch period of a single speaker has a range typically less than 5 ms wide. Most gross errors fall outside this relatively narrow range and hence can be easily detected.

The pitch-period range of an incoming speech signal depends heavily on the speaker and can change significantly when someone else begins to speak. When the algorithm detects such a change, the learning is initialized, and the new pitch-period range is estimated.

The algorithm can be described as a three-stage procedure, which is repeated for each pitch-period estimate. In the first stage, each new pitch-period estimate is included in a progressive average of all of the pitch-period estimates made since the most recent reset of the learning algorithm. Pitch-period samples taken during moments of silence are arbitrarily assigned pitch periods of zero and excluded from the average.

According to experiments, there is a high probability that the instantaneous pitch-period estimate will lie between 0.75 and 1.25 times the average. In the second stage, the algorithm tests each subsequent pitch-period estimate to determine whether, in fact, it lies within this range. If it does, the estimate is assumed correct and the averaging continues. If the estimate falls outside the range, a gross error is assumed: in this case, a new estimate for the present pitch period is made from the previous and next pitch-period estimates.

If the new estimate lies within the range, a correction counter is set to zero. If it lies outside the range, the correction counter is incremented. The third stage of the algorithm is based on the assumption that a reliable pitch-period estimate has a small number of gross errors; in this case, the allowable number of consecutive errors is arbitrarily set at three. When the correction counter indicates a higher number, the pitch-period range estimate is deemed to be in error. (This is most likely to occur when a new person begins to speak.)

When an error is detected, the pitch-period average is discarded, the averaging counters are reset, and the system begins to relearn the pitch range. Error detection and correction are suspended during the first eight nonzero pitch-period estimates, when the new average is established.

This work was done by B. R. Udaya Bhaskar of Comsat Laboratories for **NASA's Jet Propulsion Laboratory**. *For further information, Circle 106 on the TSP Request Card.*

Title to this invention has been waived under the provisions of the National Aeronautics and Space Act [42 U.S.C. 2457(f)], to the COMSAT Laboratories. Inquiries concerning licenses for its commercial development should be addressed to

COMSAT Laboratories
22300 COMSAT Drive
Clarksburg, MD 20871

Refer to NPO-17045, volume and number of this NASA Tech Briefs *issue, and the page number.*

Books and Reports

These reports, studies, handbooks are available from NASA as Technical Support Packages (TSP's) when a Request Card number is cited; otherwise they are available from the National Technical Information Service.

Reducing Drift in Computation of Spacecraft Attitude

The error in an approximation is less than the computer truncation error.

A report discusses a scheme for the reduction of computational drift in the estimation of the attitude of a spacecraft from strapdown-gyroscope measurements. Such estimates and calculations are performed aboard the spacecraft during the long intervals between sighting of stars or planets, which establish attitude references. The scheme was developed for a radar-mapping satellite that will fly to the planet Venus; it is also discussed in the report described in the preceding article, "Determining Spacecraft Attitude for Planetary Mapping."

In the case of the Venus Radar Mapper, the computational drift would be excessive if the full quaternion attitude propagation were to be performed at each step. This is because of the accumulation of truncation errors in the 32-bit floating-point attitude representation: with the attitude updates computed at the required rate of 30 times every second, the accumulated attitude drift can amount to random, systematic, or gyroscopelike drift of as much as 2.2 °/h.

The improved scheme is based on the fact that the spacecraft attitude changes so slowly that the total change during a 1/30-s update interval is very small (typically, a fraction of an arc second). Instead of performing the full quaternion propagation at each time step, the attitude increment is represented as a sum of small angles of rotation about the gyroscopic axes. This approximation is justified because at the small rotational angles encountered in practice, the commutation errors are to second order in those angles. Thus, the approximation reduces the frequency of arithmetical operations and therefore the computational drift rate, without introducing significant angle errors in the short term.

To reduce the accumulation of angle errors, the full gyroscope quaternion reset is performed, either when 500 s have elapsed since the last update or when one of the cumulative rotational angles since the last quaternion update exceeds 1 °. Thus, the gyroscope-reset algorithm can be executed at a much lower rate, and it uses much less central-processing-unit time than it would if the full calculation were repeated at 30 Hz.

For the Venus Radar Mapper, the scheme reduces the computational drift per axis to 0.00536 °/h. The maximum three-axis error per orbit around Venus is 0.0288 °, which is close to the design goal.

This work was done by Whittak H. Huang of Martin Marietta Corp. for **NASA's Jet Propulsion Laboratory**. *To obtain a copy of the report, "A Computational Drift Minimizing Technique for Spacecraft Onboard Attitude Quaternion Propagation," Circle 48 on the TSP Request Card.*
NPO-17027

Determining Spacecraft Attitude for Planetary Mapping

A new algorithm can calculate the attitude with accuracy to spare.

A report describes an algorithm for use in determining the attitude of a spacecraft from the incremental-angle output of a strapdown gyroscope and star-scanner measurements. The report highlights the detail of the underlying theories and strategies. It presents the results of a simulation to demonstrate the capability of the algorithm, and it discusses possible applications. Although the specific algorithm was developed for the Magellan Spacecraft intended for the radar mapping of Venus, the algorithm may nevertheless be extended to other spacecraft and to aircraft.

The object of the spacecraft mission is to place a synthetic-aperture radar in a nearly polar orbit around Venus to gather data on surface tectonics, geological history, geophysics, and small-scale surface physics. The radar will penetrate the Venusian clouds to gather high-resolution images of the surface. At least 70 percent — perhaps as much as 90 percent — of the surface of the planet will be mapped in a single rotational period of 243 days.

The algorithm incorporates the following key features:

- A scheme reduces the computational drift by a factor of 100 in a 16-bit onboard computer that uses floating-point arithmetic.
- A sequential Kalman filter uses gains generated at a station on the ground to account for changes in the relative positions of the Sun, Venus, and Earth. The filter is used for autonomous updates of attitude-knowledge errors.
- A bias-estimation scheme uses a profile for the reduction of the effects of errors. The scheme yields a least-square estimator that is simple to implement and easy to analyze.
- Ground-based calibrations are performed to obtain gyroscope-output scale factors and reference-axis misalignments. The gyroscope parameter calibration is based on principles like those used in bias estimation and yields a least-square solution.

According to an analysis of performance with worst-case parameter errors, the algorithm will meet mission requirements with comfortable margins. For example, the error in the knowledge of the mapping attitude during orbit about Venus should be well within the requirement of 0.110 ° per axis, by a margin of 0.079 ° per axis.

This work was done by Whitak H. Huang and Narotham S. Reddy of Martin Marietta Corp. for **NASA's Jet Propulsion Laboratory**. *To obtain a copy of the report, "Venus Radar Mapper Attitude Determination, Updates and Parameter Calibration," Circle 43 on the TSP Request Card.* *NPO-17028*

Life Sciences

Hardware Techniques, and Processes

Real-Time Keratometer

This instrument rapidly produces a contour map of a corneal surface.

NASA's Jet Propulsion Laboratory, Pasadena, California

An optical/electronic keratometer system produces a contour map of a corneal surface illuminated by infrared light pulses. This system prevents operator error and eliminates the need to apply fluorescent liquids to the cornea. The keratometer provides both video display and numerical recording for corneal-transplant and radial-keratotomy surgery and for contact-lens fitting.

The contour map results from the computer analysis of the Moiré pattern that is produced when light transmitted through one circular grating is reflected from the cornea onto an identical grating. The optical system is shown in Figure 1. Infrared light from a diode laser passes through the collimating lens, the beam-shaping prisms, the beam expander, the eye-fixation plane, the condensing lenses, the first circular grating, and then through the main collimating lens. The resulting collimated beam is linearly polarized by a prismoidal beam splitter, circularly polarized by a quarter-wave plate, and directed perpendicularly to the corneal surface by a converging lens. When the portion (about 4 percent) of this light reflected by the corneal surface has returned to the beam splitter, its plane of polarization has been rotated by 90° causing it to be reflected to the second grating rather than passing back through the beam-splitting prism to the laser.

The first-grating image is modified by spherical aberration in the optical system and by its reflection from any portions of the corneal surface that deviate from sphericity. This reflected image is superimposed on the second grating, which is laid out on a fiber-optic plate that has a receiving-surface shape identical to that of the circular grating. Moiré fringes are produced by the differences between the second grating and the reflected image of the first grating. Only these fringes, not the high-frequency grating structure, are transmitted by the plate to the Moiré fringe television camera.

If the corneal surface is aspherical, the location and number of Moiré fringes differ from those produced by the spherical aberration of the optical system alone. The difference is measured as a change of transverse aberration resulting from

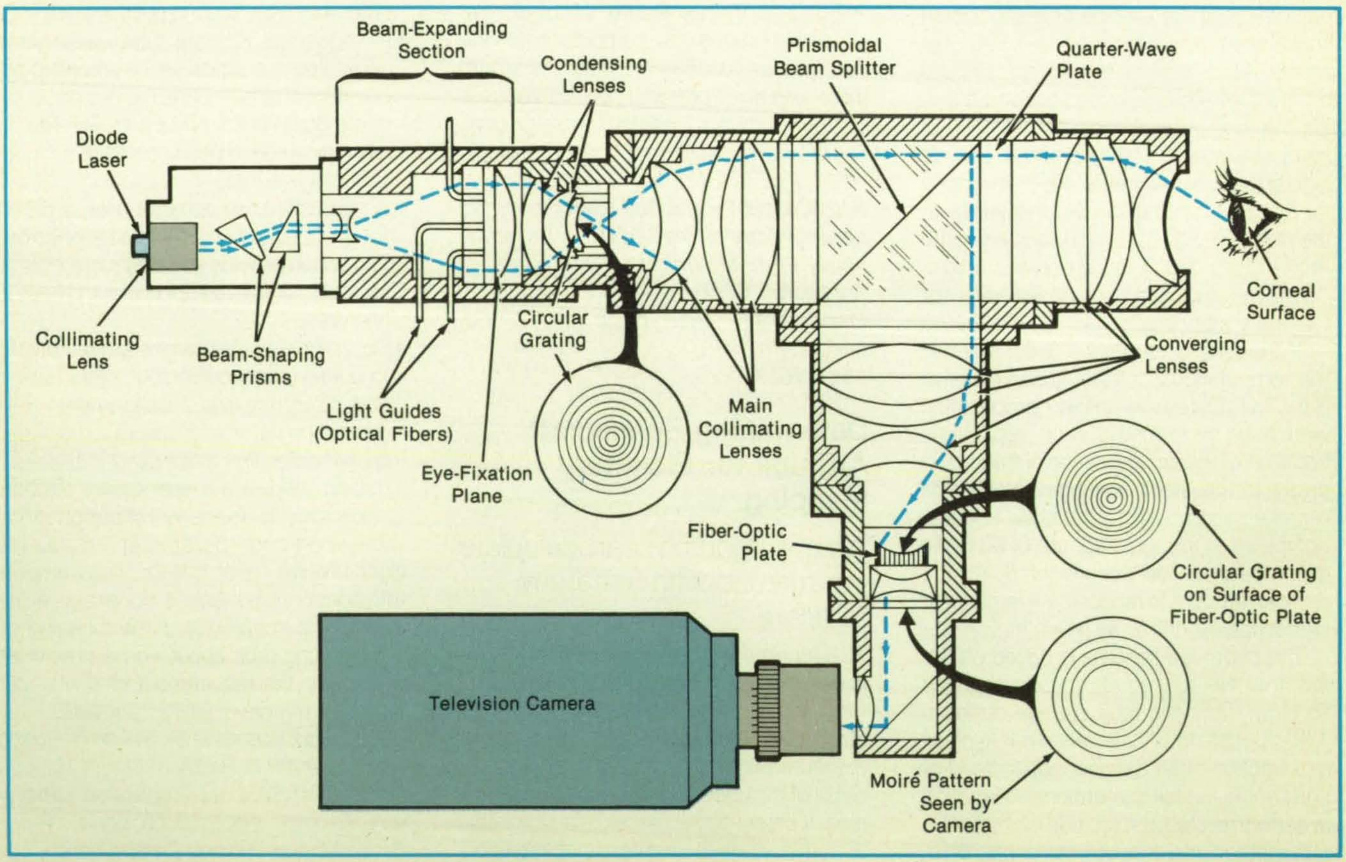

Figure 1. In the **Optical System of the Keratometer**, the circular grating pattern transmitted to the corneal surface is reflected onto an identical circular grating on the surface of the fiber plate, producing a Moiré pattern.

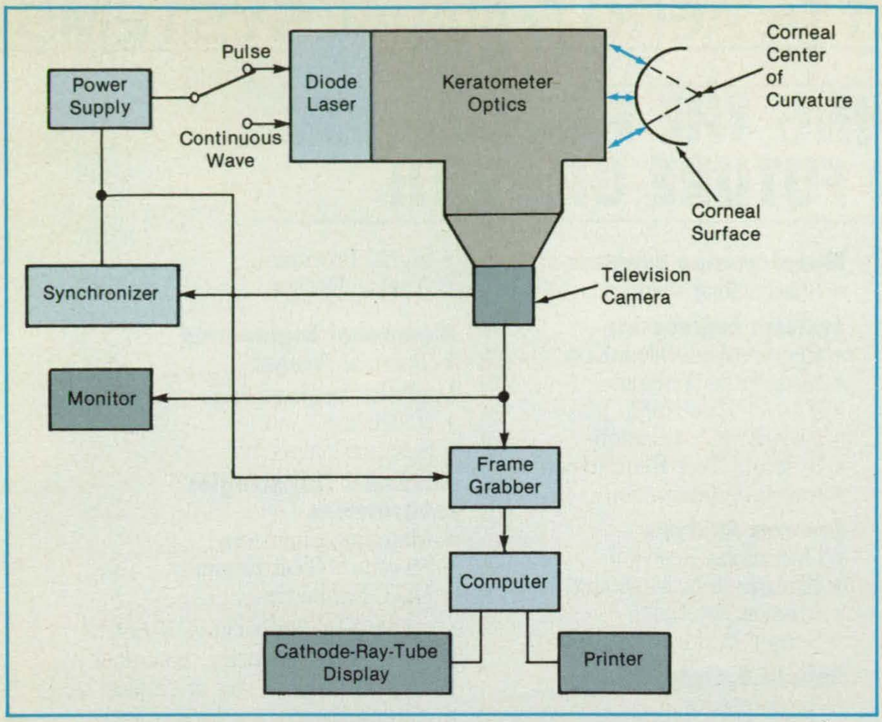

Figure 2. In the **Data-Analysis-and-Display Mode**, the laser light is pulsed, and the Moiré pattern is converted to digital information in the frame grabber. The digital picture information is sent to the computer for processing and display.

asphericity of the corneal surface. The analysis is conducted along an azimuth, and a measurement of eight azimuths suffices to define the corneal shape.

The eye-fixation plane contains the ends of eight fiber-optic guides arranged uniformly around the axis. By focusing on each of these light spots as each is illuminated in turn, the patient cumulatively presents a large portion of the corneal surface for mapping.

The data-analysis-and-display system is shown in Figure 2. The Moiré pattern is scanned at the standard television scanning rate. This rate plus the pixel resolution necessary to define a full-field Moiré pattern require analog video signals to be converted to digital at a rate about 10 to 20 times as great as the maximum transfer speed possible using a typical desktop computer; consequently, a "frame grabber" is used between the television camera and the computer. The frame grabber digitizes the signal at a high rate and transfers the data to the computer at an acceptably low rate.

Initial adjustments of the keratometer and preliminary observations are made with the laser in a continuous-wave mode. Once the measurement parameters are established, the system is switched to the automatic pulsed-laser, data-processing mode. In this mode, the short laser pulses effectively "freeze" the moving Moiré patterns from a jittering cornea. The laser pulses are synchronized with the scanning intervals of the television camera and with the analog-to-digital conversion time of the frame grabber to produce a sharp contour map of the corneal surface.

This work was done by Robert E. Frazer of Caltech and Iwao P. Adachi, and Yoshifumi Adachi of Altovac, Inc., for **NASA's Jet Propulsion Laboratory**. *For further information, Circle 125 on the TSP Request Card.*

In accordance with Public Law 96-517, the contractor has elected to retain title to this invention. Inquiries concerning rights for its commercial use should be addressed to

Edward Ansell,
Director of Patents and Licensing
Mail Stop 301-6
California Institute of Technology
1207 East California Boulevard
Pasadena, CA 91125

Refer to NPO-16701, volume and number of this NASA Tech Briefs *issue, and the page number.*

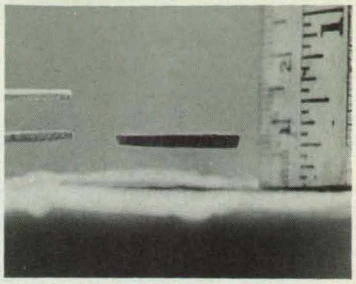

Special Report

High Tech Careers:
Strategies For Success

In today's highly competitive engineering job market technical expertise no longer guarantees long-term career success. Rising to the top of your profession requires something more: "Strategy," says Jack Schwartz, Assistant Director of Source Engineering, a nationwide recruitment firm. "An engineer needs to approach his career the same way he would a technical problem: with a clear-cut plan of action."

The first step, according to Schwartz, is to define your goals. "Engineers tend to be limited by their tunnel vision," he says. "Because they're so immersed in technology, most engineers never take the time to analyze where they'd like to be five or ten years down the road." The individual whose career has direction, whose sights are set on one area or specific position, such as Engineering Manager or Manufacturing Director, will have a distinct advantage, Schwartz says.

Once goals are established, strategy then comes into play. Though no two careers need follow precisely the same path, certain "tactics" can help almost anyone, according to employment experts. These include:

• **Establishing Checkpoints.** "I knew an engineer who, for five years, did nothing else but design the front bumper of a car," recalls James Miles, Personnel Director for the Environmental Research Institute of Michigan (ERIM). "The money was excellent, but when he wanted to change direction and get an aerospace job, he discovered that, because of his limited experience, no one would seriously consider him." By failing to develop new skills, the engineer's career had hit a dead end. To avoid such a scenario, Mr. Miles suggests reassessing your position at both the beginning and end of each new project. "It's important to ask yourself, 'Am I learning new skills and, if I am, are they going to help me achieve my goals?' If the answer is no, then it's time for a change."

• **Broadening Your Horizons.** Developing management, marketing, and communications skills may seem relatively unimportant to the novice engineer, but they are crucial to later advancement, says Carol-Lynne Cox, a partner in Novatron, a New York placement firm. "In the past," she says, "companies would hire a traditionally skilled manager, a pure people-motivator, to come in and ride herd on their technical staff. But with industry-wide budget cutting and streamlining taking place, that's a luxury most companies can no longer afford. They're expecting the technical staff to take up more and more of the slack." This is reflected, she says, in the rising demand for engineers holding MBA degrees.

Recent economic trends have also created the need for design engineers with marketing know-how. "With profit margins shrinking in so many areas of manufacturing, an engineer who understands the position of his organization in the overall economy and can design with a bottom line orientation is a very valuable commodity," says Robert Weatherall, Director of Career Services for the Massachusetts Institute of Technology. Mr. Weatherall advises engineers to supplement their technical education with courses in Economics, Finance and Marketing.

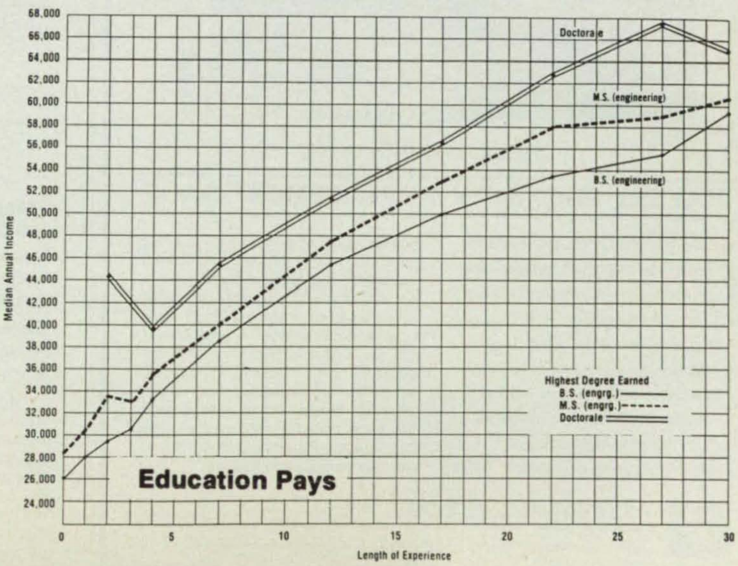

Increased education results directly in higher earnings throughout an engineer's career, as shown by these results from the 1987 Salary Survey by the National Society of Professional Engineers. Overall, engineers holding a doctorate earn 31.0% more than those with a B.S. in engineering, according to the NSPE member survey. The comparable figures in previous yers were 30.1% in 1986, 25.5% in 1985, 24.5% in 1983, and 21.0% in both 1982 and 1981.

Business Communications courses can also provide engineers with a competitive edge. "There's been an industry-wide communications problem where the managers will get together with the technical staff and neither group will have the foggiest idea what the other is talking about," explains Ms. Cox. "Companies need people who can take a technical concept or idea and translate it into clear enough English that non-technical management can understand."

- **Advancing Your Education.** "A Masters Degree is becoming more valuable with each passing year," says Sally Asmundson, Director of Career Development for the California Institute of Technology. "And in sophisticated areas such as Artificial Intelligence, a Doctorate may be necessary for long-range career growth." Adds Mr. Weatherall: "An individual who attains an advanced degree level will naturally have greater confidence in his or her ideas. Companies recognize this and in turn will place more confidence in this individual than someone holding only a Bachelors Degree." *(see graphs)*
- **Networking.** Affiliation with professional societies can be vital to your advancement in two ways: by helping you stay abreast of industry trends and by providing a means of networking with fellow professionals. "(Society membership) is a visible sign of professionalism," comments Mr. Miles. "It shows that a person is staying on top of the latest developments in his or her field." Society seminars and conferences offer the opportunity to meet key industry figures in your field and develop contacts that can "put you on the inside track for new opportunities," according to Mr. Schwartz.
- **Leaving Tracks.** "Moving up the company ladder often requires some breast-beating on your part," Schwartz says, "especially when you're involved in large group projects: It's essential that you find a way to make your supervisors notice your accomplishments." One method is to publish technical papers and articles in industry journals. This not only serves as self-promotion, Schwartz points out, but it also shines the spotlight back on your organization, which can only help come promotion time.

And what is the single most important factor contributing to career growth? "Getting results, day-in and day-out" says Mr. Weatherall. "No matter what skills you may possess, it still comes down to everyday performance, putting your ideas on the line, making them work. That's the bottom line." □

Income by Level of Education

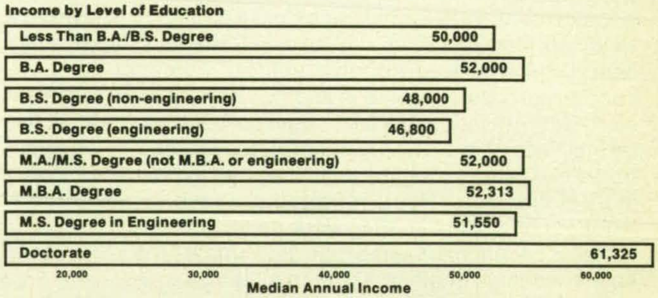

Source: National Society of Professional Engineers 1987 Salary Survey

Classifieds

Classified advertising rates and specifications are as follows: Set in 6 point light type face, with up to five words at beginning of copy in bold caps. Count box numbers as six words.

50 words or less .... $ 180
100 words .... $ 250

Check or money order must accompany order to: Classified Advertising Manager, NASA Tech Briefs, Suite 921, 41 East 42nd Street, New York, NY 10017-5391.

New on the Market

The model CWS-200 **computerized welding system** from the Astro Arc Co., Sun Valley, CA, is designed for process control in industrial manufacturing settings. The automatic gas tungsten arc welding system includes cassette storage for weld programs, a data acquisition system for real time inspection of welded parts, and remote control capabilities. The CRT screen enables all welding variable and positioning adjustments to be controlled at the touch of a finger. **Circle Reader Action Number 780.**

Foster Airdata Systems, Inc., Columbus, OH, has introduced the F4 Phoenix, **IFR Rated LORAN**. The panel mounted unit contains a push button release mechanism that facilitates removal from the plane for quick and easy pilot exchange of the data base cartridge. An optional demo kit allows the Phoenix to operate on standard house current, enabling pilots to train, practice, or load actual flight plans without having to be in the aircraft.
Circle Reader Action Number 786.

National Instruments, Austin, TX, has adopted an open architecture for integrating conventional program code into the current release of its LabVIEW® software system, a **graphical programming system** used by scientists and engineers for tasks such as data acquisition and analysis, automated test and measurement, simulation, and modeling. The first high-level language supported under the open architecture is THINK's LightspeedC®, from Think Technologies.
Circle Reader Action Number 798

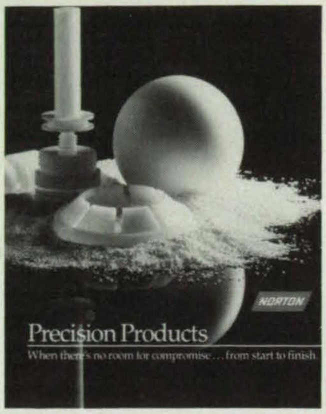

A new brochure from Norton Performance Plastics, Wayne, NJ, illustrates materials, processes and capabilities for manufacturing high-performance **plastic parts**. Products highlighted in the brochure include: EXAC® premium quality machining stock; Chemfluor® Fluid Handling Systems and PFA fittings; and Chemware® beakers, part of a full line of laboratory ware made from TFE and other fluoropolymers.
Circle Reader Action Number 790.

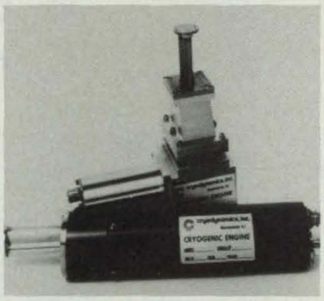

A miniature closed-cycle **cryogenic refrigerator** is now available in a choice of configurations from Cryodynamics, Inc., Mountainside, NJ. The Model M15 Series produces one watt net useable cooling at 77°K in only eight minutes, with less than 30 watts input power. The non-lubricated, hermetically sealed unit is ideal for use in infrared sensor and laser systems, low noise amplifiers and antennae, spot cooling, and range instrumentation.
Circle Reader Service Number 792.

EG&G Princeton Applied Research Corp. has announced a new **software package**, the M1461/90, that combines the computing features of the IBM-PC's and the data acquisition power of the OMA III M1461 buffered interface. The result is a cost effective, sophisticated parallel light detector system simple to use yet powerful enough to run the most complex OMA experiments.
Circle Reader Action Number 782.

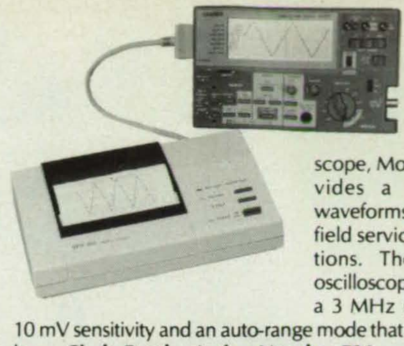

Leader Instruments Corp., Hauppauge, NY, has created a companion **printer** for the Combination Digital Multimeter/Storage Oscilloscope, Model 100P. The printer provides a hard copy of stored waveforms, making this unit ideal for field service and laboratory applications. The Model 100P storage oscilloscope section is equipped with a 3 MHz maximum sampling rate, 10 mV sensitivity and an auto-range mode that automatically sets the time base. **Circle Reader Action Number 796.**

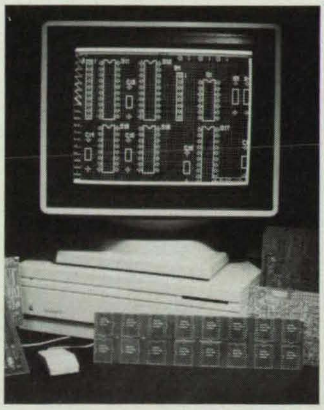

Douglas Electronics, San Leandro, CA, has added the CAD/CAM Professional System to its line of **printed circuit board software**. The system runs on the Apple Macintosh and features color and multilayer capabilities. A layout package, schematic capture, and autorouter make the Professional System a fully integrated package for CAD/CAM applications. Demonstration disks are available from Douglas.
Circle Reader Action Number 784.

Amco Engineering's 1988 catalog presents an expanded array of **electronic consoles**. Amco now offers 19" and 24" panel widths, three distinct styles, and ten color selections in one or two tone applications. The 44 page catalog also displays Amco's full line of blowers, fans, desks, accessories and hardware.
Circle Reader Action Number 794.

Varian Associates' new 200 watt Millitron **traveling wave tube**, which operates at millimeter-wave frequencies, was designed specifically for use in the extremely high frequency (EHF) commercial ground system satellite communications market. The tube incorporates an advanced ladder circuit technology pioneered by Varian. The ladder design is easy to manufacture in production quantities, and therefore costs less than tubes using structures which require exotic machining techniques and a higher part count.
Circle Reader Action Number 778.

The Philips PM 3350, a high-performance **digital oscilloscope** with real-time capability, has been introduced by John Fluke Mfg. Co., Inc., Everett, WA. The dual-channel PM 3350 features a 50 MHz bandwidth and a maximum sampling frequency of 100 Msamples/s, maintainable on both channels simultaneously for high resolution signal display and storage. The PM 3350 has a one-button AUTOSET function available in both analog and digital modes for automatic channel selection and setting of amplitude, timebase, and triggering parameters for any imput signal.
Circle Reader Action Number 800.

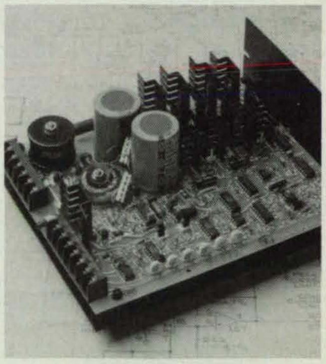

The VXA Series of modular **PWM (Pulse-Width Modulated) amplifiers** from PMI Motion Technologies, Commack, NY, features a peak-current-rating that can double torque and acceleration rate of dc servos. The compact (8.7"x2.9"x7") VXA provides precise incremental and continuous motion control for dc servos requiring up to 384 watts (768 watts peak). Servo system stabilization is simplified by adjustable compensation, and the amplifier is fault protected.
Circle Reader Action Number 788.

Subject Index

Advertiser's Index

*RAC stands for **Reader Action Card.** For further information on these advertisers, please circle the RAC number on the Reader Action Card elsewhere in this issue. This index has been compiled as a service to our readers and advertisers. Every precaution is taken to ensure its accuracy, but the publisher assumes no liability for errors or omissions

DON'T FORGET TO CHECK YOUR LABEL

0020 EXP DATE FEB 88 T9999999
JOHN DOE
XYZ COMPANY
123 MAIN BLVD
BLARNEY NJ 07335

Your NASA Tech Briefs address label contains very valuable information:

1. **Subscription Expiration Date**—a great way to remember to renew before you're caught unaware of interrupted service.
2. **Personal Identification Number**—aids in the rapid processing of your renewal.

It's fast and easy to renew when you use the convenient peel-off address label. Just attach to the subscription form in your magazine, sign, date & complete all questions. **We must have your company name and address if your copy of NTB is being sent to your home address.**

Don't take a chance on missing out on any of NTB's latest technology, new product ideas or industry trends you need to acquire the knowledge, solutions, and ideas that have inspired progressive industry leaders—look at your label, and renew early.

NASA Tech Briefs, ISSN 0145-319X. USPS 750-070. copyright © 1988 in U.S., is published monthly except July/August and November/December (10x per year) by Associated Business Publications Co., Ltd. 41 E. 42nd St., New York, NY 10017-5391. The copyrighted information does not include the individual Tech Briefs which are supplied by NASA. Editorial, sales, production and circulation offices at 41 E. 42nd Street, New York, NY 10017-5391. Subscriptions for non-qualified subscribers in the U.S., Panama Canal Zone, and Puerto Rico, $75.00 for 1 year; $125.00 for 2 years; $200 for 3 years. Single copies $15.00. Remit by check, draft, postal or express orders. Other remittances at sender's risk. Address all communications for subscriptions or circulation to NASA Tech Briefs, 41 E. 42nd Street, New York, NY 10017-5391. Second-class postage paid at New York, NY and additional mailing offices. **POSTMASTER: please send address changes to NASA Tech Briefs, 41 E. 42nd Street, Suite 921, New York, NY 10017-5391.**

The New 4180 Plug-In

SPEED TRIALS.

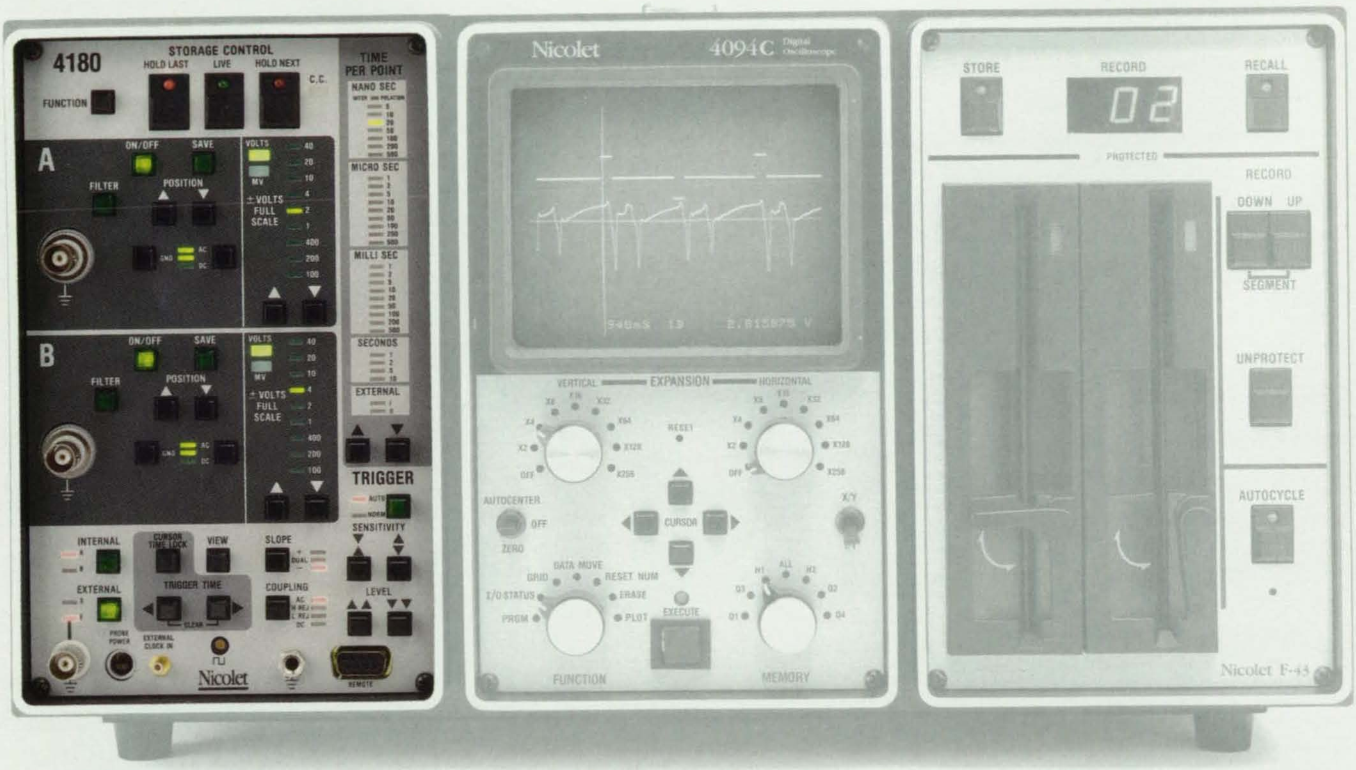

- *Multi-channel: two or four channel configurations.*
- *Unmatched single-shot capabilities.*
- *High speed, 200 MHz digitizing.*
- *100 MHz analog input bandwidth.*
- *Real-time math functions.*

- *For your Free Speed Trial call: 800-356-3090 or 608-273-5008*

Nicolet Test Instruments Division
P.O. Box 4288
5225-2 Verona Road
Madison, WI 53711-0288

Nicolet Digital Oscilloscopes

Speed. Using the latest designs in ADC technology, your input signal can be digitized at speeds up to 200 MHz (5ns per data point) and saved for analysis. The wide band input amplifiers allow signals up to the 100 MHz Nyquist limit to be input without distortion. Sophisticated trigger setup displays allow you to accurately set the level, sensitivity, and slope to make one-shot transients easy to catch; eliminating the usual hit or miss guesswork. For multi-channel applications two 4180's can operate together in one mainframe producing a four channel scope with no degradation in speed or performance.

Real-Time Math. In addition to the extensive post-processing capabilities in the mainframe, the 4180 has several useful routines which present computed results as live, real-time displays: *FFT, MAX/MIN, A+B, A−B, A×B, A/B,* and *AVERAGING.*

Nicolet

INSTRUMENTS OF DISCOVERY

Circle Reader Action No. 350